Titre: Title:	Nonlinear finite element studies of cementless knee implants
Auteur: Author:	Seid Ataolah Hashemi
Date:	1998
Type:	Mémoire ou thèse / Dissertation or Thesis
Référence: Citation:	Hashemi, S. A. (1998). Nonlinear finite element studies of cementless knee implants [Ph.D. thesis, École Polytechnique de Montréal]. PolyPublie. https://publications.polymtl.ca/6783/

INFORMATION TO USERS

This manuscript has been reproduced from the microfilm master. UMI films the text directly from the original or copy submitted. Thus, some thesis and dissertation copies are in typewriter face, while others may be from any type of computer printer.

The quality of this reproduction is dependent upon the quality of the copy submitted. Broken or indistinct print, colored or poor quality illustrations and photographs, print bleedthrough, substandard margins, and improper alignment can adversely affect reproduction.

In the unlikely event that the author did not send UMI a complete manuscript and there are missing pages, these will be noted. Also, if unauthorized copyright material had to be removed, a note will indicate the deletion.

Oversize materials (e.g., maps, drawings, charts) are reproduced by sectioning the original, beginning at the upper left-hand corner and continuing from left to right in equal sections with small overlaps. Each original is also photographed in one exposure and is included in reduced form at the back of the book.

Photographs included in the original manuscript have been reproduced xerographically in this copy. Higher quality 6" x 9" black and white photographic prints are available for any photographs or illustrations appearing in this copy for an additional charge. Contact UMI directly to order.

UMI®

Bell & Howell Information and Learning
300 North Zeeb Road, Ann Arbor, MI 48106-1346 USA
800-521-0600

UNIVERSITÉ DE MONTRÉAL

NONLINEAR FINITE ELEMENT STUDIES OF CEMENTLESS KNEE IMPLANTS

SEID ATAOLAH HASHEMI
DÉPARTEMENT DE GÉNIE MÉCANIQUE
ÉCOLE POLYTECHNIQUE DE MONTRÉAL

THÈSE PRÉSENTÉE EN VUE DE L'OBTENTION
DU DIPLÔME DE PHILOSOPHIE DOCTOR
(GÉNIE MÉCANIQUE)
SEPTEMBRE 1998

UNIVERSITÉ DE MONTRÉAL

ECOLE POLYTECHNIQUE DE MONTRÉAL

Cette thèse intitulée:

NONLINEAR FINITE ELEMENT STUDIES OF CEMENTLESS KNEE IMPLANTS

Présentée par: HASHEMI Seid Ataolah

en vue de l'obtention du diplôme de: Philosophiae Doctor

a été dûment accepte par le jury d'examen constitué de:

M., LAKIS, Aouni, Ph.D., Président

M. SHIRAZI-ADl, Aboulfazl, Ph.D., membre et directeur de recherche

M., KASRA, Mehran, Ph.D., membre

M., YAHIA, L'Hocine, Ph.D., membre

To my parents

ACKNOWLEDGMENTS

It is a special privilege to acknowledge the inspirations and influences of my teachers, friends and colleagues who have in one way or another contributed to this work.

First, I would like to thank prof. A. Shirazi-Adl the thesis supervisor, for the help and guidance along the way. Also to be recognized are the other members of the committee prof. M. Kasra, prof. A. Lakis and prof. H. Yahia.

The scholarship from the Ministry of Culture and Higher Education of I.R. Iran are highly appreciated. Thanks also go to NSERC Canada for the partial financial support and Howmedica, Inc. for providing the material used in the experiment tests.

Acknowledgment must also go to the Applied Mechanic Section professors, graduate students, and technicians. Among those, the assistance of M. Dammak in friction tests, A. Kieffer in the programming, S. Sadouk in writing résumé, and G. Giron in preparing test specimens and performing CMM measurements is also gratefully appreciated.

I would like also to express my gratitude to my uncle and his family for the help provided to me during my stay in Canada. Finally, I wish to thank my sister and brother for sustaining me with their kindness and encouragement.

RESUMÉ

Durant les deux dernières décennies, des travaux ont été effectués sur le remplacement de l'articulation du genou humain. Ceci est dans un but de trouver un remède au problème de l'arthrite du genou. Les implants cimentés et non cimentés sont deux types utilisés pour le traitement arthroplastique du genou. Les implants non cimentés présentent principalement deux types de problèmes majeurs : le descellement et l'usure. Dans ce type d'implants, le frottement à l'interface de l'os-implant et les vis/tiges sont utilisés pour assurer la stabilité requise à la fixation durant la période post-opératoire où les attachements osseux-implants ne sont pas suffisamment développés. Le présent travail a été conçu dans le but de développer un modèle du système genou - implant par éléments finis, afin d'étudier la fixation mécanique et la stabilité, avec une charge statique, de différentes conceptions et différents modèles de frottement. À cet effet, des études primaires nous ont permis d'examiner le frottement à l'interface de l'os et de l'implant, ainsi que l'arrachement des vis/tiges.

Dans la première partie, vu l'importance des frottements sur la stabilité des implants, des tests bi-directionnels de frottement ont été réalisés entre un cube de matériau osseux et une plaque métallique à surface poreuse. Ceci a permis de déterminer les propriétés mécaniques de l'interface pour pouvoir les introduire dans le code d'éléments finis (3D) d'implant non-cimentés. À cet effet, des spécimens osseux ont été extraits de différentes régions proximales de tibias et une plaque à surface poreuse a été préparée. Le montage expérimental utilisé pour les tests de frottement uni-directionnel a été modifié afin de pouvoir appliquer des charges normales entre elles et tangentielles à la surface de contact, et enregistrer les déplacements induits dans le plan. Les résultats mesurés ont montré que la courbe charge - déplacement est fortement non linéaire avec un couplage significatif entre les deux directions. Le coefficient de frottement a été trouvé presque invariant du site anatomique de la surface osseuse extraite du tibia. Des tests bi-directionnels ont suggéré que

la relation charge-déplacement, évaluée pour les valeurs résultantes, reste similaire au cas du test uni-directionnel. Par la suite, les équations constitutives considérant les termes de couplage entre les deux directions perpendiculaires ont été développées et utilisées dans un modèle d'élément finis 3D simulant le test du frottement. La validation des termes de couplage a été effectuée par comparaison des résultats du modèle d'élément finis 3D aux valeurs mesurées ce qui montre une concordance satisfaisante. Les mêmes essais ont été répétés en remplaçant l'os par du polyuréthanne donnant ainsi des résultats similaires. Les équations constitutives développées pour le frottement bi-directionnel sont alors utilisées dans les analyses par éléments finis 3D simulant le test d'arrachement et le système os-implant dans le genou.

Dans la deuxième partie, vu le rôle des vis et des tiges dans le montage implant-os, le comportement des vis/tiges (lisses et poreuses) insérées dans le cylindre en polyuréthanne a été étudié pour le cas de l'arrachement à chargement incliné. Ce comportement a été observé expérimentalement ainsi que par le modèle des éléments finis proposé. Il a été trouvé que le chargement incliné diminue la résistance d'arrachement des vis, par contre, augmente celle des tiges poreuses. Pour le cas des tiges lisses, l'influence n'est pas considérable. Ces résultats ont été confirmés par l'utilisation de la méthode expérimentale ainsi que par éléments fins. Cette validation nous a permis, alors, d'intégrer les approches proposées dans le modèle d'éléments finis 3D du système genou - implant.

Finalement, le modèle d'éléments finis 3D constitué du système genou - implant nous a permis d'étudier de l'influence des types de fixation du tibia ainsi que des types de frottement durant la période post - opératoire du genou (où les attaches biologique ne sont pas encore développées) sur le comportement du système. L'interface os-implant a été modélisée en se basant sur les équations constitutives bi-directionnelles de frottement développées dans la première partie. Les propriétés de frottement entre le fémur et le polyéthylène ont aussi été déterminées. L'os d'après

la littérature présente des propriétés mécaniques élastiques linéaires mais hétérogènes. Les caractéristiques élastoplastiques du polyéthylène ont été introduites dans le modèle présent. Les vis/tiges ainsi que les formes géométriques obtenues expérimentalement pour les différentes composantes ont été integrées dans le modéle. Différentes configurations de la plaque fixée sur le tibia ont été considérées: plaque à 3 vis, plaque à une vis et deux tiges et une plaque libre. Un poids de 2000N correspondant à trois fois celui du corps a été appliqué sur le fémur. Il a été constaté que le modèle de frottement de Coulomb sous estime le déplacement relatif à l'interface de l'os et de l'implant. Le cas de la plaque à 3 vis a donné moins de déplacements relatifs et moins de décollage (lift-off). Le déplacement relatif à l'interface de l'os et de l'implant ainsi que la distribution des contraintes ont été trouvés dépendant du type de la fixation. Dépendamment du type de la fixation, les os cortical et cancellous supportent respectivement 10 à 13% et 65-80% de la charge. Le reste est transféré sous forme de cisaillement entre les vis/tiges et l'os. Cependant les contraintes normales et de Von Mises dans le polyéthylène sont indépendantes du type de fixation. Les valeurs maximales de ces contraintes dépassent la contrainte d'écoulement et sont localisées à 1-2 mm au-dessous de la surface de contact pour tous les types de fixation. Basé sur les résultats des études par éléments finis, le rôle important de la friction et des vis/tiges sur la stabilité de la fixation a été démontré. Il a été recommandé qu'un nombre croissant de vis et de tiges et d'une localisation de ceux-ci dans le périmètre de design peuvent réduire les micro-mouvements. En utilisant des surfaces poreuses avec des grands coefficients de friction on peut aussi augmenter la force de cisaillement à l'interface ce qui assurera une fixation plus rigide.

ABSTRACT

Total joint replacement has been significantly developed in the last two decades to provide a solution to the arthritic joint. Cemented and cementless implants are two types that are currently used in the joint arthroplasty. In a cementless implant, friction at the bone-implant interface and screws/posts are employed to provide the required fixation stability of the structure in the immediate post-operative period with no biological attachment. In the cementless implant, loosening of the tibial prosthesis and polyethylene wear remain as two main causes of the implant failure. This work deals with the initial fixation and stability of cementless implants. Due to the important role of friction and screws/posts in the initial fixation, friction characteristics at the bone-implant interface and pull-out test behavior under inclined load were determined. Finally, a 3-D finite element model of the knee-implant system was developed to investigate the influence of different friction models and fixation design configurations on fixation stability under static loading. The micromotion at the knee-implant interface and stress distribution within the bone and polyethylene were studied, as well.

In the first part due to the importance of friction role in the fixation stability of implant, bi-directional friction tests between cancellous bone/polyurethane cubes and a porous-coated metal plate were performed to determine the mechanical properties of the interface required in 3-D finite element model studies of cementless implants. For this purpose, bone specimens obtained from proximal regions of tibia and a beaded porous-surfaced plate were used. The apparatus used for uni-directional friction tests was modified to apply tangential loads in perpendicular directions and monitor the corresponding displacements. Measured results showed that the interface load-displacement curve was highly nonlinear with significant coupling between two perpendicular directions. Bi-directional tests suggested that the load-displacement relation when evaluated for resultant values was similar to that obtained in a uni-directional testing condition. Constitutive

equations that account for the cross-stiffness coupling terms between perpendicular directions were also developed and used in a 3-D finite element model study of preceding bi-directional friction tests. The influence of the coupling terms on results was investigated by comparison of predictions with measurement results. A satisfactory agreement was found between the results of experiments with those of finite element studies confirming the constitutive relations as well as the importance of coupling terms. The equations developed here were used in the subsequent 3-D finite element analyses, i.e., the pull-out tests and the knee-implant system. Similar experimental/finite element investigations were repeated for the polyurethane cubes replacing cancellous bone specimens to further study the nonlinear coupled characteristics of such interfaces in bi-directional friction conditions. Polyurethane specimens yielded results comparable to those obtained using bone specimens.

Second part included the study undertaken to investigate the effect of combined loading on pull-out fixation response of bone screws, porous coated posts, and smooth-surfaced posts inserted in polyurethane material. Screws and posts are used in various implant designs to contribute to the fixation stability of artificial joints. Finite element models of the screws/posts were proposed and validated by experimental tests. The effect of inclination in posts and screws showed three different patterns. Increasing the inclination angle increased the axial pull-out load for porous coated posts. It did not, however, significantly affect that for smooth-surfaced posts while the axial pull-out load for the screw reduced with load inclination. The satisfactory agreement between numerical and experimental results confirmed the accuracy in modeling the interface, posts, and screws. The developed models were, therefore, used to investigate the post-operative short term fixation stability of various implant designs.

In the last part, a three dimensional nonlinear finite element model was developed to investigate tibial fixation designs and friction models in total knee arthroplasty in the immediate postoperative

period without biological attachment. Bi-directional friction properties were used for the bone-porous coated implant interface. Based on the measurements of friction properties at the interface between polyethylene and smooth metal surface, Coulomb's friction (μ=0.045) was considered to model the polyethylene-femoral component interface. Linear elastic isotropic but heterogenous mechanical properties were considered for bone. Tension tests were performed to obtain the mechanical behavior of the polyethylene required for the simulation. The elasto-plastic isotropic hardening mechanical model was used for polyethylene in the finite element analysis. Based on the earlier finite element and experimental pull-out studies, posts and screws were also reliably modeled. The geometry of every component was obtained through measurements. The Porous Coated Anatomical (PCA, Howmedica Inc.) tibial baseplate with three different configurations was considered; one with three screws, one with one screw and two short inclined porous-coated pegs, and a third one with no fixation for the sake of comparison. Three times body weight was applied through the femoral component on the medial plateau of articular insert. It was found that Coulomb's friction significantly underestimates the relative micromotion at the bone-implant interface. The lowest micromotion (21.8 μm) and lift-off (21.6 μm) were found for the design with screws. Cortical and cancellous bones carried, respectively, 10-13% and 65-86% of the axial load depending on the fixation configuration considered. Normal (48 MPa) and Mises (23 MPa) stresses as well as contact area in the polyethylene insert were independent of the baseplate fixation design. Maximum Mises stress in polyethylene exceeded the yield stress and was found 1-2 mm below the contact surface for all designs.

The finite element analyses revealed the significant dependency of relative micromotion and stress transfer at the bone-implant interface on the friction model and on the baseplate anchorage configuration. However, stresses within the polyethylene were found to be independent of the baseplate fixation. The study also confirmed the superior performance of screws in preventing the micromotion and the lift-off.

CONDENSÉ EN FRANÇAIS

Le remplacement du genou humain est devenu un moyen de plus en plus efficace de réduire la douleur associée à l'arthrite. Le nombre de remplacement, particulièrement l'arthoplastie de la hanche et du genou, a augmenté de façon significative avec un taux de succès clinique dépassant les 80%. Cette augmentation est amenée à se poursuivre avec le vieillissement des populations occidentales. Plus de 400 000 arthoplasties de la hanche et du genou sont effectuées chaque année aux États Unis seulement. Des défaillances ont été notées avec la méthode utilisée actuellement pour la prothèse du genou. Des problèmes comme le descellement, l'usure du polyéthylène, et le bris d'éléments métalliques ont été observés cliniquement. Le relâchement et l'usure du polyéthylène affectent la performance à long terme de la prothèse du genou de façon défavorable.

Deux types d'implants, i.e., cimentés ou non, sont actuellement utilisés dans l'arthoplastie du genou. Tandis que dans les implants cimentés, le ciment est utilisé comme agent liant entre les éléments prothétiques et les os, dans les implants non cimentés, la prothèse est directement en contact avec l'os hôte. Les études à long terme ont également révélé que le mode principal de défaillance du remplacement total du genou est le relâchement mécanique à l'interface os/implant. Afin de fournir un produit plus stable à long terme, il a été proposé de fixer la couche poreuse des implants aux os par la croissance osseuse rendant une fixation biologique. La fixation à court terme des implants non cimentés est obtenue à l'aide de vis/tiges. Le succès à long terme de l'opération dépend de la réussite d'une telle intégration biologique.

L'autre problème fréquemment rencontré relié à la prothèse du genou, est la cassure de la "ultra high molecular weight polyethylene" (UHMWPE) qui peut provoquer le mouvement de particule d'usure de polyéthylène dans le corps et peut entraîner le dysfonctionnement de l'implant. Les débris de polyéthylène peuvent causer des l'ostéolisys, la résorption et le relâchement. La cassure

du polyéthylène a été notée dans plusieurs analyses de prothèses. Il a été remarqué que certains facteurs comme la qualité du polyéthylène, les procédés de fabrication et les méthodes de stérilisation affectent gravement la résistance à l'usure du polyéthylène.

Par conséquent, la prothèse du genou et les problèmes qui y sont reliés constituent le sujet de nombreuses recherches récentes. Le présent travail a également été conçu dans le but de développer un modèle d'éléments finis du système genou-implant, afin d'étudier la fixation mécanique et la stabilité de différentes conceptions et différents modèles de frottement. Dans un implant non cimenté, le frottement à l'interface os/prothèse joue un rôle important dans la réponse mécanique du système, en particulier dans la période post-opératoire immédiate, où aucune croissance osseuse ne s'est encore produite et le frottement reste le seul moyen de transfert de la charge dans les directions tangentielles aux interfaces communes. Les propriétés du frottement uni-directionnel à l'interface entre l'os spongieux du tibia et plusieurs plaques de métal furent mesurées auparavant. Dans un problème de contact à trois dimensions, les pièces articulées peuvent subir des mouvements relatifs et développer des forces de cisaillement dans différentes directions à l'interface commune. Ces directions peuvent aussi changer durant la déformation. Le phénomène de frottement bi-directionnel entre deux corps nécessite une recherche expérimentale.

Ainsi, afin d'étudier les propriétés de friction bi-directionnel à l'interface entre la surface de l'os poreux et le métal, le montage expérimental utilisé pour des tests uni-directionnels a été modifié pour permettre l'enregistrement continu de charges et de déplacements relatifs dans des directions perpendiculaires à l'interface. Dans des conditions normales de pression, plusieurs charges testées ont été appliquées dans une direction alors que dans l'autre direction la charge était augmentée par pas successifs. La réponse dans les deux directions a été mesurée simultanément. Les mesures mènent à des courbes de force de frottement en fonction du déplacement similaires aussi bien pour les valeurs des tests bi-directionnels que pour celles des tests uni-directionnels. Les résultats

expérimentaux montrent clairement la présence de couplage entre ces deux directions perpendiculaires. C'est le cas pour l'os spongieux avec toutes les régions de l'os. Le coefficient de frottement à l'interface reste aussi presque inchangé avec l'amplitude relative des contraintes tangentielles et du lieu de coupure de l'os, et c'est pratiquement la même que celle trouvée dans les tests uni-directionnels. Les résultats de mesure de cette étude indiquent que le coefficient de friction à l'interface métal/os ne dépend pas de l'emplacement de la coupure de l'os. Les courbes de frottement mesurées sont très fortement non linéaires avec des déplacements relatifs très grands, dans un intervalle de 60 à 500 μm, dépendant de l'emplacement de la coupure de l'os. La pente initiale est plus forte dans les régions médiale et latérale, ceci est dû au fait que le module élastique de l'os dans la région proximale du tibia est plus grand dans les sites latéraux et médians que dans les autres sites. Les déplacements relatifs de l'interface sont aussi indépendants de l'amplitude des charges appliquées précédemment.

Une approche analytique basée sur les courbes charge/déplacement unidirectionnel a aussi été présentée. Ces équations ont été développées avec l'hypothèse que des micromouvements arrivent dans la direction de la force résultante et que cela suit la courbe charge/déplacement unidirectionnel. Dans les développements en cours, les propriétés de frottement dans différentes directions sont supposées être couplées. Le couplage des propriétés de friction a introduit des termes hors diagonale dans les relations de base. Ces équations ont été introduites dans les études du modèle d'éléments finis des tests de frottement bi-directionnels. Un bon accord a été trouvé entre les résultats du modèle et ceux de l'expérience. Cet accord satisfaisant n'aurait pas été obtenu si les termes de couplage de l'équation 2.3 n'avaient pas été considérés dans le modèle d'éléments finis. Des résultats similaires ont été obtenus quand des cubes de polyéthylène ont remplacé les spécimens d'os spongieux. Ainsi, dans l'étude par éléments finis en 3-D du contact entre les corps avec des interfaces isotropiques, tel qu'avec l'arthroplastie des joints non cimentés, les formulations du frottement couplé présentées dans ce travail devront être utilisées.

Depuis que dans les systèmes de prothèse du genou, les vis/tiges, supportent aussi bien les forces de cisaillement que les forces axiales, l'effet de l'inclinaison sur la force d'arrachement a été étudié à travers des méthodes expérimentales et d'éléments finis. Dans le modèle d'éléments finis 3-D des tests d'arrachements inclinés, les équations de base du frottement bi-directionnel ont été utilisées pour modéliser de façon précise l'interface entre le polyuréthane et les tiges/vis. Ainsi le but de cette partie du travail était : de proposer des modèles efficaces d'éléments finis pour l'analyse de la fixation des vis ; et de rechercher l'effet des charges de cisaillement sur la force d'arrachement des tiges (lisses et poreuses) et des vis.

Dans les premières études de mesures, les surfaces lisses des tiges ont démontré une performance supérieure d'arrachement sous des conditions de charge simple et de fatigue lorsqu'elles étaient comparées à des tiges à surface poreuse de même dimension. Les résultats expérimentaux et par éléments finis des tests d'arrachement incliné indiquent que la différence précédente diminue en présence de charges de cisaillement. La force d'arrachement axiale de tiges lisses n'est pas affectée de façon significative par l'accroissement de l'angle d'inclinaison de la force de retrait. Ceci est dû à des contraintes normales élevées à l'interface des tiges à surface lisse et du cylindre de polyuréthane. Cependant, l'inclinaison de la charge affecte la charge d'arrachement axiale pour des tiges à surface poreuse. Ceci est dû à la modification des contraintes normales à l'interface. Les vis, cependant, ont démontré une diminution constante de la force d'arrachement dans la direction axiale avec des charges combinées. Ceci peut être en partie dû à la limite placée sur la contrainte de cisaillement à l'interface qui ne doit pas dépasser la résistance en cisaillement mesurée sur le matériau.

La géométrie d'une vis étant complexe, le modèle par éléments finis, mécaniquement équivalent, d'une vis pour l'os a été proposé en remplaçant les vis par des tiges avec des propriétés modifiées à l'interface. Le coefficient de friction, approximativement de 2, a été proposé et validé après

comparaison de l'état des contraintes autour des tiges équivalentes, avec les résultats obtenus numériquement pour un modèle de vis axisymmétrique et détaillé. Le bon accord entre les résultats numériques et expérimentaux confirme la précision de la modélisation des tiges et des vis. Ces modèles vont ainsi pouvoir être utilisés dans de prochaines études sur la fixation d'implants.

Dans un dernier temps, le modèle 3-D par éléments finis de l'implant du genou a été développé afin d'étudier les mécanismes de transfert de charges et les mouvements microscopiques aux interfaces.

C'est pourquoi,

- la géométrie du tibia a été construite à partir de mesures effectuées sur le tibia droit d'un adulte de taille moyenne. Une plaque tibiale modulaire à surface poreuse avec deux configurations de fixation a été utilisée dans cette étude. Le CMM (Coordinate Measuring Machine) a été utilisé pour mesurer les surfaces articulaires des éléments fémoral et tibial. La génération de maillage a été exécutée par un programme de notre groupe de recherche. Un maillage plus raffiné a été pris en compte aux régions de contacts. Deux configurations différentes ont été utilisées, la première inclue une plaque tibiale avec trois vis (cancellous screw), la seconde possède une vis dans la région antérieure et deux petites tiges à surface poreuse inclinées postérieurement. A titre de comparaison un autre modèle à plaques tibiales à surface poreuse sans fixation reposant librement sur l'os a été utilisé. Le maillage inclus environ 10900 briques à huit nœuds et des éléments en forme de prisme triangulaire linéaire à six nœuds et un total de 14300 nœuds.

- Des études par éléments finis ont laissé supposer que l'effet d'anisotropie de l'os spongieux peut être négligé si son hétérogénéité est prise en compte. Ainsi, dans cette étude, un modèle linéaire, élastique, isotropique, mais hétérogène a été utilisé pour modéliser les propriétés du matériau spongieux et cortical. Suivant la région (20 régions au total), le

module d'élasticité pour l'os cancellous varie de 17 à 340 MPa. Le module d'élasticité pour l'os cortical est supposé augmenter de 1000 à 9800 MPa à partir de l'épiphyse jusqu'au diaphyse moyen. Un coefficient de Poisson de 0.3 est considéré aussi bien pour l'os spongieux que pour l'os cortical. Étant donné l'existence de dispersion dans les propriétés mécaniques du polyéthylène, des tests en tension ont été effectués à partir de ASTMD638-94B. Le module d'élasticité et la contrainte élastique ont respectivement été pris à 1083.0 et 13.00 MPa, tandis que le coefficient de Poisson était de 0.45. Un modèle de durcissement élastoplastique isotropique a été considéré pour le polyéthylène. Les éléments restant de la plaque fémorale et tibiale métallique sont modélisés par un matériau linéaire élastique de module d'élasticité de 220 GPa et de coefficient de Poisson de 0.3.

- L'interface entre l'os et la prothèse a été modélisée en utilisant les équations de bases développées pour des propriétés de friction non linéaire et bi-directionnelle. Les propriétés de friction à la surface polyéthylène/métal lisse ont également été mesurées et les variations du coefficient de friction avec pression de contact ont été aussi analysées pour des surfaces sèches et humides (avec une solution saline). Le coefficient de friction pour le contact sec était légèrement supérieur que celui du contact humide. Une analyse statistique révèle un effet significatif de la condition de contact et de la pression de contact sur le coefficient de friction. L'interface entre le polyéthylène et le condyle métallique fémoral était, ainsi, modélisé en utilisant un modèle de friction de Coulomb. Le coefficient de friction à l'interface a été pris égale à 0.045 pour une condition de surface humide. L'interface entre la plaque métallique et le polyéthylène inséré a été considérée fixe. Ceci est basé sur le mécanisme de blocage à l'interface qui permet la prévention du mouvement relatif.

- On a supposé la force de compression de trois fois le poids du corps (BW) à 2000 N. La force totale a été appliquée seulement sur le condyle fémoral médian pour simuler un

alignement variable. Le bout périphérique du tibia a été fixé dans toutes les directions.

Les résultats de la simulation par éléments finis montre que les déplacements prévus de la plaque sont cohérents avec ceux des précédentes études expérimentales et numériques. Les amplitudes de déplacement pour l'implant tibial varient en fonction de la conception prosthétique utilisée. Le déplacement dans la direction axiale (Z) a montré la faible dépendance sur la configuration de la fixation, particulièrement dans le plan A-P (sagittal). Les déplacements au nœud de l'interface os/implant étaient plus grands dans la direction X (M-L), i.e., environ de 160 à 200 μm, que dans la direction Y (A-P), d'environ 40 à 75 μm. Il a été trouvé que le déplacement à l'interface est plus grand à l'os qu'à l'implant. Le décollage de la région latérale mène à un espace entre l'os et l'implant réduisant ainsi la surface de contact effective et augmentant, à son tour, la pression de contact et donc un affaissement dans la région médiale opposée. La fixation utilisant des vis donne le plus petit décollage suivi par celle avec des tiges.

L'incompatibilité des déplacements entre l'os et l'implant à l'interface crée des micro-mouvements relatifs qui étaient plus grands dans la configuration sans fixation. Le design avec les vis, suivi de celui avec une vis et deux tiges amène à la réponse la plus rigide. Conformément aux autres études, le modèle de friction à l'interface influence de façon significative les micro-mouvements relatifs autant dans les directions M-L que A-P. Le frottement de Coulomb, tel que comparé avec le modèle de frottement non-linéaire, sous estime considérablement les micro-mouvements relatifs tangentiels. L'amplitude maximale d'un micro-mouvement pour un design de fixation avec vis et tiges, a été calculé numériquement pour rester sous les 28 μm, ce qui est compatible avec la croissance de l'os. Les mouvements relatifs excessifs peuvent diminuer la prolifération de l'os sur la surface poreuse de l'implant. Dans toutes les configurations de design, l'amplitude maximale du micro-mouvement est atteinte dans le périmètre de l'implant.

La contrainte de contact normale à l'interface entre l'os et l'implant varie en fonction du design. La contrainte de contact maximale à l'interface de l'os cancellous et de l'implant était de 2.81 MPa pour le design avec tiges et de 2.56 MPa pour celui avec des vis, calculée à la limite médiale adjacente à la surface supportant la charge. Le design avec des vis et tiges amène des contraintes de contact à l'interface plus faibles, ceci est dû à la transmission partielle de la charge de compression appliquée via les forces de cisaillement à travers les interfaces verticales entre l'os et les tiges/vis. Dans le design avec fixation par vis, 23 % de la charge axiale a été transmise par des vis comparée à 7 % dans un design de fixation avec des tiges. Une augmentation de l'interférence à l'interface pourrait augmenter les proportions susmentionnées. Mis à part les vis et les tiges la force totale supportée par l'os cancellous (avec une surface de contact totale d'environ 2050.0 mm^2) et un os cortical (avec une surface de contact de 16.0 mm^2) varie respectivement de 65 à 86 % et de 11 à 13 % de la force axiale totale, et dont les plus petits pourcentages sont obtenus numériquement pour le design à trois vis. De plus grandes pressions de contact sont prévues avec un os cortical. Les contraintes sous le plateau au niveau des surfaces vis/tiges sont plus faibles avec des fixations que sans.

Un autre problème majeur avec le remplacement du genou est l'usure du polyéthylène qui peut causer la fracture de composants et le l'ostéolyse périprosthétique. Des facteurs comme le poids du patient, le sexe, le niveau d'activité et l'âge peuvent jouer un rôle dans l'usure du polyéthylène. Il a été trouvé que l'amplitude prédite de la pression de contact normale (48.0 MPa) est bien au-dessus de la contrainte de l'écoulement (13.0 MPa). La contrainte de Mises maximale à la plaque de polyéthylène devait arriver en dessous de la surface de contact, pour laquelle l'emplacement avait été trouvé indépendant du design de la fixation. Il a été aussi démontré que l'amplitude de la contrainte de Mises maximale est indépendante de la configuration de la fixation. Il est apparu, par conséquent, que la modélisation idéale de l'interface plaque/os n'était pas aussi fondamentale si on s'intéresse de façon primordiale au calcul des contraintes sur le polyéthylène. Les résultats

pourraient également être modifiés pour des insertions de polyéthylène plus minces que 7 mm. Les contraintes sur le polyéthylène dépendent entre autre de son épaisseur et de sa conformité. L'épaisseur recommandée est alors d'au moins 6 à 8 mm.

Basé sur les résultats des études par éléments finis, le rôle important de la friction et des vis/tiges sur la stabilité de la fixation a été démontrée. Il a été recommandé qu'un nombre croissant de vis et de tiges et d'une localisation de ceux-ci dans le périmètre de design peut réduire les micro-mouvements. En utilisant des surfaces poreuses avec des grands coefficients de friction on peut aussi augmenter la force de cisaillement à l'interface ce qui assurera une fixation plus rigide.

En conclusion, les résultats de ce travail peuvent être résumés comme suit :

- Les résultats en pure contrainte de tension du polyéthylène montrent une déformation plastique significative sous contrainte faible. Le module et la contrainte de l'écoulement mesurées sont respectivement de 1083.0 et de 13.0 MPa,
- le coefficient de friction mesuré à l'interface métal/polyéthylène varie, respectivement, pour des surfaces sèches et humides de 0.05 à 0.10 et de 0.04 à 0.08,
- le coefficient de friction à l'interface polyéthylène/métal diminue lorsque la pression de contact augmente,
- le coefficient de friction mesuré, à l'interface entre l'os et le métal à surface poreuse, à l'aide de tests de friction bi-directionnels sont identiques à ceux obtenus par des tests de friction uni-directionnels,
- les tests en friction bi-directionnels, l'interface os/polyuréthane et métal à surface poreuse, laissent supposer la présence de couplage entre deux directions perpendiculaires,
- l'augmentation de l'angle d'inclinaison pour les tests en arrachement influence d'autant plus le comportement de la vis et de la tige poreuses,

- la friction de Coulomb sous-estime les mouvements microscopiques prévus et la friction non linéaire devrait être prise en compte dans l'analyse de l'implant du genou,
- le design de la fixation avec des vis suivi du design de la fixation avec des tiges réduit considérablement les mouvements microscopiques et le décollage,
- le mouvement microscopique maximum a été obtenu dans le périmètre de l'implant pour toutes les configurations,
- approximativement 10 à 13 % de la charge axiale totale est supportée par l'os cortical, alors que l'os cancellous transfert 65 à 85 % suivant la fixation avec la partie qui reste, transmise par les vis et les tiges,
- les contraintes du polyéthylène sont indépendantes de la configuration du design et du modèle de friction, et
- la contrainte de Mises maximale apparaît à 1-2 mm sous la surface de contact avec le polyéthylène, alors que la contrainte normale maximale était prévue à la surface de contact.

TABLE OF CONTENTS

LIST OF TABLES

LIST OF FIGURES

LIST OF APPENDICES

CHAPTER 1
INTRODUCTION

1.1 GENERAL

Over the past three decades, total joint arthroplasty has become an increasingly effective means of reducing the pain associated with arthritis. The number of total joint replacements, particularly, hip and knee arthroplasty has grown significantly with clinical success rate over 80%, a trend that is expected to continue with the aging population of the western societies. It was reported that more than 400,000 knee and hip arthroplasties are performed in the United States every year, alone (Praemer, et al. 1992). The knee joint is an unconstrained joint that is subject to loads up to several times body weight during the normal human activities. The greatest challenge in the knee arthroplasty is adequate fixation of implant to the tibia. Problems, like sepsis of surrounding tissues, loosening, polyethylene wear, and fracture of metallic components (Moreland, 1988) have been observed.

Two distinct types of implants, i.e., cemented (Figure 1.1) and uncemented implants (Figure 1.2), are currently used in the knee arthroplasty. While in cemented implants (Figure 1.3), the cement is used as the bonding agent between the prosthetic components and the bone, in cementless implants the prosthesis is in direct contact with the host bone. Many researchers have pointed to potential disadvantages of cement, including limited fatigue life, accelerated polyethylene wear and bone loss (Jones and Hungerford, 1987). The long-term studies have revealed that the major mode

of failure of total knee replacement is mechanical loosening at the bone-implant interface. To provide a more stable construct in long-term, fixation of the porous coated implants to the bone by the biological fixation has been proposed. The short-term fixation in cementless implants are achieved by the screws/posts. The porous coating is employed to promote bone ingrowth and, hence, a biologic attachment of the artificial joint to the host bone. The long-term success of the operation depends, therefore, on the achievement of such biologic integration (Peters and Rosenberg, 1995). Although using the bone cement is very successful in maintaining the initial fixation by cement polymerization, but the concern about the long-term durability and adverse histologic response to the cement has persisted. Due to this limitation, cementless fixation of total knee replacement has been advocated, particularly in younger patients. It has been shown that adequate initial fixation is needed to promote bone ingrowth. Successful total knee replacement requires a complete understanding of the biomechanics of the knee, an analysis of the nature and magnitude of the stresses created by knee replacement, and exploration of new prosthetic materials and methods of fixation (screws vs posts, number, size and location of screw/posts, . . .). Finite element methods along with experimental techniques have been used to study the mechanics of the knee-implant system.

Many parameters are known to influence the biological ingrowth and the fixation stability, such as:

- Pore size: The optimal pore size for bone ingrowth has been reported to vary between 100 μm and 400 μm (Bobyn et al., 1980; Finlay et al., 1989).
- Interface motion: Excessive interface motion has been demonstrated to have a deleterious effect on bone ingrowth into porous surfaces. Pilliar et al. have shown bone ingrowth with relative displacements of less than 28 μm but fibrous fixation with 150 μm or more of motion (Pilliar, et al., 1986). Excessive relative motions at the bone-porous coated metal interface are generally recognized as a factor which decreases bone proliferation into surface pores of implants (Cameron et al., 1973; Ducheyne et al., 1977).

- Intimate contact: Gaps at the bone-porous surface interface are known to decrease the volume fraction and progression or extension of bone ingrowth (Sumner and Turner, 1991). Intimate contact between the porous coating and the bone has been identified to increase the amount of bone ingrowth in both human and animal models (Kienapfel et al., 1992; Turner et al., 1986).
- Wear particulate debris of constituent materials (polyethylene, metal, . . .) have been associated with the bone loss (i.e., osteolysis) and, hence, implant failure (Engh et al., 1992; Jones et al., 1992).
- Implant surface treatments, graft materials and electrical stimulation are some methods of enhancing bone ingrowth (Sumner and Galante, 1990; Sumner and Turner, 1991).

The other most common problem related to the knee replacement is the failure of ultra high molecular weight polyethylene (UHMWPE). Wear debris of polyethylene results in periprosthetic osteolysis and loosening (Kilgus, et al. 1991; Nolan et al.,1992; Rose et al., 1984). The polyethylene failure has been reported in many retrieval analyses of failed prostheses in different modes, i.e., pitting, delamination, scratching, surface cracking and abrasion (Collier et al, 1991; Kilgus et al, 1991; Mintz et al., 1991; Wright and Bartel, 1986). The following factors are reported to affect the wear resistance of polyethylene:

- Quality of polyethylene (Tanner, et al., 1995; Walker, et al., 1996),
- Manufacturing processes (Jones et al, 1992; Pruitt et al., 1997),
- Sterilization methods (Bell, et al., 1997; Deng and Shalaby, 1995; Polineni, et al., 1997).

1.2 Knee joint biomechanics

In this section a brief description of the anatomy and stability of the knee joint is presented. Mechanisms of load transfer at the knee joint and knee implant characteristics are given, as well.

1.2.1 Anatomy of the knee

The largest joint in the body is the knee joint. It is formed by two of the largest bones, the femur and the tibia. Figure 1.4 illustrates the constituents of the knee joint, i.e., femur, tibia, patella, menisci, cartilage, ligaments and capsule. In the tibiofemoral articulation, the medial and lateral condyles of the femur are separated from the condyles of the tibia by two wedge-shaped cartilaginous discs called menisci (Figure 1.4). The medial meniscus is bound to the fibrous capsule and the lateral meniscus is separated from the capsule by the tendon of the popliteus muscle (Figure 1.5). This muscle medially rotates the tibia if the foot is off the ground, or it laterally rotates the femur when the leg is on the ground bearing the body's weight. The capsule is a thin and strong fibrous tissue which covers the knee joint. Two cruciate ligaments, crossing each other like the arms of an X, provide the stability to the joint. While the posterior cruciate ligament (PCL) is connected to the medial femoral condyle, the anterior cruciate ligament (ACL) is connected to the lateral femoral condyle (Figure 1.5A). These cruciate ligaments are the internal ligaments of the joint while the lateral and medial ligaments are the external ligaments. The lateral ligament is connected to the head of fibula.

Figure 1.5B shows the medial and lateral cartilaginous discs (menisci) resting on the condyles of the tibia. The larger disc is the medial one. The discs are connected to the tibia by their pointed ends (horns). The condyles of the femur are in contact with the discs. The menisci act as a shock absorber during the daily activities. Other functions of menisci include, distribution of load, lubrication and limitation of slip of one bone with respect to another. The second articulation in the knee joint occurs between the femur and patella (kneecap) known as pattelofemoral. The patella connects to the extensor muscles while the patellar ligament extends from the patella to the tibia. The tibia the second longest bone in the human body articulates at its distal end with the talus of the ankle and at its proximal end with the femur. The tibia tissue like any long bone has been classified

into two categories based on porosity. The bone (tibia) walls are made of hard, dense bone called cortical (compact) bone and inside of the cylinder is filled with less dense and hard but relatively light in weight called the cancellous bone. The strongest cancellous bone is immediately under the tibial condyles known as the subchondral bone.

1.2.2 Stability of the knee

The stability at every joint (i.e., hip, knee, ...) is maintained through three mechanisms; cartilage and bony geometry (articulating bones), muscular action, and ligamentous resistance. Contribution of each mechanism depends on the function of the joint. For example in hip joint, ligaments play a small role and muscle tension in almost every plane is required to balance the joint. In the knee joint, the bone configuration is not particularly stable (contrary to the hip) and the tensions in ligaments and muscles contribute significantly to joint stability. If these tissues are weak from disuse or lax from being overstretched, the stability of joint is reduced. Flexion-extension, abduction-adduction and internal-external rotation occur simultaneously around three axes of rotation which are not fixed. Motion can be rotational as well as translational. To allow motion in certain directions, ligaments play a larger role here than at the hip. The muscles are needed not only to control the speed of motions, particularly when high torques are present (bending, jumping, ...), but also to change the lever arms to optimize the counteracting torques they can develop (Figure 1.6). Depending on the motion specified, the role of each mechanism varies. Figure 1.7 presents the case when the medial-lateral translational motion in frontal plane of the knee is limited by the tibial spines.

1.2.3 Knee joint forces

The joint force at the knee can be resolved into three components, i.e., the anterior-posterior, the

axial, and the medio-lateral components. The anterior-posterior force in the knee joint is primarily carried by the cruciate ligaments. The medial-lateral component is a shear force carried by articulating surfaces and ligaments. This component is relatively small compared to the axial component. The axial component is a compressive force also carried by articulating surfaces. The forces of functional activity to which knees are subjected are of considerable magnitudes. Morrison (1970) estimated that peak force in the knee joint can exceed several times body weight during the daily activity (Harrington, 1990; Kluster et al., 1997; Taylor et al., 1997).

1.2.4 knee prosthesis

Replacement of a damaged joint with an artificial implant considerably alters the nature and distribution of stress in the system. Serious mechanical problems (loosening, polyethylene wear, fracture of implant components, . . .) can occur due to these changes, which can cause the failure of the implant or severe biological response. The normal joint operates within a low frictional resistance and maintain a maximum contact area under the most conditions. This is accomplished due to deformity of the both articulating bearing surfaces and their underlying bone. The lubrication mechanisms of metal on plastic bearing surfaces do not resemble that in the normal joint. Total joint replacement has higher friction resistance and employs materials which are stiffer than living tissues. The difference in stiffness between implant and bone causes relative micromotion and shear stresses at the bone-implant (baseplate) and bone-cement interfaces in cementless and cemented implants, respectively. Investigators have compared the short- and long-term performance of both types of currently used implants (Collins et al., 1991; Dodd et al., 1990; Hungerford and Krackow, 1985; Rand, 1991). In general, in-vivo examinations have suggested that clinical and functional performances of cementless prostheses are as good as those of uncemented prostheses. Using the bone cement is reported to be satisfactory in providing the initial fixation. However, the long-term performance of cemented implants in younger patients are of the main concern. Cementless fixation

of total knee arthroplasty has been devised as an alternative to cement fixation in more active patients.

1.3 Literature survey

In this section, the published studies related to initial fixation and stability of cementless knee implants in postoperative period are introduced. Many research areas, such as, mechanical model of the bone, friction characteristics of the bone-implant interfaces and pullout behavior of posts and screws are among the research topics that are associated with the study of knee-implant structure. Other included areas are in-vivo and in-vitro studies of the knee-implant, wear characteristics of the polyethylene and fracture mechanics. Here, a concise review of related studies is presented.

1.3.1 Friction properties at the bone-implant interface

In the postoperative period, the friction between implant and cancellous bone is one of the mechanisms for the transfer of shear load at the interface. To study the relative significance of friction in the joint mechanics, uni-directional friction properties at the interface between tibial cancellous bone and a number of metal plates (two beaded porous surfaces, a fiber mesh porous surface, and a smooth surface) have previously been measured under single and repetitive fatigue loading (Rancourt et al., 1990; Shirazi-Adl et al., 1993). The friction coefficient noticeably increased for the porous coated metal plates as compared with the smooth one, whereas it remained unchanged with the bone excision site on the proximal tibia, magnitude of normal stress, type of porous coated plates considered, rate of displacement, and duration of conservation in saline solution. Moreover, in contrast to the idealized Coulomb's friction, the tangential load-displacement at the interface was found to be highly nonlinear in which relatively large tangential displacements of 50-400 μm were recorded at the maximum resistance load. The range

of friction coefficient was found to be between 0.3 to 0.9 Rancourt et al. (1990) and 0.4 to 0.66, Shirazi-Adl et al. (1993).

In a study on the influence of bone density on the friction properties of porous surfaced metallic plate on femoral bone (Ploetz, 1992), it was found that friction coefficient changed with the bone density. The friction coefficient was measured to vary from 0.43 to 0.72. In the most recent study, friction properties of four distinct metal surfaces (one beaded porous metal and three cast co-cr alloy ingrowth mesh surfaces) on cancellous bone specimens were measured (Dammak et al.,1997b). The range of friction coefficient was found to vary between 0.65 to 0.70 for beaded porous metal and 0.70 to 1.00 for mesh surfaces (Dammak et al., 1997b).

The foregoing experimental studies (Dammak et al., 1997b; Rancourt et al., 1990; Shirazi-Adl et al., 1993), however, treated the friction between bone and implant only in one direction. In a three dimensional contact problem, the articulating bodies could undergo relative movements and develop shear forces in different directions on the common interface. These directions could also change during the course of deformation. The results of these uniaxial studies should not, therefore, be directly implemented in 3-D FE model of knee-implants if accurate results are expected.

1.3.2 Pull-out tests

Experimental studies: To determine the parameters affecting fixation behavior of screws and posts, pull-out tests have been performed. Finlay et al. (1989) measured the pull-out force of 3.8-mm and 6.5-mm diameter cancellous screws and a 10 mm diameter peg implanted in bovine vertebral cancellous bone and two different grades of polyurethane. For the same depth of insertion, it was found that the pull-out force of a 6.5-mm diameter screw was two times larger than that of a 3.8-mm diameter screw. Both screws performed better than the peg. The pull-out force of screw

exhibited a linear relationship with the shear strength of the material into which it was inserted. The pull-out force of a peg had a linear relationship with the modulus of elasticity of the material into which they were inserted. Dependence of pull-out force on diameter of drill size, the length of insertion, and the material properties was also shown.

George et al. (1991) measured the effect of hole preparation technique for transpedicle screws on pull-out strength in human cadaveric vertebrae. No significant difference was found in pull-out strength between screws implanted into drilled holes and those implanted into probed holes. King and Cebone (1993) investigated the effect of lateral force on the pull-out load and elastic stiffness of screws inserted in bone. It was found that pull-out force of screws decreased steadily with lateral load whereas the elastic stiffness remained relatively independent of the lateral load.

Shirazi-Adl et al. (1994) measured the response of screws and porous/smooth-surfaced posts inserted in the proximal tibial cancellous bone and polyurethane cylinders. They found that the pull-out force was significantly larger when screws and posts were inserted in the medial region of the proximal tibia followed by the lateral region. This was argued to be due to the difference in elastic modulus of the bone at these regions. The central region resulted in the least pull-out force due to its lower elastic modulus. Smooth surfaced posts showed superior performance in both static and fatigue loadings than did porous coated posts. Boundary conditions used in the pull-out tests configuration were also found to affect the pull-out force.

The abovementioned experimental studies considered the influence of many parameters on the pull-out resistance but none investigated the effect of shear force on the pull-out force of porous/smooth-surfaced posts.

FE studies: There are also a few numerical studies of the pull-out tests in the literature. The pull-out

analysis of a metallic stem and the surrounding PMMA bone cement was performed (Mann et al., 1991) using a nonlinear, axisymmetric FE model study assuming an idealized Coulomb friction at the interface. The results of this study showed a good agreement with experiments for one full cycle of axial loading-unloading. In an axisymmetric FE analysis accounting for the measured nonlinear interface friction properties, it was found that the maximum resistance force and interface stresses are highly dependent on the relative material properties, boundary conditions, and the direction of the applied load (push-out versus pull-out) (Shirazi-Adl and Forcione, 1992).

Axisymmetric FE model of pull-out tests using the measured nonlinear interface friction properties and its equivalent idealized Coulomb's friction indicated that the use of measured nonlinear curve yielded results comparable with measurements and showed that the Coulomb friction could not accurately predict the measured displacements. In agreement with experiments (Shirazi-Adl et al., 1994), smooth-surfaced posts were found to have superior fixation performance when compared to porous coated ones (Dammak et al., 1997a). This is due to larger effective interferences for smooth-surfaced posts that cause greater normal stresses at the interface.

The parameters affecting fixation behavior of screws and posts have been investigated using both experimental and FE model study of pull-out tests. It has been found that pull-out force of screws is larger than that of posts. Moreover, pull-out force of smooth surfaced posts is larger than that of porous surfaced posts with the same dimensions. However, smooth surfaced posts demonstrate better performance in fatigue loading than do the screws and porous-surfaced posts. The mechanism of load transfer from the post to the polyurethane has also been determined from the analyses of FE results. The maximum resistance force is dependent on the relative material properties, boundary conditions and interface friction characteristics. The screws and posts in an implant under external loads are, however, subjected to horizontal loads in addition to the axial load. Consideration of such inclined loads is essential for realistic biomechanical analysis of

screw/post fixation systems.

1.3.3 Effect of screws and pegs on the initial fixation of tibial components

Initial fixation of tibial components remains a problem in uncemented total knee arthroplasties. To investigate the effect of screws and sleeves on the liftoff (i.e., normal separation of implant from the bone), sinking and micromotion of implants, Miura et al. (1991) performed experiments and found that screws were effective in controlling micromovements under axial and shear loadings. Liftoff was reduced by more than 90% in presence of screws. It was suggested that the main effect of the screws is to prevent liftoff. Screws also ensured initial contact between bone and implant. Use of a sleeve alone was also effective in preventing liftoff and subsidence under axial loads but to a lesser degree than the screws. Micromotion under axial loading was not, however, markedly affected by the use of screws or sleeves. A similar study performed on canine cementless implants by Sumner et al. (1994) concluded that the components secured with screws undergo up to fivefold reductions in interface motions compared to those fixed with pegs. The addition of pegs did not further increase the stability of the tibial components in the presence of screw fixation.

Biomechanical studies have clearly shown that tibial components, when fixed to the bone with only short pegs, subside on the loaded side and liftoff on the opposite unloaded side. The effectiveness of screw and stem were also shown in the study of Volz et al. (1988). Bourne and Finlay (1986) found that removing the tibial component-cortex contact decreased the cortical strains by 33%-60% immediately under the tibial component. The results of this study demonstrated stress shielding along the entire length of the intramedullary stem causing cortical resorption of proximal tibia in long-term. Therefore, they suggested the use of tibial components with implant-cortex contact, and discouraged the use of implants with any, particularly long, intramedullary stems.

Investigations of Wyatt et al. (1991) indicated that the initial rigidity of tibial implants with screw fixation is dependent on the bone quality, type of bone purchase, and number, and position of screws. Long cancellous screws and screws with cortical purchase consistently allowed less than 150 microns (reported to be necessary to allow bone ingrowth into a porous implant) motion at the tibial baseplate interface. In this study (Wyatt et al., 1991), four short screws placed on the periphery allowed less micromotion than the three-short-screw or two-short-screw configurations, an observation in agreement with results of Lee et al. (1991). The fixation superiority of screws has been demonstrated by other researchers as well (Dammak et al., 1997a; Kaiser and Whiteside, 1990).

The aforementioned studies clearly suggest the superior performance of screws when compared to pegs and sleeves in preventing liftoff. Screws also ensure initial contact between bone and implant and limit interface micromotion. Increasing the number of screws is stated to further reduce the micromotion, as well.

1.3.4 Polyethylene failure

Another problem observed in the total knee replacement is the wear of ultra high molecular weight polyethylene (UHMWPE) which can result in migration of polyethylene fragments into the body and can cause malfunction of the implant. Polyethylene debris can cause scarring, periprosthetic osteolysis, and loosening (Nolan and Bucknill, 1992; Wright and Bartel, 1986; Rose et al., 1984; Kilgus et al., 1991; Jones et al., 1992). A number of factors play a role in the wear of polyethylene tibial components. Quality of polyethylene (Tanner et al., 1995; Whiteside and White, 1995), manufacturing processes (Jones et al., 1992; Pruitt et al., 1997) and sterilization methods (Bell et al., 1997; Deng and Shalaby, 1995; Polineni et al., 1997) can influence the wear resistance of polyethylene. The importance of polyethylene thickness and geometry of the articular surfaces has

also been shown by both experimental and numerical studies (Bartel et al, 1995; Blunn et al., 1991; Chillag and Barth, 1991; Collier et al., 1991; DeHeer and Hillberry, 1992; Engh et al, 1992; Ishikawa et al., 1996; Landy and Walker, 1985; Mintz et al., 1991; Rose et al., 1984; Sathasivam and Walker, 1997). These studies recommend the use of polyethylene greater than 6-8 mm for nonconforming surfaces. The more conforming articular geometry between the femoral and tibial components has been suggested, as well. Nonconforming designs result in low contact areas causing high contact stresses which exceed the yield stress of polyethylene. In a retrieval analysis of 48 total condylar prostheses, significant positive correlations were reported (Hood et al., 1983) for the surface damage correlated with the patient's weight and the time the prosthesis was implanted. This is known as the evidence that fatigue and cyclic loading are the cause of damage. Hood et al. (1983) identified seven modes of surface degradation, among which pitting and delamination have been reported by researchers (Collier et al., 1991; Landy and Walker, 1985; Mintz et al., 1991; Rose et al., 1984; Wright and Bartel, 1986) as the most severe damage mode in polyethylene components.

Fracture mechanic studies are used to investigate the wear mechanisms in the polyethylene components. Wear initiation is due to high contact stresses and fatigue cracks in polyethylene. It is believed that pitting and delamination result from a fatigue fracture mechanism (Heck et al., 1992; Landy and Walker, 1985; Rose et al., 1984). Pitting occurs when crack initiates at the surface and propagates at or below the surface. High axial compressive stresses at the contact point which reach material yield point can cause fracture. Once a surface crack has initiated, it can propagate in different modes (Keer et al., 1982; Keer and Bryant, 1983; Murakami et al, 1985). Delamination also takes place when a subsurface fatigue crack propagates parallel to the contact surface. In this failure mode, a layer of material peels away from the surface and creates voids. Researchers (Jahanmir and Suh, 1977) have found that microvoids in the material can initiate a fatigue crack below the contact surface. Using the linear elastic fracture mechanics, it was shown

(Fleming and Suh, 1977) that a subsurface crack can propagate parallel to the surface for a given loading condition and friction coefficient. Cyclic shear stresses below the contact surface was blamed as the main parameter promoting crack propagation resulting in delamination (Fleming and Suh, 1977; Sheppard et al., 1985; Wright and Bartel, 1986).

The studies have shown that pitting and delamination resulting from tibio-femoral contact stresses are the main causes of implant failure. The studies revealed that high normal contact stress and subsurface shear stress are the most critical parameters in the initiation and propagation of fatigue cracks. The use of more conforming articulating surfaces and thicker polyethylene components and improved quality of polyethylene and manufacturing method were reported to reduce the wear. The finite element studies performed to evaluate the contact stresses at the polyethylene-femoral component were initially limited to 2D or (half) symmetric 3D models which do not reflect the observed stress distribution. Despite the recent 3D finite element models, the influence of including the whole implant (e.g., tibial tray, resurfaced tibia, implant fixation design configurations) on computed stresses has not been determined.

Many experimental and numerical studies have been performed to quantify the stresses recognized as the cause of the polyethylene failure (Bartel et al., 1986; Bartel et al., 1995; Blunn et al., 1991; Rose et al.; Walker et al., 1996). However, the likely coupling between the articular plate and prosthesis-bone structure as particularly related to polyethylene stresses and interface motions have been overlooked. Therefore, new investigations should study the mentioned coupling by developing a detailed 3D finite element model of the bone-implant structure including all the interacting components. The synergy between micromotion and polyethylene debris in implant response has been suggested in recent studies (Bechtold et al., 1997).

1.3.5 Numerical analysis of knee prostheses

The FE method of structural analysis has long been established as a tool in orthopaedic biomechanics. Huiskes and Chao (1983) reported the detailed earlier developments and applications of FE methods in orthopedic biomechanics. Two dimensional (2-D) (Askew and Lewis, 1981; Beaupre et al., 1986; Lewis et al., 1982; Rakotomanana et al., 1992; Vasu et al., 1986), axisymmetric (Ahmed et al., 1990; Dawson and Bartel, 1992: Murase et al., 1990; Shirazi-Adl and Ahmed, 1989) and three dimensional (3-D) (Cheal et al., 1985; Keja et al., 1994; Rakotomanana et al., 1994, Strickland et al., 1989; Tissakht et al., 1995) FE models have been employed to investigate the fixation influence of different design parameters in total knee replacements.

Using a 2-D FE model of a metal tibial prosthetic component with a single post implanted with PMMA (polymethylmethacrylate) bone cement, Askew and Lewis (1981) found that in the absence of the cortical shell, the axial load is carried mainly near the post tip, particularly for the longest post. It was suggested that if the nonhomogeneity in the bone is correctly taken into account, the effect of the bone anisotropy is negligible. In agreement with this study, Cheal et al. (1985) reported that heterogeneous material properties of bone exert a more pronounced influence on local stresses than the material anisotropy. In an axisymmetric model with nonhomogeneous trabecular bone properties and 3-D (nonaxisymmetric) loading, Murase et al. (1983) showed that post length, post rigidity, and bone rigidity affected stress distribution in the bone. Use of a wider metal tibial component was recommended to reduce maximum stress in the underlying bone.

In two separate studies, stress analyses in the frontal plane and sagittal plane were conducted using 2-D equivalent-thickness FE models (Beaupre et al., 1986; Vasu et al., 1986). Equivalent-thickness models accounted for the out-of-plane thickness and material properties. The interface

conditions existing between bone and metal tray simulated bony ingrowth with the continuity assumed at the interface between implant and bone. Four different tibial plateau components along with bi-condylar and uni-condylar axial forces were considered. It was found that two-piece designs with separate components for each condyle have lower interface tensile stress than do continuous, one-piece designs. The shape of the epiphyseal plate was suggested to be used as a guideline for prosthetic design.

A parametric axisymmetric FE model study on the interface motions in porous-surfaced tibial implants (Shirazi-Adl and Ahmed, 1989) showed that the presence of both a circumferential metal flange and a more rigid prosthesis design reduced the relative interface motions. The interface was assumed frictionless in this study. In the similar study using measured nonlinear friction properties at the interface (Forcione and Shirazi-Adl, 1990), relative motions at the horizontal interface was reduced by 10%. The effect of interference fit between the peg and the bone was studied by Dawson and Bartel (1992). They used a linear elastic, axisymmetric FE model to explain observed long-term patterns of growth of bone into tibial components. Interface between bone and metal plate was modeled using a layer of elements with different elastic modulus to represent fibrous tissue or bony ingrowth. It was revealed that the interference fit results in larger residual stresses perpendicular to the bone-implant interface in the bone near the fixation peg. These stresses were suggested to be favorable for ingrowth of bone into the peg. The interference fit relieved stresses in the bone under the tray of the implant. Lack of these stresses in addition to an increase of relative motion were believed to be responsible for growth of fibrous tissue.

In a 2-D comparative study of the cemented metal tray total condylar (MTTC) and the noncemented Porous Coated Anatomic (PCA) tibial plateaus (Rakotomanana et al., 1992), debonding of the bone-peg interface was observed for the PCA. The stress peaks at the interface beneath the tray were found lower for the PCA than for the MTTC due to the PCA deformability.

In a later 3-D study by the same authors (Rakotomanana et al., 1992), Coulomb's friction at the interface between bone and implant was used to compare the PCA and MTTC implants. Keja et al. (1994) assessed the effect of perimeter fixation versus midcondylar pin fixation and the effect of plate thickness and plate stiffness by a 3-D FE model study. In this study, the interface was modeled using frictionless interface elements to yield the maximum micromotion, the bone as a heterogeneous material and pegs as a rigid area at the appropriate peg locations of the model. Under the axial loading, the component with perimeter fixation provided better resistance to reversible relative motion than that with peg fixation. The Poisson's ratio and in-plane stiffness of the prosthesis slightly influenced the relative reversible motion. It was suggested to use a prosthesis with higher in-plane stiffness when it is possible. Tissakht et al., (1996) in a 3-D FE study of total tibial component showed that screw fixation design yielded the minimum relative micromotion. The micromotion predicted (maximum 8 μm) in this study was in the range (28 μm) reported to be required for the bone ingrowth (Pilliar et al., 1986).

Apart from a few studies (Keja et al., 1994; Rakotomanana et al., 1994; Tissakht et al., 1995), the previous models were based on idealized 2-D or axisymmetric geometries. In view of the irregular bone geometry and material distribution, a 3-D representation appears necessary. Furthermore, FE studies considered the bone-implant interface frictionless (Keja et al., 1994; Shirazi-Adl and Ahmed, 1989) to represent no bony ingrowth or fixed (Beaupre et al., 1986; Cheal et al., 1985; Vasu et al., 1986) for either a complete bony ingrowth or a cemented (Askew and Lewis, 1981; Murase et al., 1983) implant. Idealized Coulomb's frictional model has also been employed (Dawson and Bartel, 1992; Rakotomanana et al., 1994; Tissakht et al., 1995). Recently, measurement-based uni-directional nonlinear friction (Dammak et al., 1997b) was demonstrated in a pull-out study to substantially improve predictions. No 3-D studies has yet been found to employ a nonlinear friction that exists at the interface between bone and implant. Some 3-D models have used computerized axial tomography to obtain the geometry of the proximal tibia and

associated mechanical properties, while, the published mechanical properties of bone using compression tests (Goldstein et al., 1983; Keaveny et al., 1983) have been incorporated in the others. Based on the above discussions, the limitations of the previous FE studies can be summarized as:

- Previous models have often been based on idealized 2D or axisymmetric geometries. Due to irregular bone and implant geometries, loading and nonhomogeneous material distribution, a 3D representation is necessary.
- Previous studies, simulated the bone-prosthesis interface as frictionless, as perfectly bonded or with idealized Coulomb's friction. No 3D study of bone-implant structure has yet employed nonlinear friction properties measured at the interface between bone and various porous-surfaced implants.
- In addition, finite element studies of bone-implant system have neglected to present an adequate model of posts and screws (with the exception of Dammak et al., 1997a simulating plate fixation on polyethylene blocks).
- Furthermore, the coupling effect of bone-implant modeling on the polyethylene stresses has been overlooked.

1.4 OBJECTIVES

The main objective of this study was to develop a finite element model of the knee-implant structure to investigate the influence of different design configurations and friction models on mechanical fixation stability under static loading. The micromotion at the knee-implant interface and stress distribution within the bone and polyethylene were studied, as well.

Due to the fact that the knee-implant experiences a two dimensional motion at the common interface bi-directional friction properties between bone and porous coated metal plate needed to

be investigated. To study bi-directional friction properties, test apparatus used earlier for uni-directional friction tests (Shirazi-Adl et al., 1993) was modified to allow simultaneous measurements of tangential force and displacements at two perpendicular directions. Proper constitutive relations were developed which accounted for the coupling terms between perpendicular directions. The foregoing nonlinear interface constitutive relations were, then, implemented in the finite element model studies of the bi-directional friction tests to further validate the developed equations and to identify the influence of coupling terms on results. The mentioned experimental/finite element investigations were repeated for the polyurethane cubes replacing cancellous bone specimens to also study the nonlinear coupled characteristics of such interfaces in bi-directional friction.

Pull-out tests were performed to determine the effect of different parameters on pull-out response. Since in a knee prosthesis system, posts/screws undergo shear force as well as axial force, the effect of load inclination on pull-out response was investigated through experimental and FE methods. In the 3-D FE model of inclined pull-out tests, bi-directional friction constitutive equations were used to accurately model the interface between polyurethane and posts/screws. The predicted results were compared to experimental results in order to validate the FE model.

Subsequently, the 3-D FE model of knee implant was developed to investigate the mechanisms of load transfer and relative micromotion at the interfaces. For this purpose, geometry of the tibia and components of the implant were obtained by direct measurement or using coordinate measuring machine (CMM). The mechanical properties of tibial trabecular bone have already been reported, using compression tests (Goldstein, 1983; Keaveny et al., 1994) ultrasonic techniques (Ashman et al., 1989) and quantitative computed tomography (Bentzen et al., 1987; Hvid et al., 1989). A linear elastic isotropic and heterogenous model was considered in the model based on the properties published in the literature. Mechanical properties of the polyethylene was measured and

compared to that in the literature. Then an elasto-plastic isotropic hardening model was considered for the articular polyethylene insert. Interface between bone and implant was modeled using the developed constitutive equations for bi-directional friction properties. The interface between polyethylene and metallic femoral condyle was modeled using Coulomb's friction model based on the measurements. An appropriate model of posts/screws was also considered in these models to present the real conditions. To simulate a case with a significant varus misalignment, a load of approximately three times body weight was applied at the medial condyle.

Since knee-implant systems undergo cyclic loading, fatigue analysis will be required to simulate daily conditions. To initiate a study on the effect of load cycle on the knee-implant system, the interface friction properties and pull out responses were investigated under cyclic conditions. For this purpose, a few cycle of friction tests and axial pull-out tests were performed and proper FE models were also developed and validated. The fatigue performance of the interface between the bone and the porous- and smooth- surfaced metallic plate, which is assigned and validated in pull-out models, could be used in the FE study of tibial knee implants to predict the permanent migration of the implant over the long term period (Ryd et al., 1988; Ryd et al., 1993).

1.5 ORGANIZATION OF THE THESIS

This dissertation was prepared based on the articles which consists the main body of the thesis. Chapter 1 provides the clinical problem associated with the total knee arthroplasty and a short description on the anatomy of the knee. The critical review of literature is also presented in this chapter. Chapter 2 presents the work performed to measure bi-directional friction properties at the bone-porous-coated metal plate and to develop proper constitutive equations required for the FE simulations of surfaces with nonlinear isotropic friction properties. This work was published in the Journal of Biomedical and Material Research (Applied Biomaterial).

Chapter 3 presents the experimental tests and 3-D finite element study of pull-out tests. The aim of this study was to evaluate the 3-D FE model presentation of pull-out tests by applying an inclined pull-out force. The pull-out finite element model validated during this work was used in the final paper presented in the next chapter. This work was issued in the proceedings of the "1996 Engineering Systems Design and Analysis (ESDA)" conference.

Chapter 4 presents the developed FE model of knee-implant structure. This study employed the outcome of the chapters 2 and 3 in order to develop the most realistic finite element model of the knee-implant. This chapter has been submitted to the journal of "Computer Methods in Biomechanics and Biomedical Engineering".

The chapter five is allocated to the general discussion of the results while the last chapter presents conclusion and recommendations for future studies. Contributions made by this study as well as the limitations of the present work are discussed, as well.

The first two addendums are placed to help the better understanding of the second and third chapters. Appendix A is in the continuation of the work presented in Chapter two in which the bone was replaced by the polyurethane. The results of this work also confirms the findings in the second chapter by providing an application of the bi-directional friction formulation in the FE simulations. This work was published in the "Numerical Implementation and Application of Constitutive Models in the Finite Element Method, ASME 1995". Appendix B also presents experimental and developed finite element model of pull-out tests under a loading/unloading cycle using measured cyclic nonlinear friction properties. This part of the study was set to propose and guide the new direction for the future studies. Additional results of the finite element model study of knee-implant (Chapter 4) are presented in the last appendix.

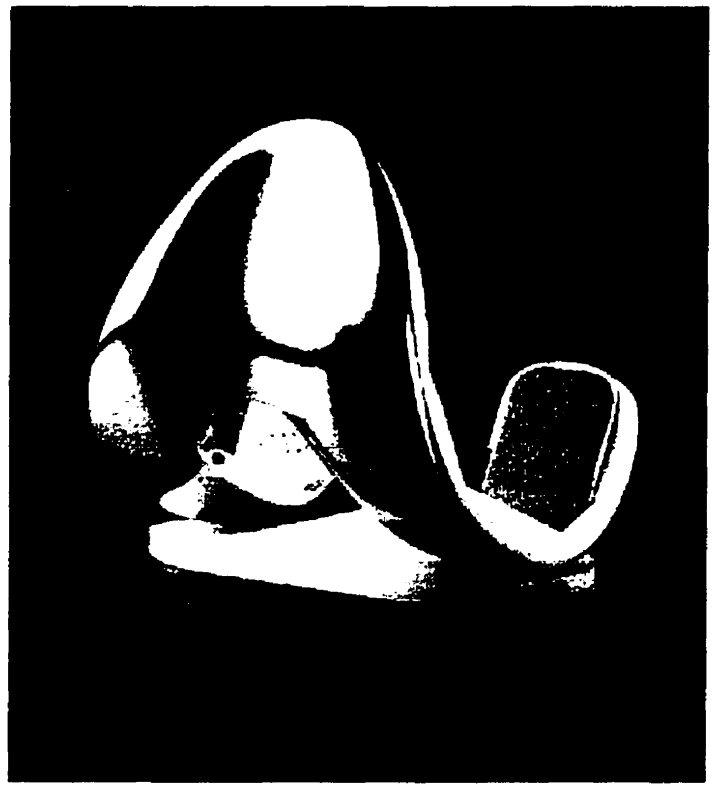

Figure 1.1 An example of cemented knee implant (Microloc Porous Coated Knee System).

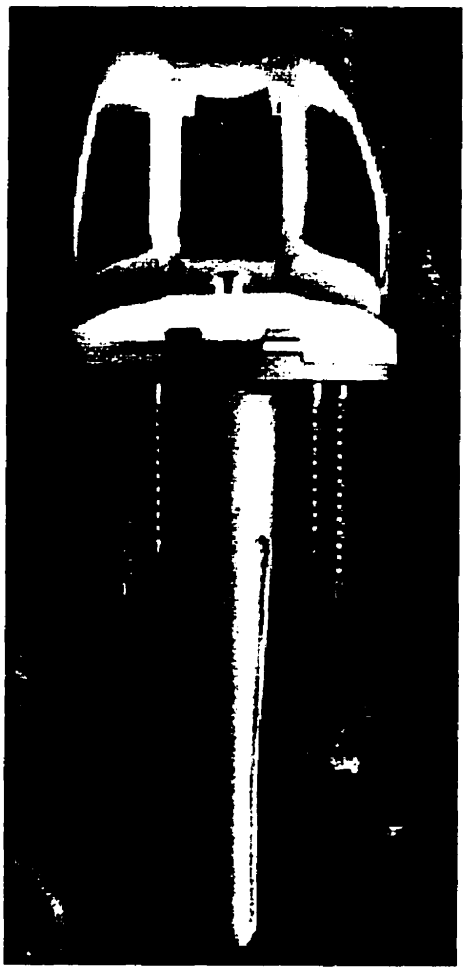

Figure 1.2 An example of cementless knee implant (AGC Total Knee System, Biomet, Inc.).

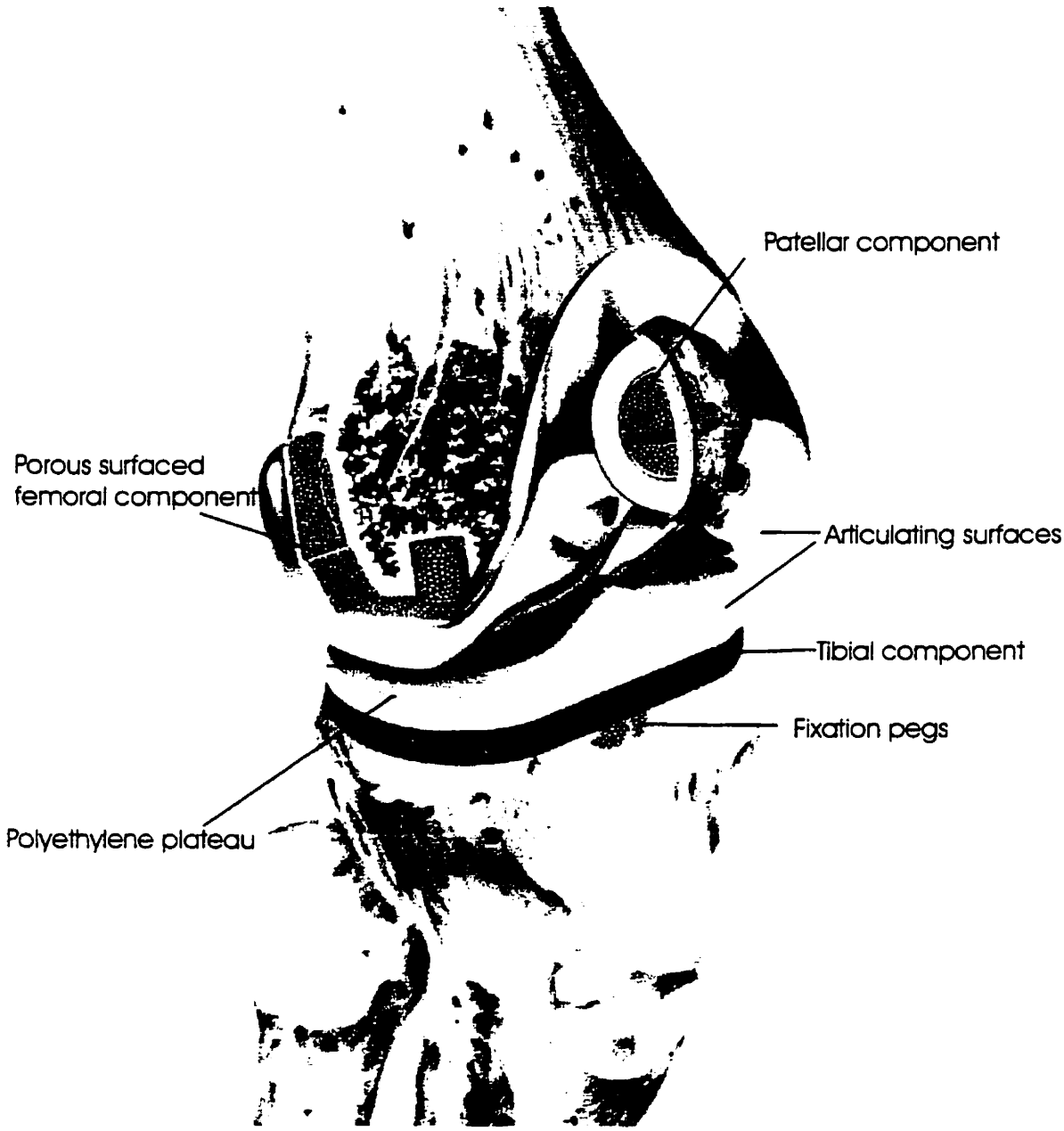

Figure 1.3 Total knee replacement (arthroplasty) by a cemented implant.

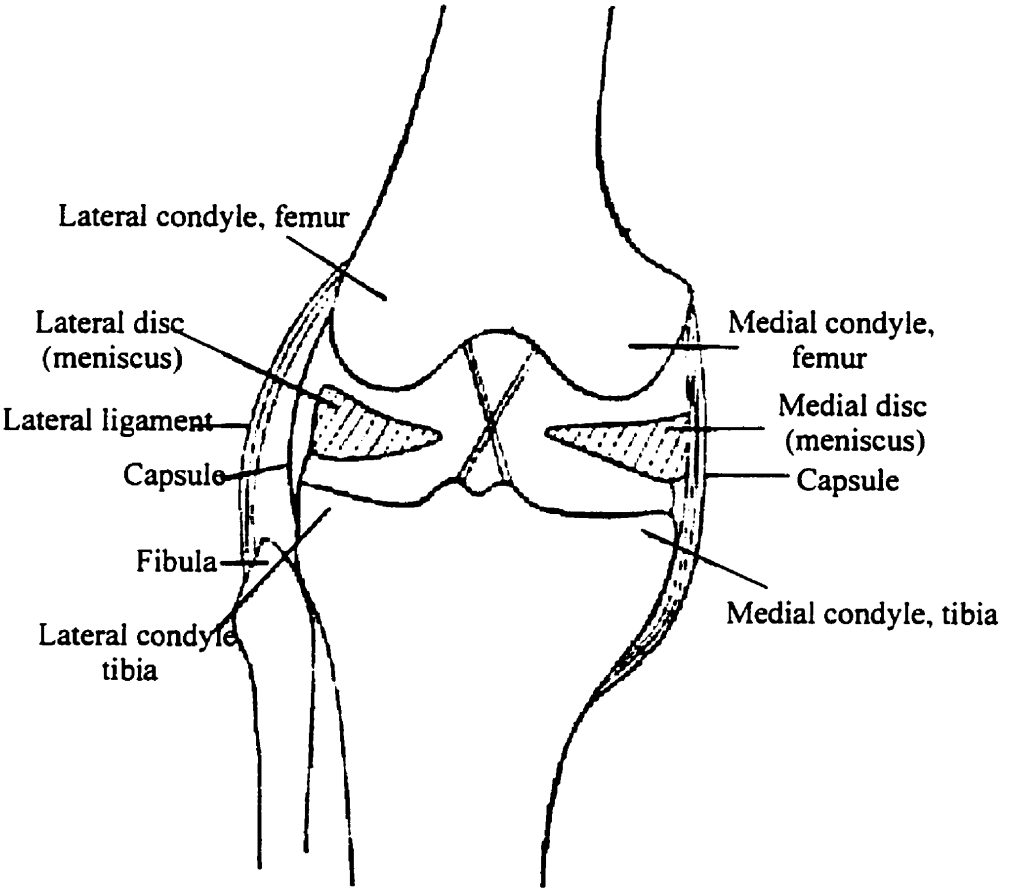

Figure 1.4 A schematic representation of knee joint.

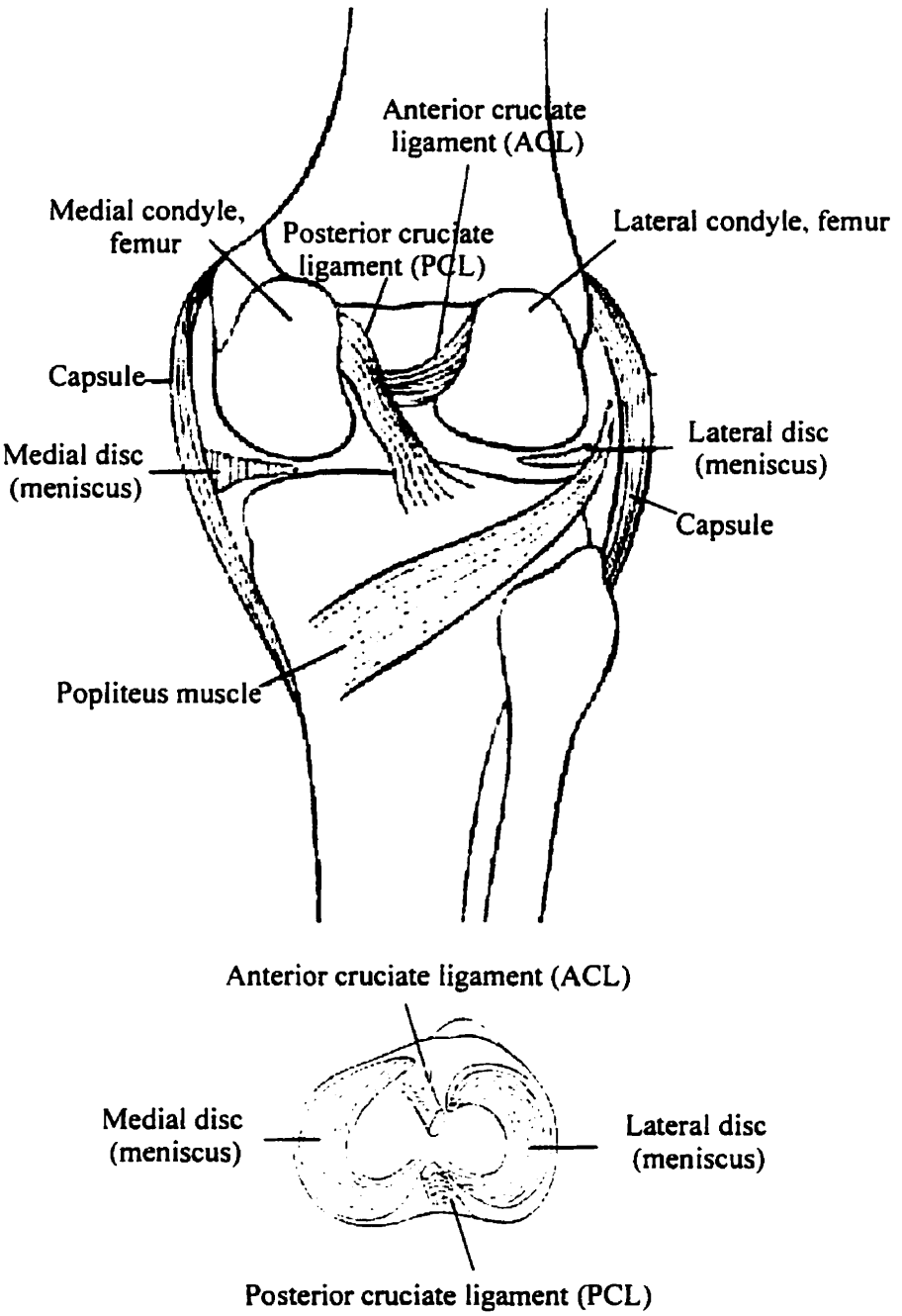

Figure 1.5 A schematic representation of knee joint ligaments and cartilaginous discs.

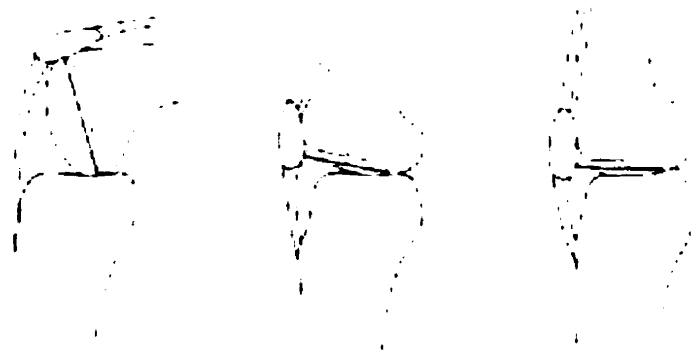

Figure 1.6 Knee position determines the lever arms of the muscles about the knee.

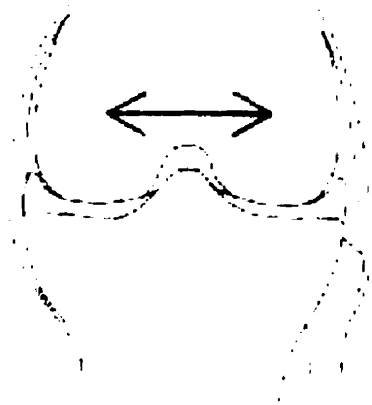

Figure 1.7 Medial-lateral translation is limited by the tibial spines.

CHAPTER 2

BI-DIRECTIONAL FRICTION STUDY OF CANCELLOUS BONE-POROUS COATED METAL INTERFACE

2.1 ABSTRACT

Bi-directional friction tests between cancellous bone cubes and a porous-coated metal plate were performed to determine the mechanical properties of the interface required in 3-D finite element model studies of cementless implants. Bone specimens were obtained from different proximal regions of four resurfaced cadaveric tibiae. A beaded porous-surfaced plate similar to those used in implants was used. Tangential loads in perpendicular directions with different magnitudes were applied at the interface in presence of constant normal pressure and the displacements were monitored in the same directions. Measured results showed that the interface load-displacement curve is highly nonlinear with significant coupling between two perpendicular directions. The interface friction coefficient (defined as the ratio of the maximum resultant tangential force divided by the normal load) was found to remain nearly unchanged with the relative magnitude of tangential stresses and the bone location. Moreover, bi-directional tests suggested that the load-displacement relation when evaluated for resultant values is similar to that obtained in a uni-directional testing condition. Constitutive equations that account for the cross-stiffness coupling terms between perpendicular directions were also developed. These relations were used in a 3-D finite element model study of preceding bi-directional friction tests. The influence of the coupling terms on results was investigated by comparison of predictions with measurement results. A satisfactory agreement

was found between the results of experiments with those of finite element studies confirming the constitutive relations as well as the importance of coupling terms.

2.2 INTRODUCTION

In an arthritic joint, the pain can be relieved and near-normal activity be regained by a prosthetic replacement (i.e., an artificial joint). The number of total joint replacements has grown significantly in the last two decades, a trend that is expected to continue with the aging population of the western societies. Cemented and cementless implants are two distinct types that are currently used in the joint arthroplasty. While in cemented implants, the cement is used as the bonding agent between the prosthetic components and the bone, in cementless implants the prosthesis is in direct contact with the host bone. In this latter, the short- and long-term fixation stability is provided by both the porous coating of the implant at the interfaces with the bone and the screws/posts. The porous coating is employed to allow for bone ingrowth and, hence, a biologic attachment of the artificial joint to the host bone. The success of the operation depends, therefore, on the achievement of such biologic integration. Many factors are known to influence the ingrowth of bone, for example, the size of surface pores and the magnitude of relative displacements at the bone-implant interface. Excessive relative motions at the bone-porous coated metal interface are generally recognized as a factor which decreases bone proliferation into surface pores of implants (1,2), (Cameron et al., 1973, Ducheyne et al., 1977), thereby resulting in adverse fibrous ingrowth (3) (Pilliar et al., 1986).

In a cementless implant, the friction at the bone-prosthesis interface plays an important role in the mechanical response of the system, particularly in the immediate post-operative period where no bony ingrowth has yet occurred and the friction is the only means of load transfer in directions tangential to common interfaces. To study the relative significance of friction in the joint mechanics,

uni-directional friction properties at the interface between tibial cancellous bone and a number of metal plates (two beaded porous surfaces, a fiber mesh porous surface, and a smooth surface) have previously been measured under single and repetitive fatigue loadings (4,5) (Rancourt et al., 1990; Shirazi-Adl et al., 1993). It was found that the friction coefficient noticeably increased for the porous coated metal plates as compared with the smooth one whereas it remained unchanged with the bone excision site on the proximal tibia, magnitude of normal stress, type of porous coated plates considered, rate of displacement, and duration of conservation in saline solution. Moreover, in contrast to the idealized Coulomb's friction, the tangential load-displacement at the interface was found to be highly nonlinear in which relatively large tangential displacements of 50-400microns were recorded at the maximum resistance load. The measured interface nonlinear properties were implemented in axisymmetric finite element analysis of push-out tests (6,7) (Shirazi-Adl and Forcione, 1992; Dammak et al, 1995) and tibial knee implants (8) (Forcione and Shirazi-Adl, 1990). These limited case studies demonstrated the important role of friction in fixation mechanics of cementless artificial joints. The earlier finite element studies of cementless tibial components in total knee replacement have been limited in either using the idealized Coulomb's friction (9-11) (Dawson and Bartel, 1992; Rakotomanana et al., 1994; Tissakt et al., 1995) or assuming a frictionless contact at the bone-implant interface (12,13) (Keja et al., 1994; Shirazi-Adl and Ahmed, 1989).

The foregoing experimental studies (4,5), however, treated the friction between bone and implant only in one direction. In a three dimensional contact problem, the articulating bodies could undergo relative movements and develop shear forces in different directions on the common interface. These directions could also change during the course of deformation. The phenomenon of bi-directional friction between two bodies, therefore, needs to be investigated in an experimental study. The results can then be employed to develop appropriate constitutive laws necessary to perform realistic model studies of cementless artificial joints that experience relative motions and shear

stresses simultaneously in different directions.

Based on the above discussion and in continuation of our earlier studies (Rancourt et al., 1990: Shirazi-Adl et al., 1993), (4,5) the aim of this study is to investigate the friction properties at the bone-porous coated metal interface in bi-directional tests. That is, horizontal loads in perpendicular directions with different magnitudes are applied at the interface in presence of some constant normal pressure and the tangential displacements are recorded. Proper tangential load-displacement constitutive equations for the bone-porous coated metal interface is accordingly developed which accounts for the cross-stiffness coupling terms between perpendicular directions. The foregoing nonlinear interface constitutive relations are, then, implemented in finite element model studies of the above bi-directional experimental tests to further validate the developed equations and to identify the influence of coupling terms on results.

2.3 MATERIALS AND METHODS

2.3.1 Preparation of specimens

Trabecular bone cubes were obtained from four cadaveric fresh-frozen proximal tibiae (2 males and 2 females with 70 ± 3 years age). Each tibia was resurfaced with a diamond saw having a posterior alignment of about 7 degrees (verified by visual inspection). A subsequent cut parallel to the first one was performed to obtain bone specimens of 10 mm height. From these bone plates, cube specimens of about 20 x 15 x 10 mm were then obtained from different anatomical sites (medial, lateral, anterior, posterior, and central) as shown in Figure 2.1. Two tibiae were large enough to obtain extra specimens from lateral and medial regions. In two specimens the central region was too soft to perform tests. One knee was so small that no specimen at the central region was cut. Overall, a total of 22 bone cube specimens were obtained; 7 medial, 6 lateral, 4 anterior,

4 posterior, and 1 central. The experiments were arranged in a way as to complete the static tests on each tibia as soon as possible in the same day as it was cut. During the tests, the bone samples were stored in plastic containers to avoid drying. At the end of the tests, the bone specimens were stored in saline solution and kept at -14 °C while the metal plates were cleaned with acetone for the subsequent tests. A beaded porous-surfaced metal plate made of Vitallium (a cobalt-chromium-molybdenum alloy) with the surface texture (bead diameter of about 0.70 mm and surface porosity of 30-40%) similar to those currently used in cementless implants was used (provided by Howmedica Inc, Pfizer Hospital Products Group Inc., Rutherford, NJ, Figure 2.2). This plate was used in the earlier studies in uni-directional friction tests (5) (Shirazi-Adl et al, 1993).

2.3.2 Test Apparatus

The experimental apparatus developed earlier for our uni-directional friction tests (5) (Shirazi-Adl et al, 1993) was slightly modified to allow for the simultaneous application of loads and measurement of motions in perpendicular directions at the interface. A schematic representation of the bi-directional friction test is shown in Figure 2.3; for more details, our previous work should be consulted (5). The normal load was applied by weights on top of a moving frame containing rigidly the specimens while the tangential loads were applied via cables attached to the same frame at the interface level to avoid undesired moments. Care was taken to apply the normal load in the direction perpendicular to the interface resulting in no additional tangential force. The bi-directional nature of the tests required the simultaneous monitoring of the load-displacement behavior in two perpendicular directions, x and y.

2.3.3 Experimental Procedures

To perform the tests, bone specimens were placed on top of the beaded porous-surfaced metal

plate and a normal pressure of 0.1 MPa was applied which remained constant during the test. Previous extensive friction studies have demonstrated that the interface friction resistance does not depend on the magnitude of the normal load and the rate of loading (4,5). The low magnitude of 0.1 MPa was used also to assure that the surface of the bone specimens was not damaged for subsequent tests (Rancourt et al, 1990, Shirazi-Adl et al., 1993). A constant tangential preload was applied in one direction (say x) while another tangential load was applied and incrementally varied to its maximum value in the perpendicular direction (say y). The tests were terminated as soon as the maximum interface resistance was reached at which load the cube started sliding on the metal plate. These tests were repeated for different preload magnitudes expressed as percentage of the mean maximum tangential force evaluated from prior (minimum of 3) uni-directional friction tests for each specimen. The percentage of preloads was 0%, 37%, 65%, or 84%.

2.3.4 Frictional Contact Formulation

Measured nonlinear friction properties of the uni-directional contact tests have been used to develop following constitutive relations. In this formulation, the frictional properties in different directions are coupled. That is, a shear stress in one direction depends not only on the relative displacement in its own direction but also on that in the other direction perpendicular to the first one. This dependency introduces off-diagonal terms in constitutive matrix that causes coupling effects. In these developments, it is actually assumed that the resultant tangential forces and relative displacements occur in the same direction and follow the corresponding nonlinear uni-directional friction curve. Taking the τ_{eq} and γ_{eq} as the resultant shear stress and relative displacement, respectively, shear stress components in perpendicular directions can be expressed as

$$\tau_i = \tau_{eq} \frac{\gamma_i}{\gamma_{eq}} \qquad i = x, y \tag{2.1}$$

in which

$$\tau_{eq} = f(\gamma_{eq}) \tag{2.2}$$

where f is the uni-directional nonlinear friction function obtained from measurements (e.g., the nonlinear curve in Figure 2.5 for the uni-directional test $F_x=0$).

The gradients of the interface friction stress with respect to the relative displacements $\gamma_i (i=x,y)$ yield both diagonal and off-diagonal stiffness terms as follows

$$\frac{\partial \tau_i}{\partial \gamma_j} = \begin{cases} \left(\dfrac{\partial f(\gamma_{eq})}{\partial \gamma_{eq}} - \dfrac{f(\gamma_{eq})}{\gamma_{eq}} \right) \dfrac{\gamma_i^2}{\gamma_{eq}^2} + \dfrac{f(\gamma_{eq})}{\gamma_{eq}} & \text{when} \quad i = j \\ \left(\dfrac{\partial f(\gamma_{eq})}{\partial \gamma_{eq}} - \dfrac{f(\gamma_{eq})}{\gamma_{eq}} \right) \dfrac{\gamma_i \gamma_j}{\gamma_{eq}^2} & \text{when} \quad i \neq j \end{cases} \tag{2.3}$$

One observes that all stiffness terms are function of both perpendicular relative tangential displacements. Moreover, it is noted that the cross-stiffness parameters (i.e., coupling terms) in Eq. 2.3 disappear if the friction response becomes linear or uni-directional. The earlier uni-directional friction measurements (4,5) (Rancourt et al., 1990; Shirazi-Adl et al., 1993) demonstrated the linear dependence of the shear stress and the independence of the tangential displacement on the normal stress at the interface. In the foregoing developments given in Eqs. 1-3, therefore, the normal pressure term was left out, without loss of completeness.

The formulation without coupling terms assumes that the friction response in each direction is independent on that in the other perpendicular direction. The shear resistance is, therefore, a function of relative displacement at that direction only; i.e., no coupling between different directions.

In this event $\tau_i = f(\gamma_i)$ where i=x,y and, hence,

$$\frac{\partial \tau_i}{\partial \gamma_j} = \begin{cases} \dfrac{\partial f(\gamma_i)}{\partial \gamma_j} & \text{when} \quad i = j \\ 0 & \text{when} \quad i \neq j \end{cases} \tag{2.4}$$

The tangential stiffness of the interface in each direction is a function of the relative displacement at that direction only. In this case, as is seen in Eq. 2.4, the cross-stiffness parameters are nil and no coupling between different perpendicular directions is introduced in constitutive equations. The resultant tangential force, nevertheless, can not exceed the maximum uniaxial interface resistant force, i.e., μF_N.

2.3.5 Finite Element Model

To investigate the relative accuracy and performance of the foregoing constitutive laws, a finite element model was developed and analyzed using the ABAQUS program (Hibbit, Karlsson and Sorenson Inc., Pawtucket, RI, 1992). The foregoing nonlinear friction constitutive relations were input in the program through an interface subroutine.

In this model study, the experimental friction tests of a bone specimen (medial region) on metal plate were simulated using a three dimensional model that includes 52 eight-node brick elements, 148 nodes and 16 contact elements, as shown in Figure 2.4. The nonlinear bi-directional constitutive equations were used in this study to evaluate the foregoing constitutive developments. To compare the predictions with the results of experimental friction tests, the geometry, boundary conditions, and loading were taken identical to those used in tests.

The elastic moduli of the plate and cancellous bone (medial region) materials for these studies were taken as 200,000 MPa and 300 MPa (14,15), respectively. The Poisson's ratio was 0.3 for the metal and 0.2 for the bone (15). To perform these studies, appropriate uni-directional friction data obtained from experiments have been implemented in the program.

2.4 RESULTS

2.4.1 Experimental study

Typical experimental results of bi-directional friction tests performed on the porous-surfaced metal plate and a bone specimen (from the medial region) are shown in Figures 2.5 and 2.6 for different preload magnitudes. Similar nonlinear and coupling behaviors were obtained for different regions considered in this study. To distinguish the effect of preload on the relative displacements, initial displacements due to the preload in the x direction have been removed in Figure 2.6. The load-displacement is highly nonlinear exhibiting relatively large displacements before the maximum interface resistance is reached. As in the uni-directional tests (i.e., $F_x=0$), interface sliding occurs right from the beginning as the load is applied. It is seen that the presence of a preload in the x direction affects the response not only in the y direction (Figure 2.5) but also the coupled tangential motion in the x direction (Figure 2.6). Moreover, the coupling effect is seen to increase as the relative magnitude of the preload increases. The measured variation of resultant forces with displacements evaluated from these bi-directional tests is verified to be similar to that measured in uni-directional tests (i.e., $F_x=0$).

2.4.2 Friction Coefficient

The friction coefficients (mean ± standard deviation) at the interface between cancellous bone and

porous-surfaced metal under an interface normal stress of 0.1 MPa are listed in Table 2.1. The friction coefficient for such nonlinear curves is defined as the ratio of the maximum resultant tangential load resisted at the interface divided by the normal load. The number of bone cubes used was six for lateral, seven for medial, four for anterior/posterior each and one for central. Despite relatively close mean values for different cases, the statistical analysis (2-way ANOVA with post hoc LSD test, Statistica program, StatSoft, Inc., Tulsa, OK) indicates significant p-levels ($p<0.05$) for 0% and 37% preloads versus higher preloads and anterior site versus lateral and posterior sites.

2.4.2 Interface Tangential Displacements

The interface relative displacements (μm, mean±SD) at the maximum resistance force for different bone excision sites and various amount of preloads are listed in Table 2.2. The statistical analysis indicates that the effect of preloads on the relative displacements is not significant($p>0.05$). As for different bone regions, significant differences are noted between lateral site and remaining regions as well as medial site versus posterior one.

2.4.3 Finite Element Studies

The predicted variation of tangential load-displacement in the y direction in presence of various preloads in the x direction using the formulation with coupling terms (i.e., Eq. 2.3) are shown in Figures 2.7 and 2.8 for a bone cube (on medial region, for which Figures 2.5 and 2.6 are given) on the porous-surface metal plate. The predictions with and without coupling terms (i.e., Eqs. 3 and 4, respectively) as well as the measured values (mean ± SD) under a preload of $F_x = 0.37 F_{max}$ are given in Figures 2.9 and 2.10. These finite element studies simulate the bi-directional experimental tests the results of which are shown in the same Figures 2.9 and 2.10. Comparison of predictions with measurements suggests a satisfactory agreement. It also confirms the constitutive

formulation accounting for the coupling terms and indicates that the response cannot be accurately computed if these terms are neglected. when the coupling terms are neglected (Eq. 2.4), the F_y-D_y curves for different preloads (Figures 2.7 and 2.9) would shift horizontally to overlap the corresponding unidirectional curve for $F_x=0$. Moreover, the force in y direction would generate no additional interface displacements in the x direction (see Figure 2.10), in contrast to the predictions in Figures 2.8 and 2.10 and measurements in Figures 2.6 and 2.10. It is to be noted that similar to the case in Figure 2.6, the initial displacements due to preloads have been removed in Figures 2.8 and 2.10 for all cases except for $F_x=0$ in the former figure and finite element results without coupling in the latter figure where no initial displacement exists.

2.5 DISCUSSION

The objective of the present study was to investigate the friction characteristic at the bone-metal interface in bi-directional motions required in nonlinear 3-D finite element analysis of contacting bodies as is the case in the cementless artificial joints. For this purpose, the experimental apparatus used for the earlier uni-directional tests (4,5) was modified to allow the continuous recording of loads and relative displacements in perpendicular directions at the interface. In the presence of normal pressure, various preloads were applied in one direction and the response in both directions were simultaneously measured as an incrementally increasing load was applied in the other direction.

The measurements yield similar load-displacement friction curves for the resultant values in bi-directional tests as those in uni-directional tests (i.e., $F_x=0$), regardless of the bone excision site (Tables 2.1 and 2.2). Experimental results clearly suggest the presence of coupling between these two perpendicular directions (Figures 2.6 and 2.10). This is found to be the case for the cancellous bone at all bone regions. The interface friction coefficient evaluated as the ratio of the interface

resultant tangential resistance to the normal pressure is also found to remain nearly unchanged with the relative magnitude of tangential stresses and the bone excision site, and is nearly the same as that found in uni-directional tests (i.e., $F_x=0$). The measured results of this study indicate that the coefficient of friction at the bone-metal interface does not depend on the excision site of bone and this is in agreement with those of the earlier studies (4,5) (Rancourt et al., 1990, Shirazi-Adl et al., 1993). The measured friction curves are highly nonlinear with large relative displacements with range of 60-500 μm depending on bone excision sites. The initial slope is found to be higher at the medial and lateral regions, due to the fact that elastic modulus of bone in the proximal region of the tibiae is larger at the medial and lateral sites than at the remaining sites. These are found in the earlier studies as well (5) (Shirazi-Adl et al., 1993). The interface relative displacements are also found to be independent of the preload magnitudes (Table 2.2).

An analytical approach based on uni-directional load-displacement curves, which could be used as a substitute for bi-directional experiments, was also presented. These equations were developed with the assumptions that micromotion occurs in the direction of the resultant force and that it follows the uni-directional load-displacement curve. In the current developments, the friction properties in different directions were assumed to be coupled. The coupling of friction properties introduced off-diagonal terms in the constitutive relations (i.e., Eq. 2.3). These equations were implemented in the finite element model studies of bi-directional friction tests. A good agreement was found between the results of predictions and those of experiments (Figures 2.5-2.10). This satisfactory agreement would not have been achieved had the coupled terms in Eq. 2.3 not been considered in the finite element models (see Figures 2.9 and 2.10). Use of Eq. 2.4 in which the friction response is independent in each perpendicular direction (i.e., with no coupling terms) yields different results in complete disagreement with measurements. That is, the primary F_y-D_y response follows the uni-directional curve (i.e., $F_x=0$) irrespective of the magnitude of the preload (i.e., F_x) while the coupled F_y-D_x response entirely disappears.

The coupled terms were, therefore, essential if accurate results were to be expected from model studies. Such coupling terms properly account for the softening in coupled responses when preloads in other directions are present. The analytical constitutive expressions with coupling terms (Eq. 2.3) were, hence, validated and could be used in future model studies of the human joint implant systems. Based on the Eq. 2.3, it is seen that the cross-stiffness terms (i.e., coupling terms) vanish in a uni-directional friction analysis or when a linear friction behavior is implemented for an interface. Thus, these equations can be simplified and accurately used in an axisymmetric or two-dimensional analysis where there is only one shear component at the interface. The idealized Coulomb's friction in which no displacement occurs before the maximum resistance force is reached, was found in our earlier studies (7) (Dammak et al, 1995) not to perform satisfactorily even when compared with measured nonlinear uni-directional friction constitutive law and, hence, was not considered in this study. In 3-D cases in which one component of shear stress at the interface is much larger than the other one, these coupling terms can be neglected without noticeable loss of accuracy. This is verified by the present model studies of friction tests when a small preload is applied in one direction and response is calculated in both perpendicular directions.

Finally, it is to be noted that the formulation presented here is limited only to interfaces with isotropic friction properties; i.e., where uni-directional friction properties are not direction dependent. This has been verified by our friction tests to be the case at the porous coated implant interfaces with the cancellous bone. Therefore, in 3-D finite element study of contacting bodies with isotropic interfaces as in cementless joint arthroplasty, the experimental results coupled with constitutive formulations presented in this work should be used.

ACKNOWLEDGMENTS This work was supported by a grant from the Natural Sciences and Engineering Research Council of Canada (NSERC). The porous coated metal plate was provided by the Howmedica Inc. (USA).

REFERENCES

1. Cameron, H. U.; Pilliar, R.M.; Macnab I., "The effect of movement on the bonding of porous metal to bone.", J. Biomed. Mater. Res., 7:301-311; 1973.
2. Ducheyne, P.; DeMeester, P.; Aernoudt, E.; Martens, M.; Mulier, J.C., "Influence of a functional dynamic loading on bone ingrowth into surface pores of orthopedic implants.", J. Biomed. Mater. Res., 11:811-838; 1977.
3. Pilliar, R.M.; Lee, J.M.; and Maniatopoulos, C., "Observations on the effect of movement on bone ingrowth into porous-surfaced implants.", Clin. Orthop. Rel. Res., 208:108-113; 1986.
4. Rancourt, D.; Shirazi-Adl, A.; Drouin, G., "Friction properties of the interface between porous-surfaced metals and tibial cancellous bone.", J. Biomed. Mater. Res., 24:1503-1519; 1990.
5. Shirazi-Adl, A.; Dammak, M.; Paiement, G., "Experimental determination of friction characteristics at the trabecular bone/porous-coated metal interface in cementless implants.", J. Biomed. Mater. Res., 27:167-175; 1993.
6. Shirazi-Adl, A.; Forcione, A., "Finite element stress analysis of a push-out test part II: Free interface with nonlinear friction properties.", J. Biomech. Eng., 114:155-161; 1992.
7. Dammak, M.; Shirazi-Adl, A.; Zukor, D., " Analysis of cementless implants using interface nonlinear - Experimental and finite element studies.", J. Biomechanics., 30(2): 121-129, 1997.
8. Forcione, A.; Shirazi-Adl, A., "Biomechanical analysis of a porous-surfaced knee implant: A finite element contact problem with nonlinear friction.", Mechanical Engineering Forum, Canadian Society of Mechanical Engineers, Toronto., 2:19-24; 1990.
9. Dawson, J.M.; Bartel, D.L., "Consequences of an interference fit on the fixation of porous-coated tibial components in total knee replacement.", J. Bone Joint Surg.,

74-A(2):233-238; 1992.

10. Rakotomanana, L. R.; Leyvraz, P.F.; Curnier, A.; Meister, J-J.; Livio, J-J., "Comparison of tibial fixations in total knee arthroplasty: An evaluation of stress distribution and interface micromotions.", The Knee, 1(2):91-99; 1994.

11. Tissakht, A.; Eskandari, H.; and Ahmed, A. M., "Micromotion analysis of the fixation of total knee tibial component.", Computers and Structures, 56:365-375; 1995.

12. Keja, M.; Wevers, H.W.; Siu, D.; Grootenboer, H., "Relative motion at the bone-prosthesis interface.", Clin. Biomech., 9(5):275-283, 1994.

13. Shirazi-Adl, A.; Ahmed, A. M., "A parametric axisymmetric model study on the interface motions in porous-surfaced tibial implants.", Annals of Biomedical Engineering 17:411-421; 1989.

14. Goldstein, S.A.; Wilson, D.L.; Sonstegard, D.A.; Matthews, L.S., "The mechanical properties of human tibial trabecular bone as a function of metaphyseal location.", J. Biomechanics, 16:965-969, 1983.

15. Cheal, E.J.; Hayes, W.C.; Lee C.H.; Snyder, B.D.; Miller, J., "Stress analysis of a condylar knee tibial component: Influence of metaphyseal shell properties and cement injection depth.", J. Orthop. Res., 3:424-434, 1985.

Table 2.1 : Variation of Friction Coefficient (mean ± SD) at the Maximum Resistance With the Bone Excision Site and Preload Magnitude for Porous-Surfaced Metal Plates Under a Normal Pressure of 0.1 MPa.

Bone Cube Site	Preload			
	0%	37%	65%	84%
Lateral	0.57 ± 0.05	0.54 ± 0.04	0.58 ± 0.04	0.65 ± 0.08
Medial	0.58 ± 0.02	0.58 ± 0.07	0.65 ± 0.03	0.60 ± 0.09
Anterior	0.61 ± 0.02	0.61 ± 0.07	0.62 ± 0.04	0.66 ± 0.05
Posterior	0.55 ± 0.06	0.53 ± 0.05	0.60 ± 0.10	0.61 ± 0.06
Central	0.54	0.53	0.60	0.59

Table 2.2 : Variation of Relative Displacement (μm, mean ± SD) at the Maximum Resistance With the Bone Excision Site and Preload Magnitude for Porous-Surfaced Metal Plates Under a Normal Pressure of 0.1 MPa.

Bone Cube Site	Preload			
	0%	37%	65%	84%
Lateral	122 ● 33	110 ± 56	117 ± 58	174 ● 68
Medial	142 ± 53	186 ± 53	203 ± 83	263 ±118
Anterior	243 ± 30	223 ± 84	239 ± 105	265 ±134
Posterior	228 ● 56	352 ± 294	326 ±236	301 ± 183
Central	475	380	310	262

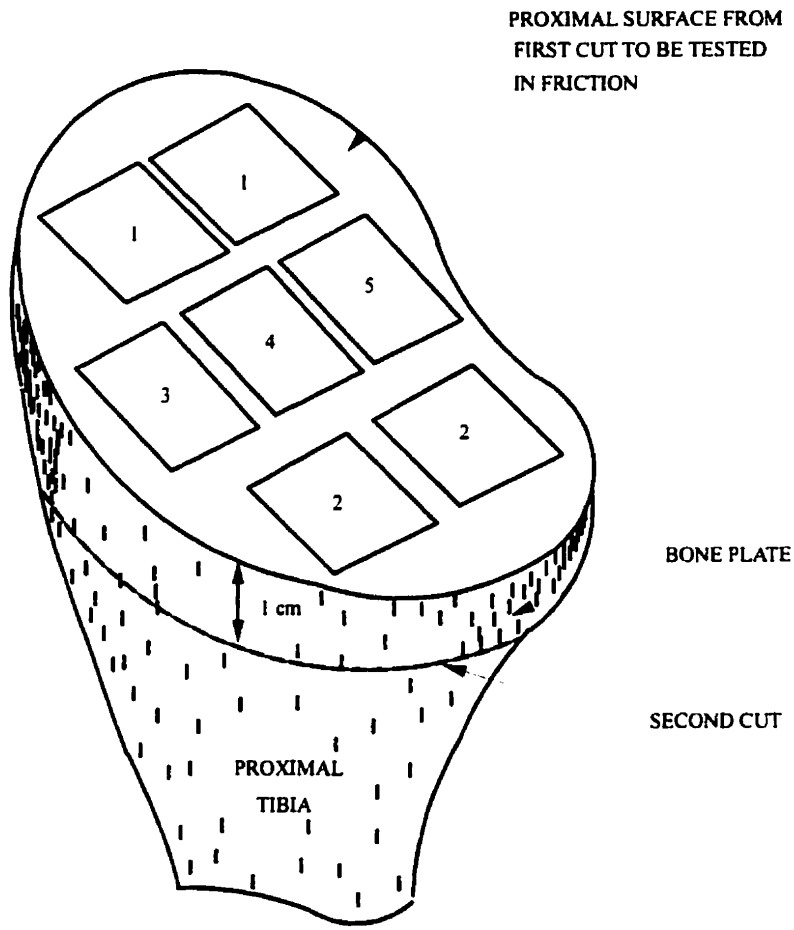

Figure 2.1 The excision sites of the cancellous bone specimens from the proximal region of a resurfaced tibia: (1) lateral, (2) medial, (3) anterior, (4) central, (5) posterior.

Figure 2.2 Specimens used in the experimental study; the vitallium bead porous-coated plate (Howmedica, Inc.) And two typical bone cubes.

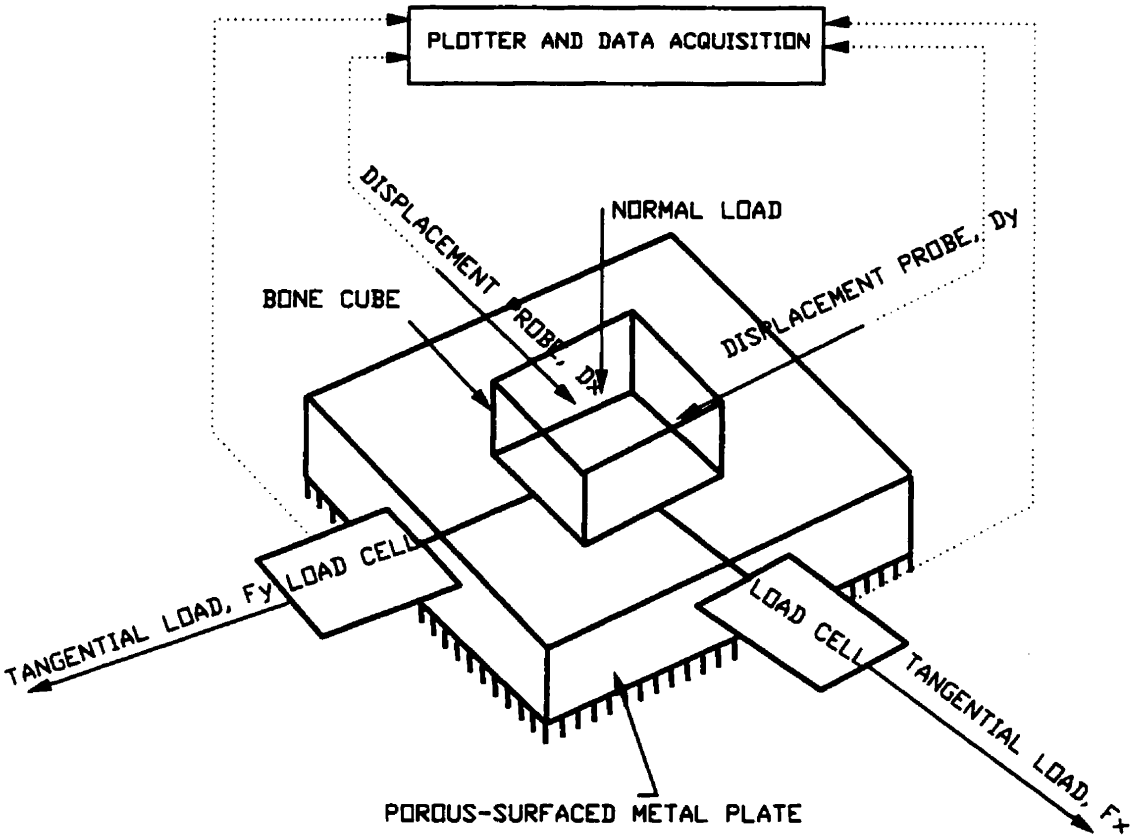

Figure 2.3 A schematic representation of the experimental setup for bidirectional friction tests of bone samples on a porous-surfaced metal plate.

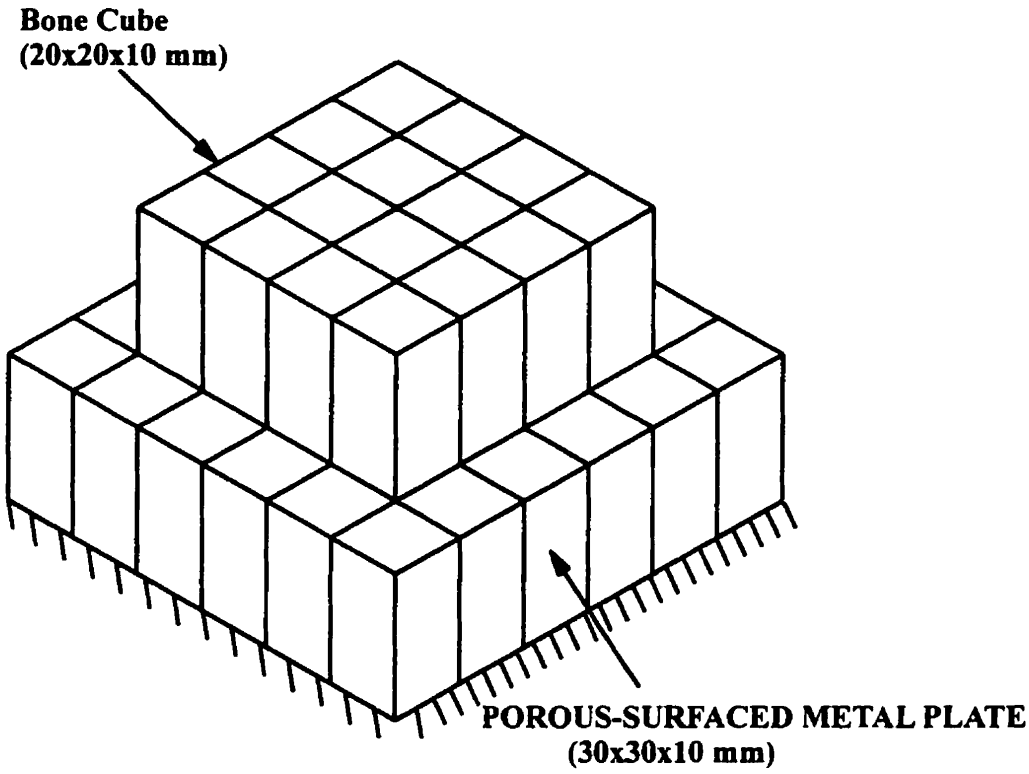

Figure 2.4 The 3-D finite element model of the experimental friction test of Figure 3 simulating a bone cube resting on top of a porous-surfaced metal plate.

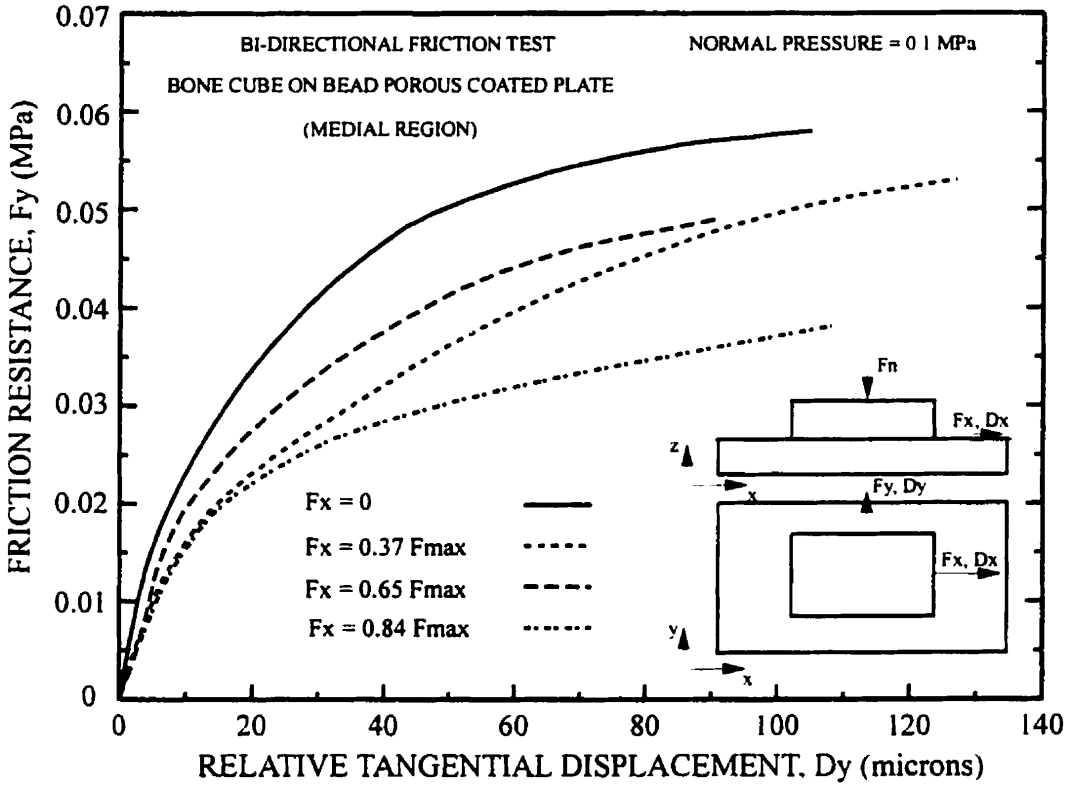

Figure 2.5 Typical friction load (y) - displacement (y) curves measured for a bone specimen at the medial region under monotonically increasing tangential load F_y preloaded in the perpendicular direction x by F_x expressed as a percentage of F_{max}, which is the mean interface resistance force in corresponding unidirectional tests, F_x=0.

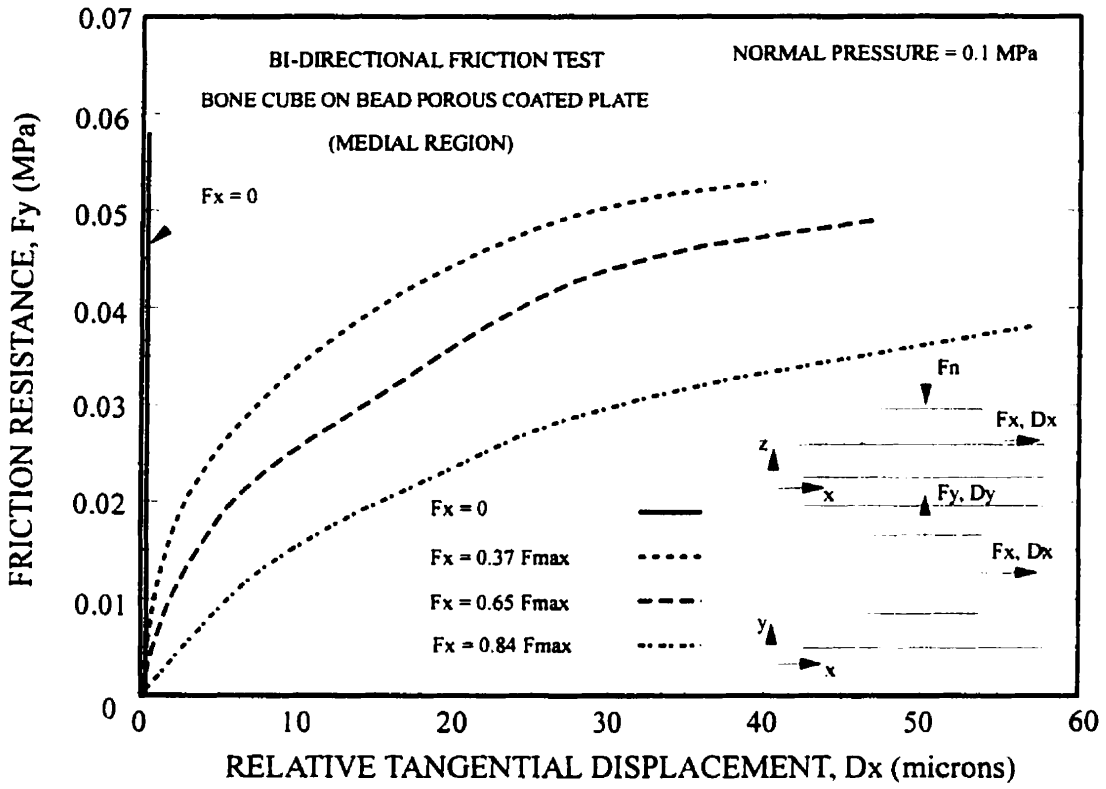

Figure 2.6 Typical friction load (y) - displacement (x) curves measured for a bone specimen at the medial region under monotonically increasing tangential load F_y preloaded in the perpendicular direction x by F_x expressed as a percentage of F_{max}, which is the mean interface resistance force in corresponding unidirectional tests, F_x=0.

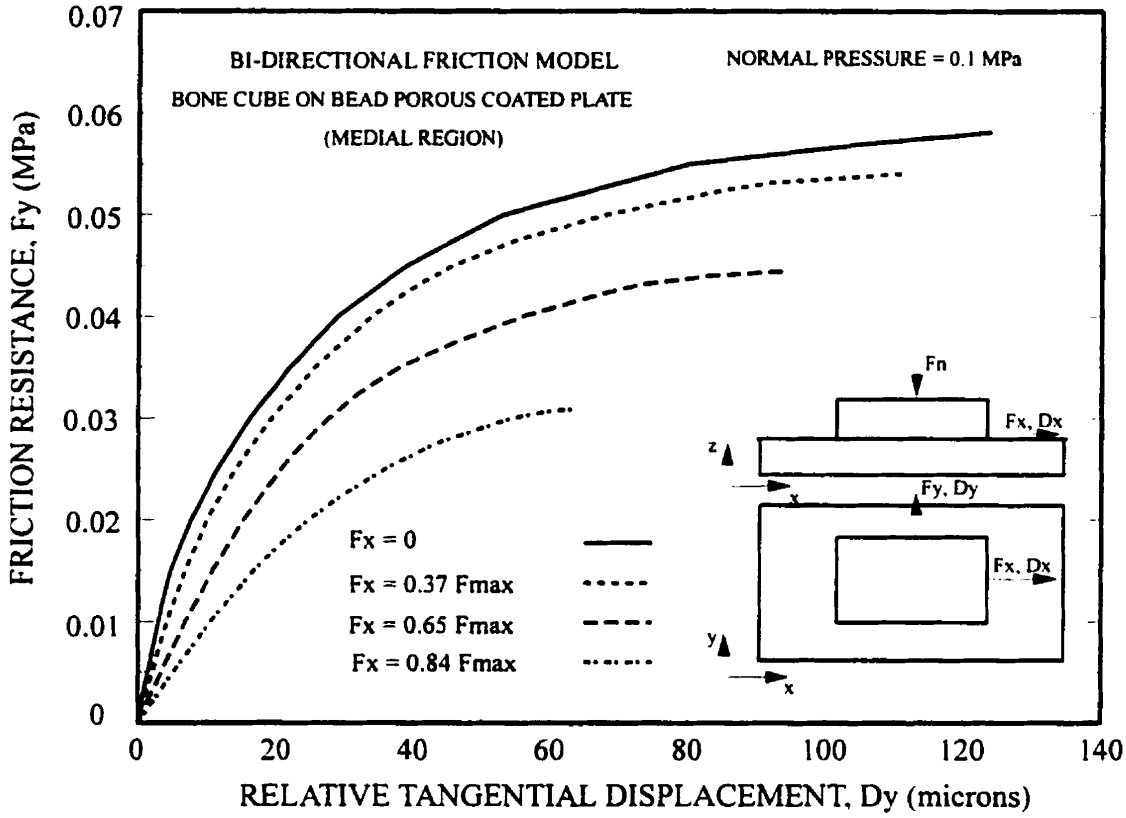

Figure 2.7 Predicted load (y) - displacement (y) curves of a bone specimen (medial region) on metal for bidirectional friction tests in the presence of various preloads in the x direction. F_{max} is the maximum tangential force measured in unidirectional tests, F_x=0.

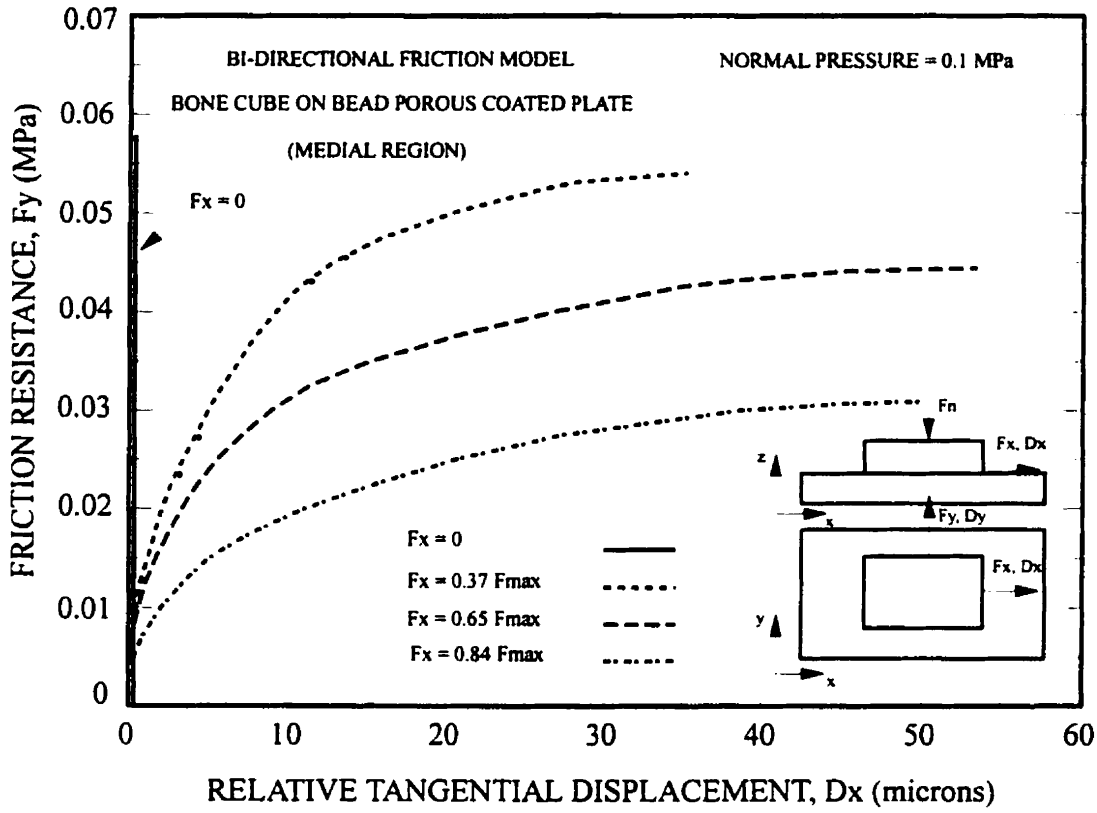

Figure 2.8 Predicted load (y) - displacement (x) curves of a bone specimen (medial region) on metal for bidirectional friction tests in the presence of various preloads in the x direction. F_{max} is the maximum tangential force measured in unidirectional tests, F_x=0.

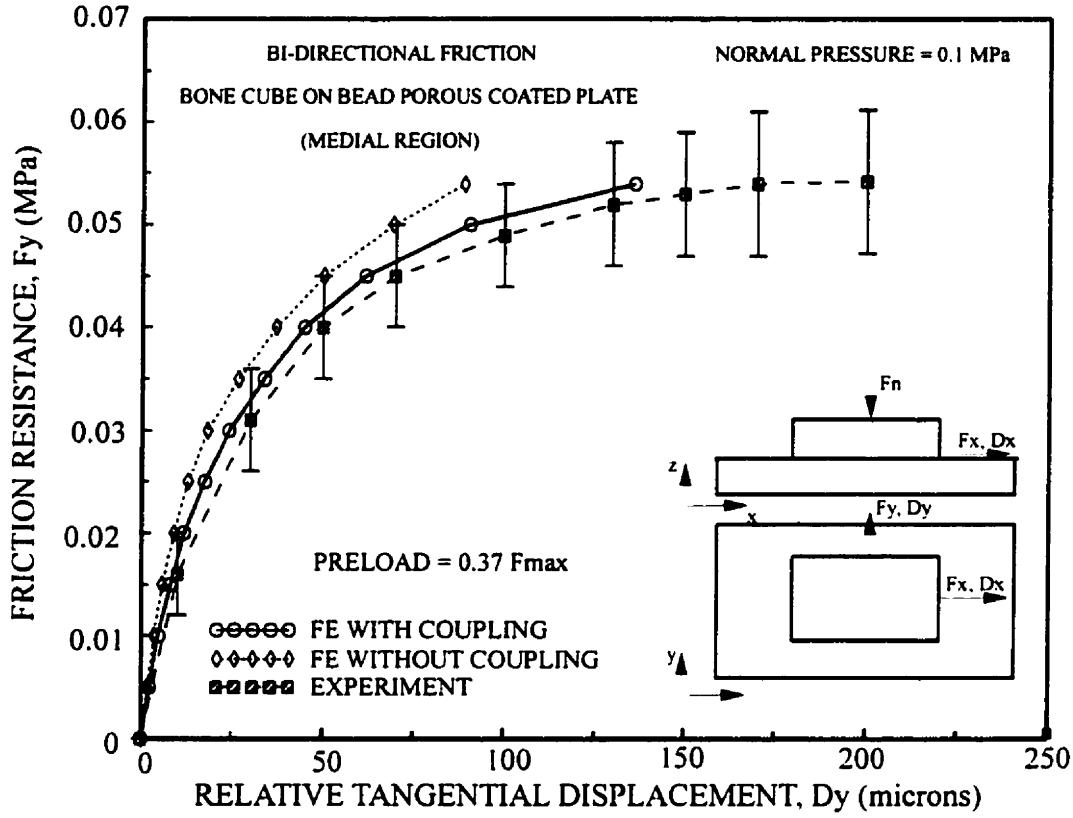

Figure 2.9 Finite element (FE) and experimental (mean ∓ SD) friction load (y) - displacement (y) curves for bone specimens at the medial region under monotonically increasing tangential load F_y preloaded in the perpendicular direction x by $F_x = 0.37\ F_{max}$. F_{max} is the mean interface resistance force measured in corresponding unidirectional tests, $F_x=0$.

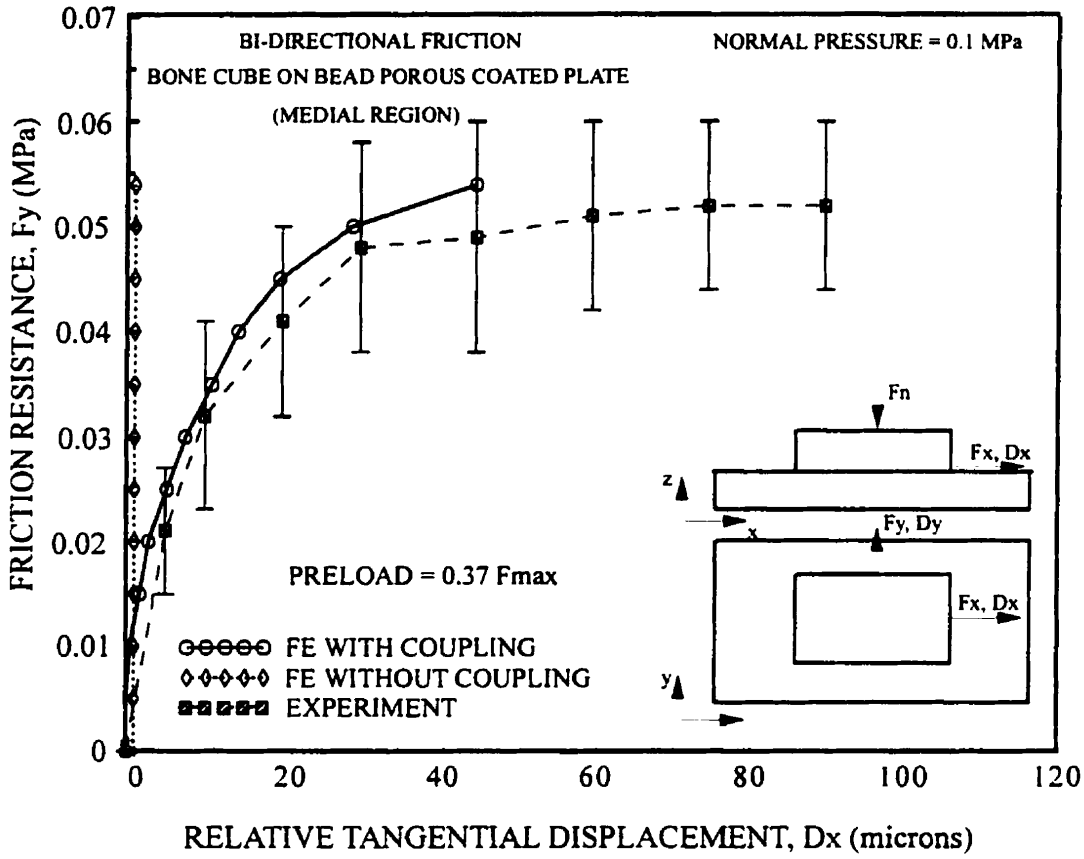

Figure 2.10 Finite element (FE) and experimental (mean ∓ SD) friction load (y) - displacement (x) curves for bone specimens at the medial region under monotonically increasing tangential load F_y preloaded in the perpendicular direction x by $F_x = 0.37\ F_{max}$. F_{max} is the mean interface resistance force measured in corresponding unidirectional tests, $F_x=0$.

CHAPTER 3

EXPERIMENTAL AND FINITE ELEMENT FIXATION STUDIES OF POSTS AND SCREWS

3.1 ABSTRACT

Screws and posts are used in various implant designs to contribute to the short- and long- term fixation stability of artificial joints. This study was undertaken to investigate the effect of combined loading on pull-out fixation response of bone screws, beaded porous coated posts, and smooth-surfaced posts inserted in polyurethane material. Mechanically-equivalent finite element models for bone screws are proposed by replacing the screws by posts with modified properties at the interface. The finite element results corroborated measurements on the effect of combined load on the fixation response. The pull-out response as well as interface stresses of a screw fixation can be represented by an equivalent post with a friction coefficient of about 2. The satisfactory agreement between numerical and experimental results confirms the accuracy in modeling the interface, posts, and screws. The developed models can, therefore, be used to investigate the post-operative short term fixation stability of various implant designs.

3.2 INTRODUCTION

In total joint arthroplasty, adequate fixation of prosthetic components to the host bone represents a great challenge. Stable fixation is a prerequisite to the satisfactory long-term performance of a

joint replacement system. In cementless arthroplasty, a porous-surfaced implant is used to permit biological fixation by the ingrowth of bone. The long-term success of uncemented implants is dependent upon achievement of the initial stability (Hungerford and Kenna, 1983; Landon et al., 1986; Waugh, 1985). Excessive motions at the bone/porous-surfaced metal interface are generally recognized as a factor to limit bone proliferation into surface pores of implants (Cameron et al., 1973; Ducheyne et al., 1977), resulting in fibrous ingrowth (Pilliar et al., 1981). The existing implant designs for total knee arthroplasty, cementless as well as cemented, utilize a wide range of screw and peg designs to provide the initial and long-term stability of tibial components. The initial rigidity of tibial components has been demonstrated by in-vitro studies to be significantly increased by the use of screws and pegs (Kaiser and Sumner et al., 1992; Lee et al., 1991; Miura et al., 1990; Sumner et al., 1992; Volz et al., 1988; Wyatt et al., 1991). The number, length, and location of bone screws as well as the quality of bone purchase have been identified as important factors in the screw fixation of implants (Finlay et al., 1989, Lee et al. 1991, Volz et al., 1988; Wyatt et al., 1991).

In a cementless implant, bone/prosthesis interface friction plays an important role in the fixation stability of the system, particularly in the immediate post-operative period where no bony ingrowth has yet occurred. The friction properties at the interface between porous- and smooth-surfaced metals and tibial cancellous bone have previously been measured under single and repetitive loadings (Rancourt et al., 1990; Shirazi-Adl et al., 1993). It was found that, in contrast to the Coulomb's friction, the tangential load-displacement at the interface is nonlinear. The friction coefficient was independent of the cancellous bone site, the magnitude of normal contact pressure, and the rate of relative displacement at the interface. The porous bead and fibre mesh surfaces, however, had significantly higher friction coefficient than the smooth surface. The incorporation of these measured nonlinear friction properties in the axisymmetric finite element analysis of push-out tests (Shirazi-Adl and Forcione, 1992) and tibial knee implants (Forcione and Shirazi-Adl, 1990)

has demonstrated the important role of friction in fixation mechanics of cementless orthopaedic implants.

It is evident that realistic 3-D nonlinear models are required in order to perform numerical experiments to accurately compute interface motions and stresses for various tibial fixation configurations. These models can then be used to evaluate the relative merits of each design in providing the short- and long- term fixation stability. In order to develop a realistic model of a prosthetic joint, we have also investigated the pull-out response of posts and screws in proximal tibia (Shirazi-Adl et al., 1994; Dammak et al., 1994). In these studies, the load was applied axially and was gradually increased to its maximum value beyond which gross debonding occurred. In an implant, however, screws and posts are subjected to combined loading cases consisting of both axial and horizontal shear forces. The relative magnitude of these components depends, amongst others, on the design, loading, and position on the implant. The effect of the shear load on the pull-out fixation response of screws and posts has not yet been determined. The objectives of this work are, therefore, set as: to investigate the influence of horizontal shear loading on the pull-out strength of bone screws and smooth/porous-surfaced posts; and to propose a simple and effective finite element model of screw fixation. Both experimental and finite element model studies are performed.

3.3 MATERIALS AND METHODS

Cylinders of diameter D=30 mm and length L=40mm made of polyurethane with properties similar to the tibial cancellous bone (measured mean values: elastic modulus=40 MPa, Poisson's ratio=0.3) were used for the experiments part. Two types of post, porous coated and smooth surfaced, were considered (D=8.75mm, insertion length L=20mm, drill size DS=8mm). Bone screws of 8 mm in diameter were also considered (L=23mm, DS=3mm). Screws and porous coated posts were manufactured from Vitallium (a cobalt-chromium-molybdenum alloy) and were

provided by the Howmedica (Howmedica Division, Pfizer Hospital Products Group Inc., Rutherford, N. J.). A base support was designed to hold these cylinders in place with different inclinations during pull-out tests with the MTS machine (MTS Bionix Test System, Materials Testing systems Corp., Minneapolis, Minnesota). Polyurethane cylinders were fixed along the outer surface. The load was applied through a cable making from 0 deg. 45 deg. with the axis of polyurethane cylinders (Fig. 3.1).

A nonlinear finite element model of experimental pull-out tests of bone screws (D=8mm, L=23mm, DS=3mm) inserted into polyurethane cylinders (D=30mm, L=40mm) was developed using ABAQUS program (ABAQUS, 1992). Given the complex geometry of a screw, it was approximated by a post with modified properties at the interface in a manner as to yield identical pull-out fixation response. In this model, different values of friction coefficient were "μ" considered (i.e., 0.2, 0.5, 1.0, 2.0, 4.0, 5.0, 6.0). The value of effective interference "e" is then chosen by matching the numerical and experimental pull-out results. The elastic moduli of screw and polyurethane materials were taken as 220,000 MPa and 40 MPa, respectively, with the Poisson's ratio of 0.3 for both materials. The finite element grid used for pull-out test of screws in polyurethane cylinders is shown in Fig.3.2. This is an axisymmetric model with 179 three to four-node elements, 15 contact elements, and 214 nodal points. Finite element results are compared with those obtained experimentally (Shirazi-Adl et al., 1994). An additional analysis of the screw pull-out test, assuming more realistic axisymmetric geometry for the screw pull-out test, was also performed to determine the state of stress at and adjacent to the thread-polyurethane interface (Fig.3.3). This model was subsequently used to determine the optimal friction coefficient among those given above that also generates similar stresses at and around the interface. Shear strength of polyurethane material was measured, according to the ASTM standards D732-93, to be 1.4±0.35 MPa. In all foregoing pull-out test models, therefore, a maximum allowable shear stress of 1.4 MPa was given at the metal-polyurethane interface beyond which sliding occurs. The applied

load was increased step by step and the nonlinear response was computed. In this manner, the interface stresses were determined for every load step until the applied load reached the final pull-out resistance of the post, at which step no additional shear stress could be carried along the interface.

Three-dimensional nonlinear finite element models of experimental inclined pull-out tests of posts and screws inserted in polyurethane cylinders were developed and analyzed using the ABAQUS program. The simplified model developed for screw was used for inclined pull-out test of screws. A typical 3-D finite element model for inclined pull-out tests is shown in Fig. 3.4. This is the half symmetric solid elements, and 64 contact elements. The measured nonlinear friction curves with friction coefficients of 0.38 and 0.2 for the polyurethane-porous and -smooth metal interfaces, respectively, were incorporated. The effective interference at the polyurethane-metal interface was 0.025 mm for porous coated posts and 0.15 mm for smooth surfaced posts. These effective interference values were directly based on measurements of the hole diameter before and after the pull-out tests (Shirazi-Adl et al., 1994).

3.4 RESULTS

The measured load-displacement response for a screw (D=8 mm, L= 23 mm, DS=3 mm) inserted in polyurethane cylinders and the computed response for its equivalent post compare well as shown in Fig. 3.5. For this case, the effective interference at the polyurethane-metal interface and the friction coefficient are 0.09 and 2 mm, respectively. Based on the detailed analysis of predicted displacements and stresses in the polyurethane for various friction coefficients, a smooth-surfaced post with an interface friction coefficient of about 2 is found to be the most suitable to replace the screw as its mechanically-equivalent structure. This is determined by comparing the post pull-out predictions with both load-displacement measurements and stress values computed from detailed

axisymmetric model of the screw pull-out test.

The measured and predicted load-displacement responses for porous-coated and smooth posts inserted in polyurethane cylinders are shown in Fig. 3.6. The predicated finite element results yield similar trends as those measured. The results of finite element model and experimental studies of axial pull-out force vs inclination for porous, smooth-surfaced posts and screws are presented in Fig. 3.7. The effect of load inclination in posts and screws shows three distinct patterns. Increasing the inclination angle increases the axial pull-out load of porous posts. It does not, however, significantly affect that for smooth posts while the axial pull-out load for screws reduces as the load is inclined. The maximum shear stress that can be transferred at the interface was limited in all models to 1.4 MPa based on our shear strength tests. Increasing the inclination can not increase the shear resistance beyond 1.4 MPa, but could reduce the shear resistance in some areas due to smaller normal stresses yielding a considerable reduction in axial pull-out resistance force in screws. The above results are confirmed by both experimental and finite element studies.

3.5 DISCUSSION

The objective of the present work was: to propose effective finite element models for the fixation analysis of screws; and to investigate the effect of shear loading on the pull-out strength of smooth/porous-surfaced posts and screws.

In the earlier measurements studies (Shirazi-Adl et al., 1994), smooth-surfaced posts demonstrated superior pull-out performance under both single and fatigue loading conditions when compared with porous-surfaced posts of the same dimensions. The current experimental and finite element results of inclined pull-out tests indicate that the foregoing difference diminishes in the presence of shear loads. The axial pull-out force of smooth posts was not affected significantly by increasing the

inclination angle of pull-out force. This is due to higher normal stresses at the interface of smooth surfaced post and polyurethane cylinder. However, it is found that the inclination of the load affects the axial pull-out load for porous-coated posts. This is due to alteration in the normal stresses at the interface. Screws, however, demonstrated a constant reduction in axial pull-out resistance force under combined loads. This could partly be due to the limit placed on the interface shear stress not to exceed the measured shear strength of the material. The above predicted and measured influence of the load inclination on the axial component of the pull-out force in screw is in agreement with experimental results reported by others (King and Cebone, 1993).

Given the complex geometry of a screw, mechanically-equivalent finite element model for bone screws was proposed by replacing the screws by posts with modified properties at the interface. For different friction coefficients varying from 0.2 to 0.6, proper interference values were chosen by matching the computed and experimental pull-out load-displacement results. The friction coefficient of about 2 was then selected as an acceptable value after comparing the state of stresses around the equivalent posts with those computed based on a detailed axisymmetric model of the screw. The equivalent post, therefore, generates nearly the same response as measured for the screw (Fig. 3.5) along with reliable stress field in the surrounding body. The good agreement between numerical and experimental results confirms the accuracy in modeling the posts, and screws. These models can, hence, be used in future implant fixation studies.

ACKNOWLEDGMENT This work is supported by a grant from the Natural Sciences and Engineering Research Council of Canada.

REFERENCES

ABAQUS, Finite element program, version 5.2, Hibbit, Karlsson and Sorenson, Inc., Pawtucket, 1992.

Cameron, H.U., Pilliar, R.M., and Macnab, I., 1973, "the effect of movement on the bonding of porous metal to bone", J. Biomed. Mat. Res., 7, 301-311.

Dammak, M., Shirazi-Adl, A., Hashemi, A., and Zukor, D.J., 1994, "Fixation mechanics of posts in joint arthroplasty - Comparison of various friction properties," Advances in Bioengineering, ASME WAM, Chicago, 411-412.

Ducheyne, P., DeMeester, P., Aernoudt, E., Martens, M., and Mulier, C., 1977, "Influence of a functional dynamic loading on bone ingrowth into surface pores of orthopaedic implants", J. Bomed. Mat. Res., 11, 811-838.

Finlay, J.B., Harada, I., Bourne, R.B., Rorabeck, C.H., Hardie, R., and Scott, M.A., 1989, "Analysis of the pull-out strength of screws and pegs used to secure tibial components following total knee arthroplasty", Clin. Orthop. Rel. Res., 247, 220-231.

Forcione, A. And Shirazi-Adl, A., 1990, "Biomechanical analysis of a porous surfaced knee implant: A finite element contact problem with nonlinear friction", Mechanical Engineering Forum, Canadian Society of Mechanical Engineers, Toronto, 2, 19-24.

Hungerford, D.S. and Kenna, R.V., 1983, "Preliminary experience with a total knee prosthesis with porous coating used without cement", Clin. Orthop. Rel. Res., 176, 95-107.

Kaiser, A.D. and Whiteside, L.A., 1990, "The effect of screws and pegs on the initial fixation stability of an uncemented unicondylar knee replacement", Clin. Orthop. Rel. Res., 259, 169-178.

King, T. STJ. And Cebone, D., 1993, "An alternative to screws for plating osteoporotic bone," J. Biomed. Eng., 15, 79-82.

Landon, G.C., Galante, J.D., and Maley, N.M., 1986, "Noncemented total knee arthroplasty", Clin. Orthop. Rel. Res., 205, 49-57.

Lee, R.W., Volz, R.G. and Sheridan, D.C., 1991, "The role of fixation and bone quality on the

mechanical stability of tibial knee components", Clin. Orthop. Rel. Res., 273, 177-183.

Miura, H., Whiteside, L.A., Easley, J.C., and Amador, D.D., 1990, "Effects of screws and sleeve on initial fixation in uncemented total knee tibial components", Clin. Orthop. Rel. Res., 259, 160-168.

Pilliar, R.M., Cameron, H.U., Welsh, R.P., and Binnington, A.G., 1981, "Radiographic and morphologic studies of load-bearing porous-surfaced structured implants", Clin. Orthop. Rel. Res., 156, 249-257.

Rancourt, D., Shirazi-Adl, A., Drouin, G., and Paiement, g., 1990, "Friction properties of the interface between porous-surfaced metals and tibial cancellous bone", J. Biomed. Mat. Res., 24, 1503-1519.

Shirazi-Adl, A., Dammak, M., and Paiement, G., 1993, "Experimental determination of friction characteristics at the trabecular bone/porous-coated metal interface in cementless implants", J. Biomed. Mat. Res., 27, 167-175.

Shirazi-Adl, A., Dammak, M., and Zukor, J., 1994, "Fixation pull-out response measurement of bone screws and porous-surfaced posts", J. Biomechanics, . 27(10), 1249-1258.

Shirazi-Adl, A. and Forcione, A., 1992, "Finite element stress analysis of a push-out test -Part II: Free interface with nonlinear friction properties", J. Biomech. Eng., 114, 155-161.

Sumner, D.R., Berzins, A., and Turner, T.M., 1992, "Stability of the tibial tray in cementless TKA: Initial versus late post-operative motion", Transactions of the Orthop. Res. Soc., 38th Annual Meeting, 268.

Volz, R.G., Nisbel, J.K., Lee, R.W. and McMurtry, M.G., 1998, "The mechanical stability of various noncemented tibial components", Clin. Orthop. Rel. Res., 226, 38-42.

Waugh, T.R., 1985, "Total knee arthroplasty in 1984", Clin. Orthop. Rel. Res., 192, 40-45.

Wyatt, R.W.B., Alpert, J.P., Daniels, A.U., Hofmann, A.A., and Dunn, H.K., 1991, "The effect of screw fixation on initial rigidity of tibial knee components", J. Appl. Biomat., 2, 109-113.

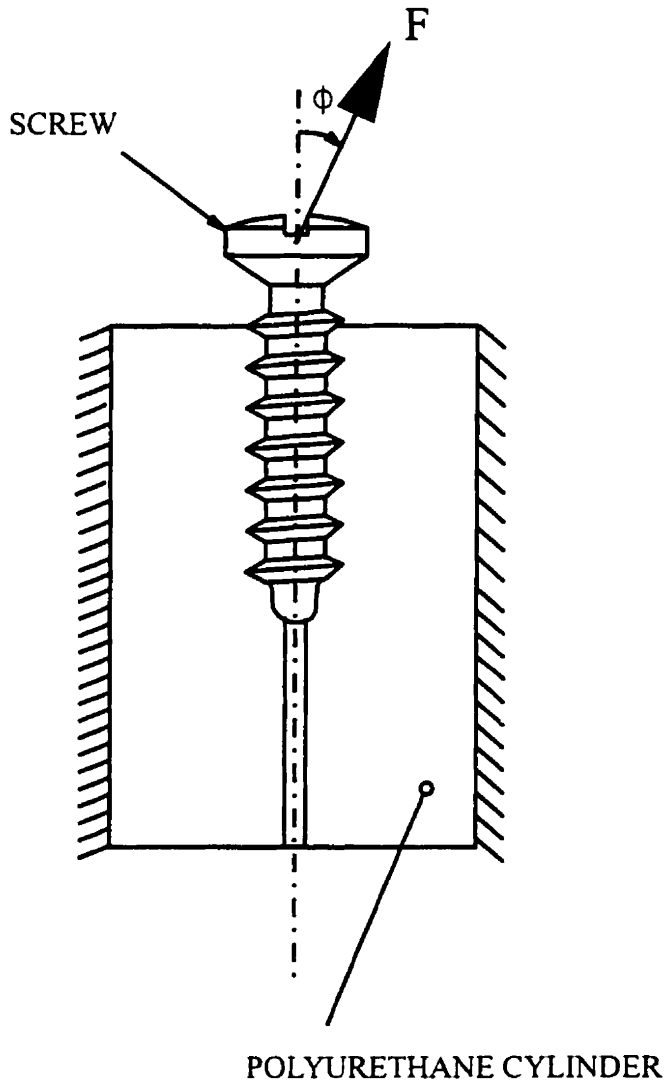

Figure 3.1 The experimental set up for the pull-out tests under inclined loads (i.e., combined loads).

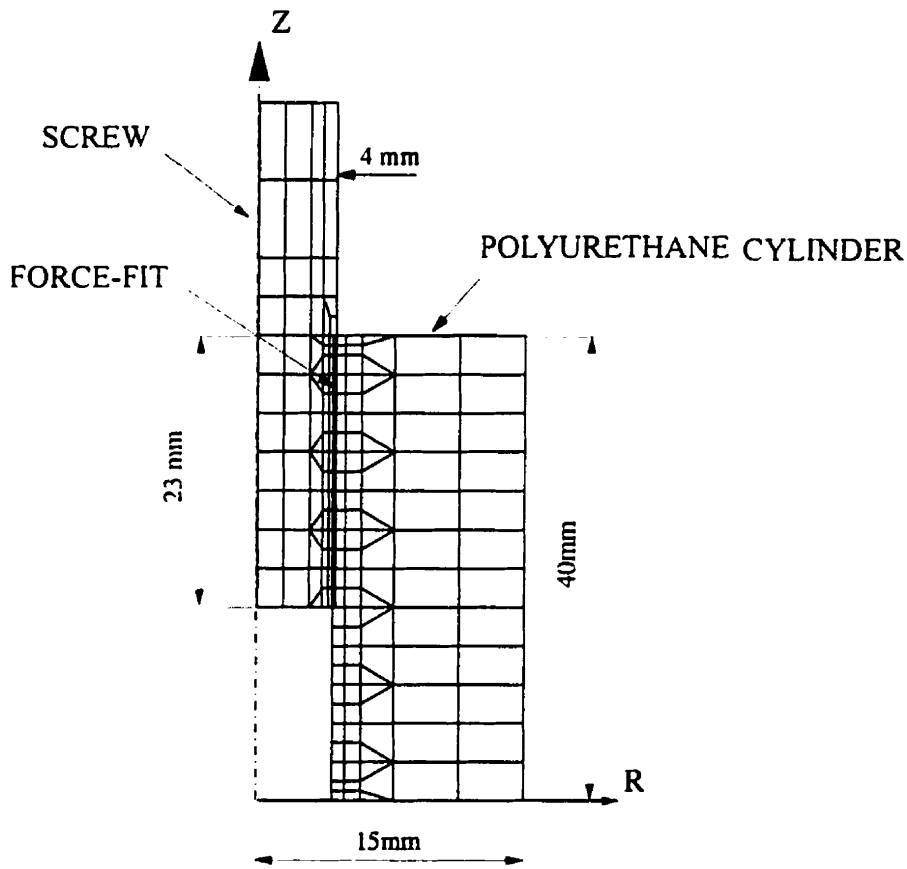

Figure 3.2 The axisymmetric finite element model of the pull-out test of a screw inserted in a polyurethane cylinder.

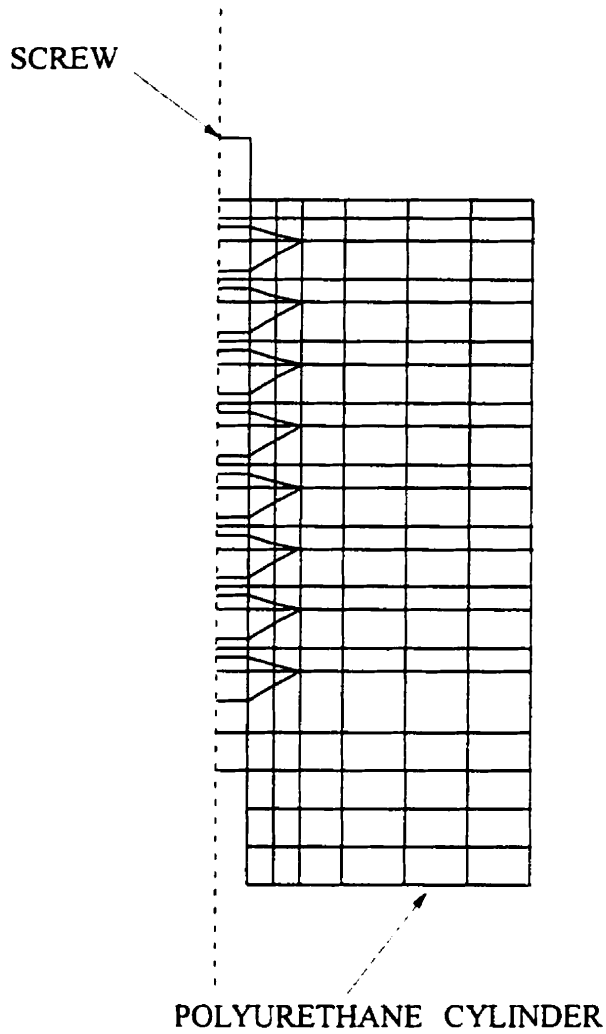

Figure 3.3 Detailed axisymmetric finite element model of the pull-out test of a screw.

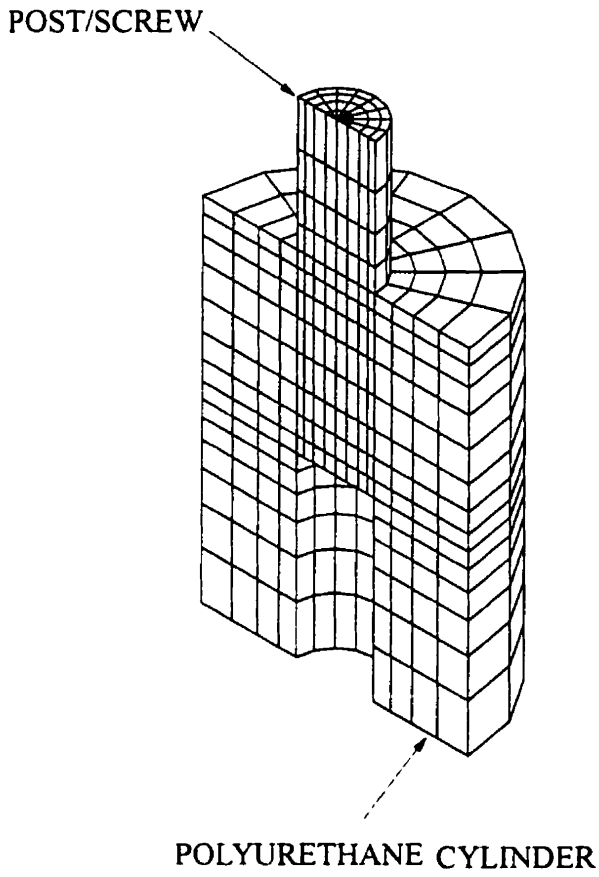

Figure 3.4 A 3D finite element model of the pull-out under combined loads.

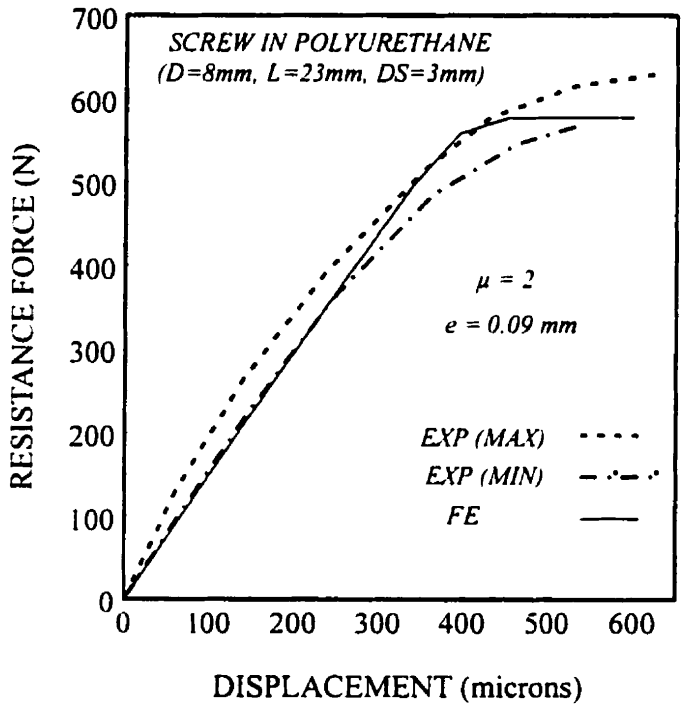

Figure 3.5 Experimental (Shirazi-Adl et al., 1994) and finite element (based on equivalent post) load-displacement responses of a screw inserted in polyurethane cylinder.

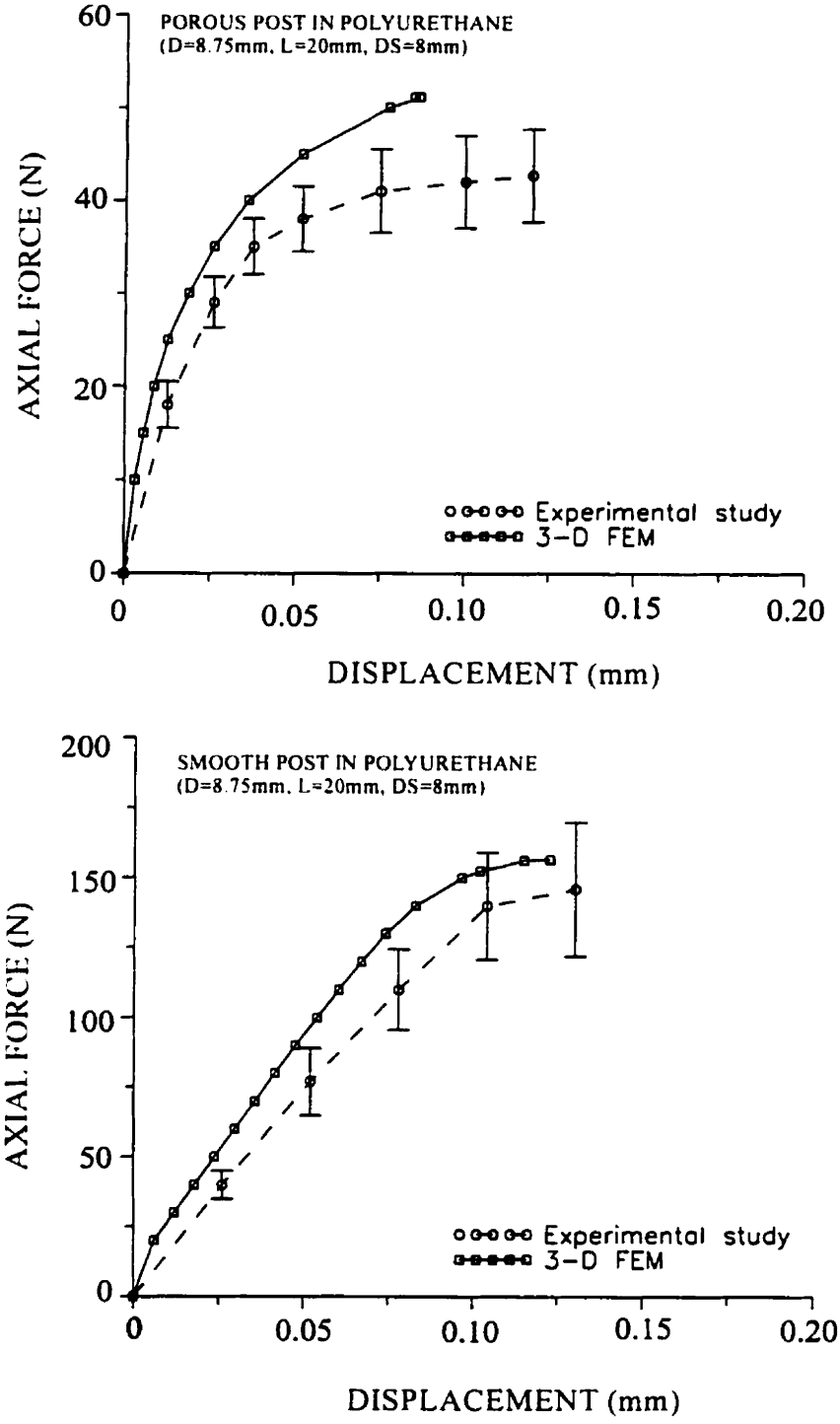

Figure 3.6 Axial pull-out load-displacement behaviour of porous- and smooth-surface posts. Experimental and finite element results (0 deg inclination).

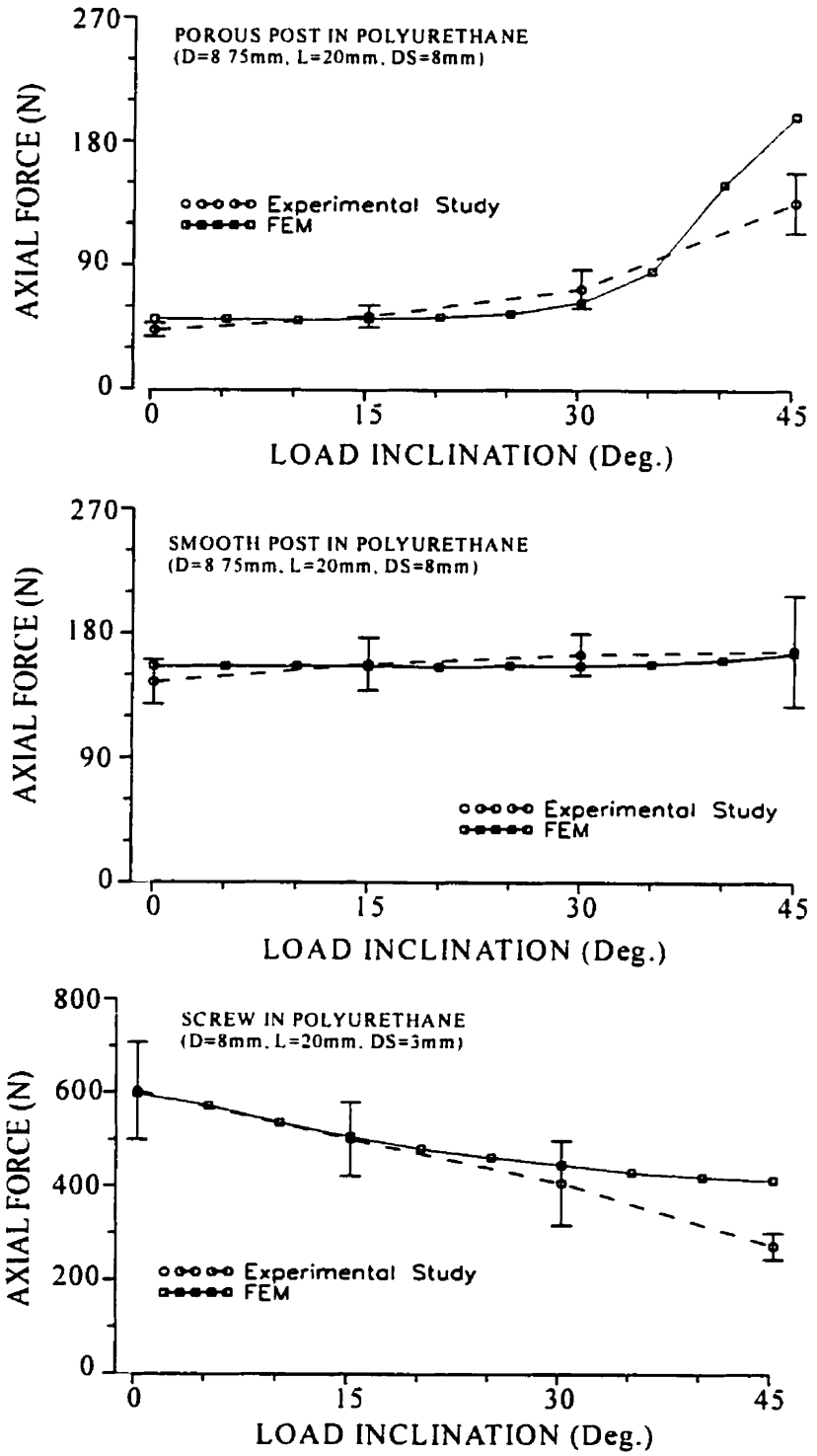

Figure 3.7 The effect of inclination of load on measured (mean ± SD) and predicted axial pull-out forces for posts and screws.

CHAPTER 4

FINITE ELEMENT ANALYSIS OF TIBIAL IMPLANTS - EFFECT OF FIXATION DESIGN AND FRICTION MODEL

4.1 ABSTRACT

A three dimensional nonlinear finite element model was developed to investigate tibial fixation designs and friction models (Coulomb's vs nonlinear) in total knee arthroplasty in the immediate postoperative period with no biological attachment. Bi-directional measurement-based nonlinear friction constitutive equations were used for the bone-porous coated implant interface. Friction properties between polyethylene and femoral component were measured for this study. Linear elastic isotropic but heterogeneous mechanical properties taken from literature were considered for the bone. Tensile behavior of polyethylene was measured and subsequently modeled by an elasto-plastic model. Based on the earlier finite element and experimental pull-out studies, pegs and screws were also realistically modeled. The geometry of every component was obtained through measurements. The PCA tibial baseplate with three different configurations was considered; one with three screws, one with one screw and two short inclined porous-coated pegs, and a third one with no fixation for the sake of comparison. The axial load of 2000N was applied through the femoral component on the medial plateau of articular insert. It was found that Coulomb's friction significantly underestimates the relative micromotion at the bone-implant interface. The lowest micromotion and lift-off were found for the design with screws. Relative

micromotion and stress transfer at the bone-implant interface depended significantly on friction model and on the baseplate anchorage configuration. Cortical and cancellous bones carried, respectively, 11-13% and 65-86% of the axial load depending on the fixation configuration used. The remaining portion was transmitted as shear force by screws and pegs. Normal and Von Mises stresses as well as contact area in the polyethylene insert were nearly independent of the baseplate fixation design. Maximum Von Mises stress in polyethylene exceeded the yield and was found 1-2 mm below the contact surface for all designs.

4.2 INTRODUCTION

During the last three decades considerable interest has been generated in the use of total knee replacement (TKR) as an effective means of reducing the pain associated with arthritis. The success of this technique to restore near-normal mobility at the joint in older subjects has prompted confidence to use the TKR in younger patients as well. Despite its success, failures of the TKR have been observed mainly due to loosening and failure of implant components. Design of implants for adequate fixation to surrounding host bone remains still as a challenge. Various fixation systems are presently used in two distinct types of implants, i.e., cemented and cementless. While in cemented implants, the polymethylmetacrylate (PMMA) is used as the bonding agent to attach the prostheses to the bone, in cementless implants the prostheses is intended to be fixed by biological attachment through bony ingrowth. Therefore, the long-term success of the cementless operation may depend on the achievement of such biological integration (1). Excessive micromotions, stresses, and wear particles at the interface have been suggested to inhibit biological ingrowth and fixation stability.

The finite element (FE) method of structural analysis is recognized as a powerful tool in orthopaedic biomechanics (2). Two dimensional (2D) (3-7), axisymmetric (8-11) and 3D (12-17) FE models

have been employed to investigate the fixation role of different design parameters in total knee replacements. Post length, post rigidity, and bone rigidity have been shown (10,11) to influence stress distribution in the bone. Use of a wider metal tibial plate was recommended to reduce maximum stress in the underlying bone. Two-piece designs with separate components for each condyle have been indicated to lower interface tensile stress as compared with one-piece designs (4,7). In previous model studies, bone mechanical response has been represented as elastic (3-4,7,9-12,16-17) or elasto-plastic (6,14). Nonhomogeneous material properties have been demonstrated to exert greater effect on local stresses than do anisotropic material properties (3,17). In 2-D (6) and 3-D (14) comparative studies of cemented metal tray total condylar (MTTC) and noncemented porous coated anatomic (PCA) tibial plateaus using Coulomb's friction, micromotions and stresses at the interface were found to vary depending on the anchorage design. Keja *et al.* (12) assessed the effects of perimeter fixation versus mid-condylar pin fixation and plate thickness/stiffness on the relative bone-implant micromotion in a 3-D FE model study with frictionless interface elements and heterogeneous bone material properties. Under the axial loading, the component with a perimeter fixation provided better resistance to reversible relative motion than that with peg fixation. Another 3D FE study (16) on the micromotion of total knee tibial component suggested the use of screws for immediate post-surgical fixation to enhance bone ingrowth.

Previous studies considered the bone-implant interface frictionless (11,12) to represent no bony ingrowth or fixed (4,7,17) for either a complete bony ingrowth or a cemented (3,10) implant. Idealized Coulomb's frictional model has also been employed (9,14,16). Recently, measurement-based uni-directional nonlinear friction (18) was demonstrated in a pull-out study to substantially improve predictions. Previous models have often been based on idealized 2D or axisymmetric geometries. Due to irregular bone and implant geometries, loading and nonhomogeneous material distribution, a 3D representation is necessary. Furthermore, majority of the FE studies, simulated the bone-prosthesis interface as frictionless, as perfectly bonded or with idealized Coulomb's

friction. No 3D study of bone-implant structure has yet employed nonlinear friction properties (19-21) measured at the interface between bone and various porous-surfaced implants. In addition, the simulation of posts and screws has often been inadequate.

Wear debris of polyethylene results in periprosthetic osteolysis (bone resorption) and loosening (22-26). A number of factors could play a role in the polyethylene wear; quality of polyethylene (27,28), manufacturing process (26,29) and sterilization method (30-32). The importance of polyethylene thickness, geometry and kinematic conditions has been indicated (24,33-42) recommending the use of polyethylene thickness greater than 6-8 mm for nonconforming surfaces. The more conforming articular geometry has also been suggested; nonconforming designs result in low contact area and high contact stresses exceeding the yield stress of polyethylene. In a retrieval analysis of 48 total condylar prostheses, significant positive correlations were reported for the surface damage with the patient's weight and the time of prosthesis implantation (43) indicating fatigue and cyclic loadings as the cause of damage. Pitting and delamination as a result of fatigue fracture (24,42,44) have been reported as the most severe surface damage modes in articular polyethylene component (23-24,33,41-42). Pitting occurs when crack initiates at the surface and propagates at or below the surface. Once a surface crack has initiated, it can propagate in different modes (45-47). Delamination also takes place when a subsurface fatigue crack propagates parallel to the contact surface. In this failure mode, a layer of material peels away from the surface and creates voids. Microvoids in the material can also initiate a fatigue crack below the contact surface (48). Using the linear elastic fracture mechanics (LEFM), it was shown (49) that a subsurface crack can propagate parallel below the surface for a given loading condition and friction coefficient. Cyclic shear stresses below the contact surface was the main parameter promoting crack propagation resulting in delamination (23,49,50). It is apparent from the above studies that pitting and delamination are a major cause of implant failure. The FE studies performed to evaluate contact stresses at the polyethylene-femoral component interface were initially limited to 2D or

symmetric models. Despite the more recent 3D FE models, the influence of including the whole implant (e.g., tibial tray, resurfaced tibia, implant fixation design configurations) on computed stresses has not been determined. The synergy between micromotion and polyethylene debris in implant response has been suggested in recent studies (51).

The likely coupling between the articular plate and prosthesis-bone structure as particularly related to polyethylene stresses and interface motions have been overlooked. The objectives of the present work were, hence, set to develop a detailed 3D FE model of the bone-implant structure including all the interacting components and to:

-calculate total and relative displacements at the bone-implant interface;

-investigate the effect of different friction models (Coulomb vs nonlinear) on predictions;

-obtain the stress distribution at the cortical and cancellous bone;

-predict the effect of different configuration designs on predictions; and

-obtain the maximum compressive contact and shear stresses in polyethylene insert.

For the purpose of this model study, the Howmedica porous coated anatomic (PCA) knee implant system with two different baseplate fixations were digitized. An additional configuration with no pegs/screws was also used for the sake of comparison. Measured friction and pull-out properties were considered for the representation of bone-implant interface properties (21) and of posts/screws (52). To obtain input data for the model, tensile properties of polyethylene and friction properties at metal-polyethylene interface were measured. It was hypothesized that the design configuration with screws would yield the stiffest response and that the type of interface friction, Coulomb vs nonlinear, would markedly influence the results.

4.3 METHODS

4.3.1 Geometry and meshes

To construct the 3-D geometry of tibia, an adult right tibial specimen of medium size was used. The cancellous bone appeared to be defect and disease free. After removing the soft tissues, the tibia was serially sectioned into parallel slices with thickness of 2.5 mm near the articular surface to 10mm in the diaphyseal region. The sequential slices were digitized to define the boundaries of the model. The thickness of the cortical shell were also measured in different locations. A porous coated modular tibial baseplate (medium size implant, M-2, with 9mm thick insert) (Howmedica, Rutherford, New Jersey) with two fixation configurations was used in the present study. The geometry of the components was obtained by coordinate measuring machine(CMM) and direct measurements. The CMM is a 3D measuring device that uses a probe, generally a sensitive pressure-sensing device, to detect the surface of the object. The linear distances moved along the three axes are recorded, thus providing the X, Y, Z coordinates. The CMM was used to measure the articulating surfaces of the femoral and tibia components. In the directions with larger curvature, points were spaced 1.0 mm apart while in the flat regions 2 mm spacing was considered. These points were entered into an IGES file that was transferred to a CAD system to generate the drawing of each part. The mesh generation was performed by an in-house program. A more refined mesh was considered at the contact regions.

Two different configurations were used, the first included a tibial baseplate with three cancellous screws (8 mm diameter and 32mm length) (Fig. 4.1), the second had one screw in anterior region and two small posteriorly inclined porous coated pegs (8 mm diameter and 10 mm length). For the sake of comparison, another model with a porous coated tibia baseplate with no fixation resting freely on the bone was used. The contact between cortical bone and tibia component was

established everywhere except at a few regions. The mesh included about 10900 eight-node linear brick and six-node linear triangular prism elements and a total of 14300 nodes. Prism elements consisting less than 2% of whole elements were used to fill places with lower stress gradient. About 2500 elements were generated internally by FE software to model the interfaces. The general purpose FE program ABAQUS (ABAQUS, Ver 5.7, 1997) used to carry out this study.

4.3.2 Material properties

Cancellous bone has anisotropy in material properties due to its lattice network structure (53,54). Finite element studies (3,17) have suggested that the effect of the anisotropy of the cancellous bone can be neglected if its heterogeneity is taken into account. Linear elastic modulus in both tension and compression has been suggested for cancellous bone (55). In this study, therefore, a linear elastic isotropic but heterogeneous model was used to model cancellous and cortical material properties. Depending on the region (total of 20 regions), the modulus of elasticity for cancellous bone was varied between 17-340 MPa (56). The modulus of elasticity for cortical bone was considered to increase from 1000 to 9800 MPa from the epiphysis to the mid-diaphysis (11,16). Poisson's ratio of 0.3 was considered for both cancellous and cortical bones (12,57).

The yield stress and modulus of elasticity of polyethylene have been reported to vary between 5-32 MPa and 324-1390 MPa, respectively (58,59). In view of the existing scatter in reported properties, tension tests were performed to obtain the mechanical behavior required for the simulation. Four specimens were obtained from polyethylene inserts (Howmedica) and prepared based on ASTM D638-94B (60) tension tests. The true stress-strain results used in FE studies showed a significant amount of plastic deformation at low stresses (Fig. 4.2). The tension results were in good agreement with those of other studies (38,61). The modulus of elasticity and yield stress were taken as 1083.0 and 13.00 MPa, respectively, while Poisson's ratio was assumed to

be 0.45. An elasto-plastic isotropic hardening model was considered for the polyethylene. The remaining metallic femoral and tibia baseplate components were modeled as linear elastic material with Modulus of elasticity of 220 GPa and Poisson's ratio of 0.3.

4.3.3 Friction properties at bone-implant and polyethylene-metal interfaces

Based on the earlier studies (19-21) the porous coated baseplate-bone interface was modeled using nonlinear friction properties (Fig. 4.3). The same apparatus used to obtain friction characteristics at the bone-metal interface (20,21) was used to obtain friction properties at the polyethylene-smooth metal surface. Specimens of polyethylene block with the contact area of 250mm^2 (12.5mm x 20mm) and 100mm^2 (10mm x 10mm) were obtained directly from polyethylene components (GUR 415 resin, gamma irradiated at 2.5 Mrads, Howmedica Inc). Metallic surface (Vitallium, Howmedica Inc) was prepared to match the surface of femoral component. Mean surface roughness of 1.75 microns and 0.025 microns c.l.a (center line average) were measured for polyethylene and metallic surfaces, respectively. Variation of friction coefficient with contact pressure were also investigated for both dry and wet (with saline) surfaces. Bi-directional tests were performed to investigate the possible coupling phenomenon in response to tangential loads applied in two perpendicular directions. The complete load-displacement response was recorded for each of four specimens used.

Typical experimental results of uni-directional friction tests obtained at the polyethylene-metal interface, wet and dry, are shown in Fig. 4.4a. Friction coefficient for dry contact was slightly higher than that for wet contact. Friction behavior can be represented by Coulomb's friction model; the relative displacement at the interface prior to sliding remained always under 5 microns (not altered by contact pressure or contact surface condition). Statistical analysis revealed a significant effect of contact condition ($p<0.05$) and contact pressure ($p<0.05$) on friction coefficient

(Fig.4.4b). The surface roughness for both polyethylene and metallic surfaces remained unchanged before and after static friction tests. Figure 4.4c shows the insignificant effect of preload ($p>0.05$) on friction coefficient. The interface between polyethylene and metallic femoral condyle was, hence, modeled using Coulomb's friction model. Friction coefficient at the interface was taken as 0.045 for a wet surface condition. The interface between metal baseplate and polyethylene insert was considered to be fixed. This was based on the lock mechanism at the interface which prevents relative motion.

4.3.4 Post and screw models

In the previous pull-out test studies on screws and posts (52), it was found that mechanical behavior of bone screw can be obtained using an equivalent post with friction coefficient of about 2.0. Based on this finding, screws were modeled as posts with the equivalent dimensions. Friction coefficient and initial interference for screws were considered to be 2.0 and 0.025mm, respectively. Since posts used in this study were porous coated, a nonlinear friction curve similar to that at baseplate-bone interface was considered for the bone - post interface. Interference for the post model was 0.025 mm (62). This value was also found to adequately represent the pull-out response under combined loads (52).

4.3.5 Loading and boundary conditions

The compression force of three times body weight (BW), 2000N, was assumed (Morrison, 3 x BW; Collins, 3.9 x BW; Harrington, 3.5 x BW; Kluster *et al.*, 3.9 x BW; Taylor *et al.*, 2.2-2.8 x BW) (63-67). The total force was applied only on the medial femoral condyle to simulate a varus alignment. The distal end of the tibial was fixed in all directions. To prevent rigid body motion, the femoral condyle was constrained in to move vertically only.

4.4 RESULTS

4.4.1 Displacements

Predicted displacements along two typical perpendicular lines at the bone-baseplate interface are shown in Figs. 4.5-4.7 for three design configurations (no fixation, post-fixation and screw-fixation). In contrast to the bone, the baseplate deformation pattern is nearly the same for different designs. In the axial direction, the metallic baseplate shows greater deformation gradient (i.e., bending) at the medial plateau due to the varus compression loading considered. A lift-off (i.e., normal separation of baseplate from the underlying bone) is evident at the far lateral side of the plate. Differences in displacements given in these figures, being largest for the case with no fixation, indicate relative micromotion. Figure 4.8 depicts the final deformed shape of bone-implant structure for the design with pegs. The deformation of the structure to the right is due to the presence of horizontal force at the polyethylene-femoral interface. Similar deformations were also obtained for the other two design configurations.

4.4.2 Micromotions

Figures 4.9a and 4.9b compare the horizontal relative micromotions at the bone-implant interface for three designs. The horizontal micromotions (resultant of X and Y components) and the maximum lift-off (Z component) at the interface are listed in Table 4.1. The largest relative micromotion for all models was obtained at the perimeter of the implant. Figures 4.9a and 4.9b, also, illustrate the relative horizontal micromotions at the bone-baseplate interface for the design with no fixation comparing two interface friction models, i.e., Coulomb's friction and nonlinear bi-directional friction. In this design, friction is the only means for the transfer of shear loads at the interface. Coulomb's friction significantly underestimates the relative displacement in both X and

Y horizontal directions. The maximum relative displacement found at the bone-implant interface is 13.2 and 2.3 microns for Coulomb's friction and 30.0 and 14.8 microns for nonlinear friction in X and Y directions, respectively.

4.4.3 Stresses

Normal contact stress at the bone-implant interface along the M-L and A-P directions are shown in Fig. 4.10 for different fixation systems. Posts and screws transmit a portion of the applied axial load through shear stresses (Table 4.2) thereby resulting in lower normal contact stress at the bone-baseplate horizontal interface (Table 4.3). For the design with screws, the medial screw alone carries nearly half the total 22.9% resisted by all three screws. In fixations with screws or screw/pegs, nearly 5.5% of the load is resisted by the anterior screw. Figure 4.11 presents the normal contact stress distribution in which maximum contact stress at medial region reaches 2.99 MPa for no fixation design, 2.81 MPa for the design with pegs and 2.56 MPa for that with screws. In both cortical and cancellous bone, the lowest maximum normal contact stress is found for the design with screws as listed in Table 4.3. Interface resultant shear stress, not shown, follow the same pattern as those given for normal contact stresses. Contact surface area is about 16.0 mm^2 and 2050.0 mm^2 for the baseplate-cortical bone and baseplate-cancellous bone, respectively. The average normal stress at the interface between post/screw and bone are 1.2, 1.2 and 0.4 MPa for medial, lateral and posterior regions, respectively.

As for the polyethylene insert, maximum Von Mises and contact stresses computed are listed in the Table 4.4, for all design configurations. Due to negligible differences between contact and Mises stresses between design configurations, the stress distribution is presented only for the design with no fixation. The maximum contact stress occurs at the contact surface while maximum Mises stress is 1-2 mm below the articular surface. Maximum normal axial stress is found to be 48.1 MPa

and compressive, for this design configuration. Figure 4.12 presents the Mises stress, minimum principal stress, and normal axial stress within the polyethylene at the medial site. Minimum principal stress is 49.4 MPa (in compression) and occurs at the contact surface similar to that of maximum normal compression stress. Maximum Mises stress of 23.10 MPa occurs about 1 mm below the contact surface. Total articular contact area is computed to be about 61.5mm^2 for all fixation configurations resulting in an average contact stress of 33.0 MPa.

4.5 DISCUSSION

The objective of this study was to develop a 3D finite element model of a knee-implant structure to investigate the mechanical fixation and stability of different design configurations under static conditions. For this purpose, nonlinear bi-directional friction properties between bone and porous coated metal plate were considered and compared with the idealized Coulomb's friction. Geometry of the tibia and implant components were obtained by direct measurements whereas the required mechanical properties of constituent materials and contacting interfaces were either measured experimentally or taken from the literature. An elasto-plastic isotropic hardening model was considered for the articular polyethylene insert. A load of approximately three times the body weight was applied at the medial condyle simulating a case with a varus alignment. The number of loading and design configurations considered were limited due to the complexity of models/analyses (~35000 degrees of freedom). It should be emphasized that the material and interface properties used in this study are adversely affected by fatigue loadings; the predictions, hence, should not be applied over longer term conditions. Moreover, the interface conditions considered here represent those at the immediate post-surgical period in which neither bony ingrowth nor fibrous attachment has occurred, not at least to an important extent. In such cases, the friction is the sole mechanism of shear transfer between two opposing surfaces. Any substantial deviation expected in a longer term would violate the basic assumptions and require additional attentions.

4.5.1 Mechanical and friction properties of the polyethylene

A good agreement was obtained between the measured mechanical properties for polyethylene (Fig.4.2) and those presented by others (38,61). The stress-strain curve for polyethylene was highly nonlinear which should be accounted for in realistic model studies; linear elastic model has been shown to overestimate stresses by 25% (37). The measured friction coefficient at the metal-polyethylene interface varying between 0.05-0.10 and 0.04-0.08 for dry and wet surfaces, respectively, was found in the range of values reported in the literature using pin-on-disc testing apparatus (68-71). It was also noticed, in agreement with the previous friction tests (68,70), that the maximum interface resistance (or friction coefficient) diminishes as the contact pressure increases. Bi-directional tests revealed that the friction coefficient remained almost unchanged irrespective of the presence of a tangential preload suggesting a weak or no coupling between different directions. This is in contrast to the friction results obtained at the cancellous bone-porous coated metal interfaces (21). An idealized Coulomb's curve was, hence, taken for the metal-polyethylene interface whereas the bone-porous coated metal interface was represented with a nonlinear bi-directional friction.

4.5.2 Displacements

Plate displacements predicted in this study were consistent with those reported in the previous experimental and numerical studies (5,14,16,72). Displacement magnitudes (Figs. 5-7) for the tibial implant varied depending on the prosthetic design used. Displacement in the axial (Z) direction showed the least dependency on the fixation configuration, particularly in the A-P (sagittal) plane. Displacements at the bone-implant interface nodes were higher in the X (M-L) direction (i.e., about 160-200 μm) than in the Y (A-P) direction (i.e., about 40-75 μm). Displacement at the interface was found to be greater at the bone than at the implant. The lift-off at the lateral region led to a gap

between bone and the implant reducing the effective contact area (73) and increasing, in turn, the compressive load and, hence, subsidence in the opposite medial region. Screw fixation (Table 4.1) provided the least lift-off followed by the post fixation. Miura *et al.* (74) found that, in presence of screws, the lift-off was reduced by more than 90%.

4.5.3 Micromotion

Incompatibility between the bone and implant displacements at the interface generates relative micromotions which were largest in the design with no fixation. The design with screws followed by that with a screw and two pegs yielded the stiffest response which is in agreement with the literature (18,73-78). In accordance with other studies (16,18,21), it was found that the interface friction model significantly influenced the relative micromotion in both M-L and A-P directions. Coulomb's friction, as compared with the nonlinear friction model, considerably underestimated tangential relative micromotions, an observation made by others as well (18,21). The maximum micromotion for screw and post fixation designs was computed to remain below 28 μm which has been reported (79-80) to be compatible with bony ingrowth. Excessive relative motions can decrease bone proliferation into surface pores of implant (81,82). For all design configurations, the maximum micromotion occurred at the perimeter of the implant.

Tissakht et al. (16) measured the maximum relative micromotion to be 5 μm at the bone-implant interface. They applied a 1000 N load in the center of top of the surface of the implant fixed with 4 short pegs/screws. The 3-D FE study predicted that the maximum relative micromotion varies from about zero for interface with friction coefficient of 0.45 to 7.5 μm for the frictionless interface. For screw fixation, even lower micromotion was predicted. The magnitude of the maximum relative micromotion they obtained experimentally and numerically is the lowest reported in the literature. On the other hand, Keja et al. (12) predicted the largest maximum relative micromotion for peg

(PCA) (up to 100 μm) and knife edge design configurations (up to 90 μm). They applied a symmetric load of 2500 N on each condyle and modeled the interface between implant and bone as frictionless to yield the maximum possible relative micromotion. Considering the differences in the location and magnitude of the load, geometry and friction model used by others, the results of the present study is well situated in the range of the reported results (4-5,7,12,14,16).

4.5.4 Stresses and load transfer

Normal contact stress at the bone-implant interface varied depending on the design. The maximum contact stress at the cancellous bone-implant interface (i.e., 2.81 MPa for the design with pegs and 2.56 MPa for that with screws computed at the medial boundary adjacent to the loaded area) is in the range of values reported by other finite element studies (4-5, 10, 14). Design with screws/pegs yielded lower interface contact stresses due to the partial transmission of the applied compression load via shear forces across the vertical interfaces between bone and screws/pegs. In screw-fixation design, 23% of axial load was transmitted in this manner as compared with 7% in the post-fixation design (Table 4.2). An increase in interface interference (force-fit) could increase the foregoing proportions whereas repetitive fatigue loading tends to decrease them (63). An increase in interference is known (9) to be favorable to bone ingrowth due to larger resistance to micromotion.

Apart from the screws/pegs, the total force carried by the cancellous bone (with a total contact area of ~ 2050.0 $mm^{2)}$ and cortical bone (with contact area of ~16.0 mm^2) varied between 65-86% and 11-13% of total axial force, respectively, with the least values computed for the design with three screws. In the present study the contact between the cortical bone and tibial baseplate occurred almost everywhere except in some regions due to the irregularity in the bone geometry. The use of implant-cortex contact to transmit loads has been encouraged (10,83). Such contact

can reduce excessive stresses in the underlying cancellous bone. However, resting of the implant edge on the cortical shell has been indicated by finite element studies (11) to have negligible effect on the interface micromotions. Due to higher stiffness of the cortical bone to that of cancellous bone, higher normal contact stresses are expected for cortical bone (Table 4.3). Stresses under the tray at the screw/post areas are lower for plates with fixation than that without fixation (Figures 10,11). The reduction of the normal stress at these regions can explain the clinical observations (83-84) in which formation of fibrous tissue and not bone ingrowth was seen at the bone-implant interface around the screw/post areas.

4.5.5 Polyethylene

A major problem reported in the TKR is the polyethylene wear which could cause component failure and periprosthetic osteolysis. Factors such as patient weight, gender, level of activity and age could play a role in the rate of polyethylene wear (23-24,41-43,36,58). Fracture mechanics studies have identified the high contact stresses and fatigue cracks in polyethylene as the cause of wear. In agreement with previous studies (34,41,85), the predicted magnitude of normal contact stress (48.0 MPa) was found well beyond the yield stress (13.0 MPa). High axial compressive stress which exceeds material yield point can initiate crack and cause fracture. Once a surface crack has initiated, it can propagate in different modes (42-44). The hydrostatic component of stress is not, however, associated with damage; it has been shown (36) that polyethylene can withstand contact stresses that are significantly greater than its yield stress. The damage is mainly caused by the distortion of the material as reflected in the Mises stress. Maximum Mises stress at polyethylene plate was predicted to occur below the contact surface the location of which was found to be independent of the fixation design. The magnitude of the maximum Mises stress, being comparable to that of others (38,58), was found to be independent of the fixation configuration, as well. It appears, therefore, that the adequate modeling of bone-baseplate interface might not be

as crucial if calculation of polyethylene stresses are of primary concern. The results could also alter for thinner polyethylene inserts less than 7mm. Stresses in polyethylene have been reported to depend amongst others on its thickness and conformity (26-30). The thickness has been recommended to be at least 6-8 mm. Retrieval analyses have indicated that wear resistance depends on the relative conformity of the articulating surfaces (33-34,42). It has been indicated (41) that the capture mechanism of the insert to baseplate affects the rate of polyethylene wear. In the current study, however, a fixed interface between the polyethylene and the metal tray was assumed due to the presence of a lock mechanism preventing polyethylene from sliding.

In summary, -friction coefficient for polyethylene measured between 0.045 to 0.09 depending on the surface condition and contact pressure; -the Coulomb's friction underestimated the predicted micromotions and nonlinear friction should be considered in the knee-implant analysis; -screw fixation design followed by post fixation design considerably reduced micromotions and lift-off; -maximum micromotion was obtained at the perimeter of the implant for all the configurations; -about 11-13% of total axial load was carried by the cortical bone while cancellous bone transferred 65-86% depending on the fixation with the remaining portion transmitted through screws and pegs; -polyethylene stresses were independent of design configuration; -maximum Mises stress occurred at 1-2 mm below the contact surface within the polyethylene while the maximum normal stress was predicted to be at the contact surface.

Acknowledgment The first author is grateful for a scholarship granted by the Ministry of Culture and Higher Education, I.R. Iran. The present work was partly supported by a grant from the NSERC-Canada. The implant was provided by Howmedica. The assistance of Dr. M. Dammak in friction tests, Y. Mir in providing information concerning CMM and G. Giron in performing the CMM measurement is also gratefully appreciated.

REFERENCES

1. C.L. Peters and A.G. Rosenberg (1995), "Bone ingrowth and total knee replacement", *The knee*, **1**, 189-196.
2. R. Huiskes and E. Y. S. Chao (1983), "A survey of finite element analysis in orthopaedic biomechanics: the first decade", *Journal of Biomechanics*, **16**, 385-409.
3. M.J. Askew and J.L. Lewis (1981), "Analysis of model variables and fixation post length effects on stresses around a prosthesis in the proximal tibia", *Journal of Biomechanical Engineering*, **103**, 239-245.
4. G. S. Beaupre. R. Vasu, D. R. Carter, and D.J. Schurman (1986), " Epiphyseal-based designs for tibial plateau components-ii .stress analysis in the sagittal plane", *Journal of Biomechanics*, **19**, 663-673.
5. J.L. Lewis, M.J. Askew, and D.P. Jayeox (1982), "A comparative evaluation of tibial component designs of total knee prostheses", *The Journal of Bone and Joint Surgery*, **64A**, 129-135.
6. R. L. Rakotomanana, P.F. Leyvraz, A. Curnier, J.H. Heegaard, and P.J. Rubin (1992), "A finite element model for evaluation of tibial prosthesis-bone interface in total knee replacement", *Journal of Biomechanics*, **25**, 1413-1424.
7. R. Vasu, D.R. Carter, D.J. Schurman, and G.S. Beaupre (1986), "Epiphyseal-based designs for tibial plateau components-i. stress analysis in the frontal plane", *Journal of Biomechanics*, **19**, 647-662.
8. A. M. Ahmed, M. Tissakht, S.C. Shirvastava, and K. Chan (1990), "Dynamic stress response of the implant/cement interface : An axisymmetric analysis of a knee tibial component", *Journal of Orthopaedic Research*, **8**, 435-447.
9. J. M. Dawson and D.L. Bartel (1992), "Consequences of an interface fit on the fixation of porous-coated tibial components in total knee replacement", *The Journal of Bone and*

Joint Surgery, **74A**, 233-238.

10. K. Murase, R.D. Crowninshield, D.R. Pedersen, and T.S. Chang (1983),"An analysis of tibial component design in total knee arthroplasty", *Journal of Biomechanics*., **16**, 13-22.
11. A. Shirazi-Adl and A.M. Ahmed (1989),"A parametric axisymmetric study on the interface motions in porous-surfaced tibial implant", *Annuals of Biomedical Engineering*, **17**, 411-421.
12. M. Keja, H.W. Wevers, D. Siu, and H. Grootenboer (1994), "Relative motion at the bone-prosthesis interface", *Clinical Biomechanics*, **9**, 275-283.
13. R. Natarajan and T.P. Andriacchi (1989), "New analytical method for the analysis of bone ingrowth in porous tibial component", *San Diego, ASME Biomechanics Symposium*, 281-284.
14. R. L. Rakotomanana, P.F. Leyvraz, A. Curnier, J-J. Meister, and J-J. Livio (1994), "Comparison of tibial fixations in total knee arthroplasty: An evaluation of stress distribution and interface micromotions", *The Knee*, **1**, 91-99.
15. A.B. Strickland, R. Natarajan, and T.P. Andriacchi (1989), "Transverse motion at the interface between the tibial component and bone in a total replacement: an analytical model", *AMD (ASME, Applied Mechanics Division), Biomechanics Symposium, Third joint ASCE/ASME Mechanics Conference*, 285-288.
16. A. Tissakht, H. Eskandari, and A. M. Ahmed (1995), "Micromotion analysis of the fixation of total knee tibial component", *Computers and Structures*, **56**, 365-375.
17. E. J. Cheal, W. C. Hayes, C. H. Lee, B. D. Snyder, and J. Miller (1985), "Stress analysis of a condylar knee tibial component: Influence of metaphyseal shell properties and cement injection depth", *Journal of Orthopaedic Research*, **3**, 424-434.
18. M. Dammak, A. Shirazi-Adl and D. J. Zukor (1997), "Analysis of cementless implants using interface nonlinear friction - Experimental and finite element studies",*Journal of Biomechanics*, **30**, 121-129.

19. D. Rancourt, A. Shirazi-Adl, G. Drouin and G. Paiment (1990), "Friction properties of the interface between porous-surfaced metals and tibial cancellous bone", *J. Biomed. Mater. Res.*, **24**, 1503-1519.

20. A. Shirazi-Adl, M. Dammak and G. Paiement (1993), "Experimental determination of friction characteristics at the trabecular bone/porous-coated metal interface in cementless implants", *Journal of Biomedical Materials Research*, **27**, 167-175.

21. A. Hashemi, A. Shirazi-Adl and M. Dammak (1996), "Bi-directional friction study of cancellous bone-porous coated metal interface", *Journal of Biomedical Materials Research(Applied Biomaterials)*, **33**, 257-267.

22. J. F. Nolan and T. M. Bucknill (1992), "Aggressive granulomatosis from polyethylene failure in an uncemented knee replacement", *The Journal of Bone and Joint Surgery*, **74B**, 23-24.

23. T.M. Wright and D. L. Bartel (1986), "The problem of surface damage in polyethylene total knee components", *Clinical Orthopaedics and Related Research*, **205**, 67-74.

24. R. M. Rose, M. D. Ries, I. L. Paul, A. M. Crugnola, and e. Ellis (1984), "On the true wear rate of ultrahigh molecular weight polyethylene in the total knee prosthesis", *Journal of Biomedical Materials Research*, **18(2)**, 207-224.

25. D. J. Kilgus, J. R. Moreland, G. A. M. Finerman, T. T. Funahashi, and J. S. Tipton (1991), "Catastrophic wear of tibial polyethylene inserts", *Clinical Orthopaedics and Related Research*, 273, 223-231.

26. S. M. G. Jones, I. M. Pinder, C. G. Moran, A. J. Malcolm (1992), "Polyethylene wear in uncemented knee replacements", *The Journal of Bone and Joint Surgery*, **74B**, 18-22.

27. M. G. Tanner, L. A. Whiteside, and S. E. White (1995), "Effect of polyethylene quality on wear in total knee arthroplasty", *Clinical Orthopaedics and Related Research*, **317**, 83-88.

28. P. S. Walker, G. W. Blunn and A. Lilley (1996), "Wear testing of materials and surfaces for total knee replacement", *Journal of Biomedical Materials Research (Applied Biomaterials)*, **33**, 159-175.

29. L. Pruitt, L. Bailey, and R. Nassiri (1997), "The role of manufacturing process on the fatigue crack propagation resistance of medical grade ultra high molecular weight polyethylene", *43rd Annual Meeting, Orthopaedic Research Society*, 790.

30. C. J. Bell, J. Simmons, P. King, P. S. Walker, and G. W. Blunn (1997), "Is oxidation of ultra high molecular weight polyethylene the main cause of delamination wear in total knee replacement", *43rd Annual Meeting, Orthopaedic Research Society*, 96 - 16.

31. M. Deng and S. W. Shalaby (1995), "Effects of gamma irradiation, gas environments, and post irradiation aging on ultrahigh molecular weight polyethylene", *Journal of Applied Polymer Science*, **58**, 2111-2119.

32. V. K. Polineni, A. Essner, A. Wang, C. Stark, and J. H. Dumbleton (1997), "Effect of sterilization methods on the wear behavior of UHMWPE acetabular cups - A hip joint wear simulator study", *43rd Annual Meeting, Orthopaedic Research Society*, 779.

33. J. P. Collier, M. B. Mayor, J. L. McNamara, V. A. Surprenant, and R. E. Jenses (1991), "Analysis of the failure of 122 polyethylene inserts from uncemented tibial knee components", *Clinical Orthopaedics and Related Research*, **273**, 232-242.

34. K. J. Chillag, and E. Barth (1991), "An analysis of polyethylene thickness in modular total knee components", *Clinical Orthopaedics and Related Research*, **273**, 261-263.

35. G. W. Blunn, P. S. Walker, A. Joshi, and K. Hardinge (1991), "The dominance of cyclic sliding in producing wear in total knee replacements", *Clinical Orthopaedics*, **273**, 253-260.

36. G. A. Engh, K. A. Dwyer, C. K. Hanes (1992), "Polyethylene wear of metal-backed tibial components in total and unicompartmental knee prostheses", *The Journal of Bone and Joint Surgery*, **74B**, 9-17.

37. D. C. DeHeer and B. M. Hillberry (1992), "The effect of thickness and nonlinear material behavior on contact stresses in polyethylene tibial components", *38th Annual Meeting, Orthopaedic Research Society*, 327.

38. D. L. Bartel, J. J. Rawlinson, A. H. Burstein, C. S. Ranawat and W. F. Flynn (1995), "Stresses in polyethylene components of contemporary total knee replacements", *Clinical Orthopaedics and Related Research*, **317**, 76-82.

39. H. Ishikawa, H. Fujiki, and K. Yasuda (1996), "Contact analysis of ultra high molecular weight polyethylene articular plate in arthificial knee joint during gait movement", *Journal of Biomechanical Engineering*, **118**, 377-386.

40. S. Sathasivam and P. S. Walker (1997), "A computer model with surface friction for the prediction of total knee kinematics", *Journal of Biomechanics*, **30(2)**, 177-184.

41. L. Mintz, A. K., Tsao, C. R. McCrae, S. C., Stulberg, and T. Wright (1991), "The arthroscopic evaluation and characteristics of severe polyethylene wear in total knee arthroplasty", *Clinical Orthopaedics and Related Research*, **273**, 215-222.

42. M. Landy and P. S. Walker (1985), "Wear in condylar replacement knees - A 10 year follow up", *31st Annual Meeting, Orthopaedics Research Society*, 96.

43. R. W. Hood, T. M. Wright, and A. H. Burstein (1983), "Retrieval analysis of total knee prostheses: A method and its application to 48 total condylar prostheses", *Journal of Biomedical Materials Research*, **17**, 829-842.

44. D. A. Heck, J. K. Clingman, and D. G. Kettelkamp (1992), "Gross polyethylene failure in total knee arthroplasty", *Orthopaedics*, **15**, 23-28.

45. L. M. Keer, M. D. Bryant, and G. K. Hariots (1982), "Subsurface and surface cracking due to Hertzian contact", *Journal of Lubrication Technology*, **104(3)**, 347-351.

46. L. M. Keer and M. D. Bryant (1983), "A pitting model for rolling contact fatigue", *Journal of Lubrication Technology*, **105(2)**, 198-205.

47. Y. Murakami, M. Kanata, and H. Yatsuzka (1985), "Analysis of surface crack

propagation in lubricated rolling contact", *ASLE Transactions*, **28(1)**, 60-68.

48. S. Jahanmir and N. P. Suh (1977), "Mechanics of subsurface void nucleation in delamination wear", *Wear*, **44(1)**, 17-38.

49. J. R. Fleming and N. P. Suh (1977), "Mechanics of crack propagation in delamination wear", *Wear*, **44(1)**, 39-56.

50. S. Sheppard, J. R. Barber and M. Comninou (1985), "Short subsurface cracks under conditions of slip and stick caused by a moving compressive load", *Journal of Applied Mechanics*, **52(4)**, 811-817.

51. J.E. Bechtold, K. Soballe, S. Overgaard, J.L. Lewis and R.B. Gustilo (1997), "Synergy between implant motion and particulate polyethylene in the formation of an aggressive periprosthetic membrane", *43rd Annual Meeting, Orthopaedic research Society*, 767.

52. M. Dammak, A. Hashemi, A. Shirazi-Adl and D. J. Zukor (1996), "Experimental and finite element fixation studies of posts and screws", *Engineering Systems Design and Analysis, ASME*, **PD-Vol.77**, 11-18.

53. L.J. Gibson (1985), "The Mechanical behavior of cancellous bone", *Journal of Biomechanics*, **18(5)**, 317-328.

54. R. B. Ashman, J. Y. Rho and C. H. Turner (1989), "Anatomical variation of orthotropic elastic moduli of the proximal human tibia", *Journal of Biomechanics*, **22**, 895-900.

55. T. M. Keavney, X. E. Guo, E. F. Wachtel, T. A. McMahon and W. C. Hayes (1994), " Trabecular bone exhibits fully linear elastic behavior and yields at low strains", *Journal of Biomechanics*, **27**, 1127-1136.

56. S. A. Goldstein, D. L. Wilson, D. A. Sonstegard and L. S. Matthews (1983), "The mechanical properties of human tibial trabecular bone as a function of metaphyseal location", *Journal of Biomechanics*, **16**, 965-969.

57. R. B. Little, H. W. Wevers, D. Siu and T. D. V. Cooke (1986), "A three dimensional finite element analysis of the upper tibia", *Journal of Biomechanical Engineering*, **108**,

111-119.

58. D. L. Bartel, V. L. Bicknell and T. M. Wright (1986), "The effect of conformity, thickness, and material on stresses in ultra-high molecular weight components for total joint replacement", *Journal of Bone and Joint Surgery*, **68A**, 1041-1051.

59. J.L. McNamara, J.P. Collier, M.B. Mayor and R.E .Jensen (1994), "A comparison of contact pressures in tibial and patellar total knee components before and after service in vivo", *Clinical Orthopaedics and Related Research*, **299**, 104-113.

60. American Society for Testing and Materials: Standard D638M-94b; Tensile properties of plastic (metric) (1994), *In: Annual Book of ASTM standards*, part 8.01, 167-175.

61. S. M. Kurtz, C.M. Rimnac, T. J. Santner and D. L. Bartel (1996), "Exponential model for the tensile true stress-strain behavior of as-irradiated and oxidatively degraded ultra high molecular weight polyethylene.", *Journal of Orthopaedic Research*, **14**, 755-761.

62. A. Shirazi-Adl, M. Dammak and D. J. Zukor (1994), " Fixation pull-out response measurement of bone screws and porous-surfaced posts", *Journal of Biomechanics*, **27**, 1249-1258.

63. J.B., Morrison (1970), "The mechanics of the knee joint in relation to normal walking", *Journal of Biomechanics*, **3**, 51-61.

64. J. J. Collins (1995), "The redundant nature of locomotor optimization laws, *Journal of Biomechanics*, **28**, 251-267.

65. I. J. Harrington (1976), "A bioengineering analysis of force actions at the knee in normal and pathological gait", *Biomedical Engineering*, **11**, 167-172.

66. M.S. Kluster, G.A. Wood, G.W. Stachowiak, and A. Gachter (1997), "Joint load considerations in total knee replacement", *The Journal of Bone and Joint Surgery*, **79B**, 109-113.

67. S.J. Taylor, P.S. Walker, J. Perry, S.R. Cannon and R. Woledge (1997), "The forces in the distal femur and knee during different activities measured by telemetry", 43rd Annual

Meeting, *Orthopaedic Research Society*, 259.

68. S.H. Benabdallah (1993), "The running-in and steady-state coefficient of friction of some engineering thermoplastics", *Polymer Engineering and Science*, **33(2)**, 70-74.

69. B.B., Seedhom, D. Dowson, and V. Wright (1973), "Wear of solid phase formed high density polyethylene in relation to the life of arthificial hips and knees", *Wear*, **24**, 35-51.

70. W.R. Jones, (1984), "Friction and wear properties of a Charnley artificial hip joint", *ASLE Transactions*, **28(3)**, 389-399.

71. R.L. Fusaro, (1983), "Friction, wear, transfer, and wear surface morphology of ultrahigh-molecular-weight polyethylene", *ASLE Transactions*, **28(1)**, 1-10.

72. L. Ryd, A. Lindstrand, A. Stenstorm, and G. Selvik (1990), "Porous coated anatomic tricompartmental tibial components: the relationship between prosthetic position and micromotion", *Clinical Orthopaedics*, **251**, 189-197.

73. R. W. B. Wyatt, J. P. Alpert, A. U. Daniel, A. A. Hofmann and H. K. Dunn (1991), " The effect of screw fixation on the initial rigidity of tibial knee components", *Journal of Applied Biomaterials*, **2**, 109-113.

74. H. Miura, L. A. Whiteside, J. C. Easley and D. D. Amador (1991), "Effects of screws and a sleeve on the initial fixation in uncemented total knee tibia components", *Clinical Orthopaedic and Related Research*, **259**, 160-168.

75. A. D. Kaiser and L. A. Whiteside (1990), " The effect of screws and pegs on the initial fixation stability of an uncemented unicondylar knee replacement", *Clinical Orthopaedics and Related Research*, **259**, 169-178.

76. R. W. Lee, R. G., Volz and D. C. Sheridan (1991), " The role of fixation and bone quality on the mechanical stability of tibia knee components", *Clinical Orthopaedics and Related Research*, **273**, 177-183.

77. R. G. Volz, L. K. Nisbet, R. W. Lee and M. G. McMurtry (1988), " The mechanical stability of various noncemented tibial components", *Clinical Orthopaedics and Related*

Research, **226**, 38-42.

78. D. R. Sumner, A. Berzins, T. M. Turner, R. Igloria, R. N. Natarajan (1994), "Initial in vitro stability of the tibial component in a canine model of cementless total knee replacement", *Journal of Biomechanics*, **27**, 929-939.

79. R. M. Pilliar, J. M. Lee and C. Miniatopoulos (1986), "Observations of the effects of movement on bone ingrowth into porous-surfaced implants", *Clinical Orthopaedic*, **208**, 108-113.

80. M. Jasty, C. Bragdon, D. Burke, D. O'Connor, J. Lowenstein and WH Harris (1997), "In vivo skeletal responses to porous-surfaced implants subjected to small induced motions", *Journal of Bone and Joint Surgery*, **79-A(5)**, 707-714, 1997.

81. H. U. Cameron, R. M. Pilliar and I. Macnab (1973), "The effect of movement on the bonding of porous metal to bone", *Journal of Biomedical Materials Research*, 7, 301-311.

82. P. Ducheyne, P. DeMeester, E. Aernoudt, M. Martens and C. Mulier (1997), "Consequences of an interface fit on the fixation of porous-coated tibial components in total knee replacement", *Journal of Biomedical Materials Research*, **11**, 811-838.

83. R. B. Bourne, J. B. Finlay, "The influence of tibia component intramedullary stems and implant - cortex contact on the strain distribution of the proximal tibia following total knee arthroplasty", *Clinical Orthopaedic and Related Research*, **208**, 95-99.

84. B. F. Morrey, E. Y. S. Chao (1988), "Fracture of the porous-coated metal tray of a biologically fixed knee prosthesis", *Clinical Orthopaedic and Related Research*, **228**, 182-189.

85. J. A. Szivek, P. L. Anderson, and J. B. Benjamin (1996), "Average and peak contact stress distribution evaluation of total knee arthroplasties", *Journal of Arthroplasty*, **11**, 952-963.

Table 4.1. Average and Maximum Magnitude of Relative Micromotion at the Bone-Implant Interface for all Fixation Configurations.

Fixation configuration	Micromotion [μm]				Maximum lift-off [μm]
	Average		Maximum		
	X	Y	X	Y	
Free	9.3	3.0	30.0	14.8	25.4
Posts and screw	6.2	1.7	27.4	13.9	23.1
Screws	3.2	3.9	21.2	5.1	21.6

Table 4.2: Percentage of Normal Load Carried by Each Component at the Bone-Implant Interface for all Fixation Configurations.

Fixation configuration	Percentage of normal load carried by		
	Cancellous	Cortical	Screws/Posts
Free	86.5%	13.5%	-
Posts and screw	81.5%	11.3%	7.2%
Screws	65.5%	10.6%	22.9%

Table 4.3. Maximum Normal Contact Stresses (MPa) Predicted at the Cortical/Cancellous-Implant Interface.

Fixation configuration	Maximum normal contact stress	
	Cortical	Cancellous
Free	18.4	2.99
Posts and screw	13.1	2.81
Screws	12.5	2.56

Table 4.4: Maximum Mises and Normal Compressive Stresses (MPa) in the Polyethylene

Fixation Configuration	Mises	Stress (S_{zz})
Free	23.10	48.03
Posts and screw	23.23	48.47
Screws	23.22	48.31

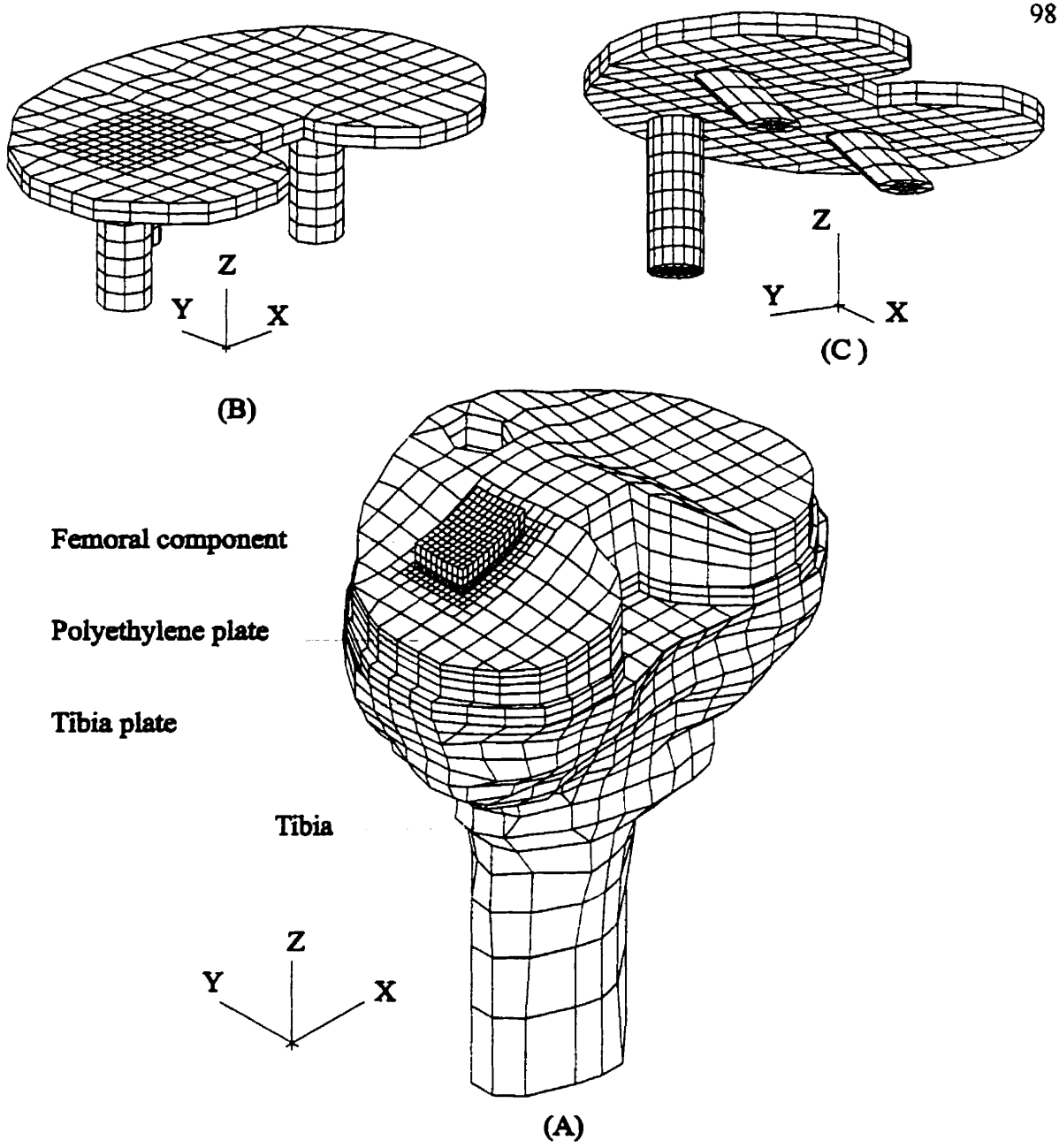

Figure 4.1 Finite element grid used in the study; A) Proximal tibia, metallic baseplate, polyethylene insert and a part of the femoral component used to apply compression, B) tibial baseplate for the design with screws, and C) tibial baseplate for the design with two inclined pegs and one screw at the anterior region. Pegs and screws are modeled as cylinders with interference and friction properties representing their measured pull-out response.

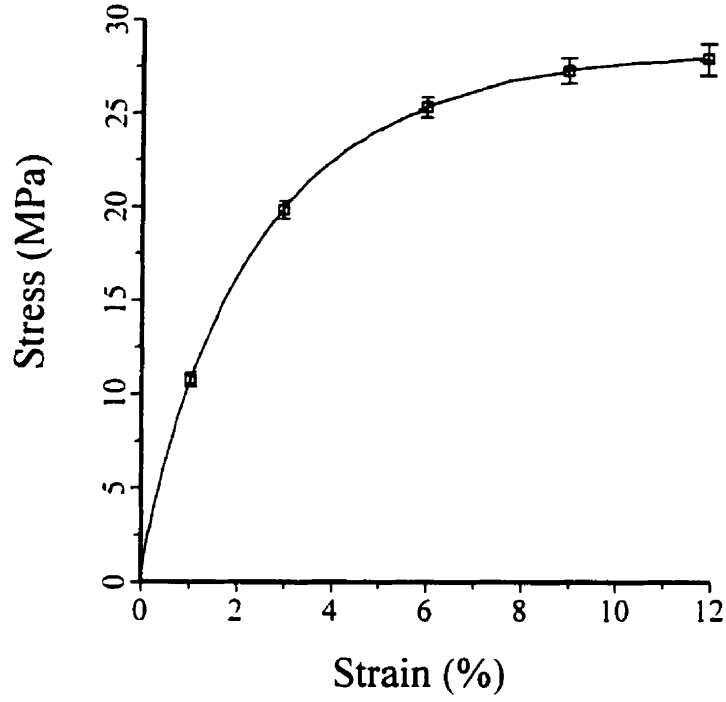

Figure 4.2 Measured (mean ± standard deviation) true stress-logarithmic strain curve for polyethylene.

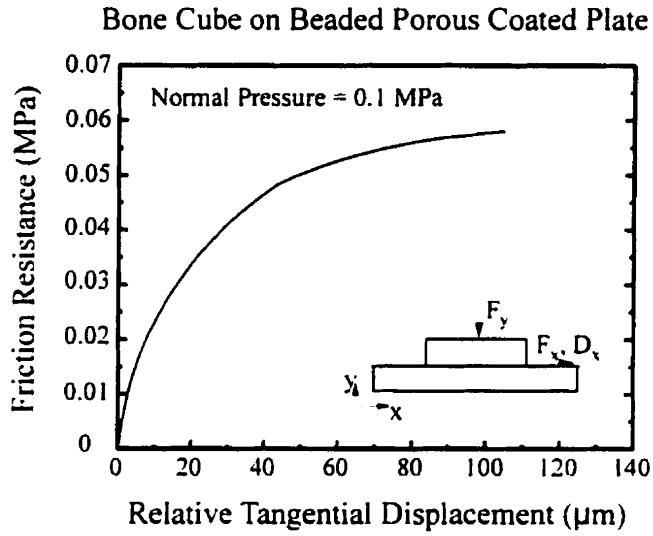

Figure 4.3 Nonlinear friction curve used for the bone-porous coated metal plate interface.

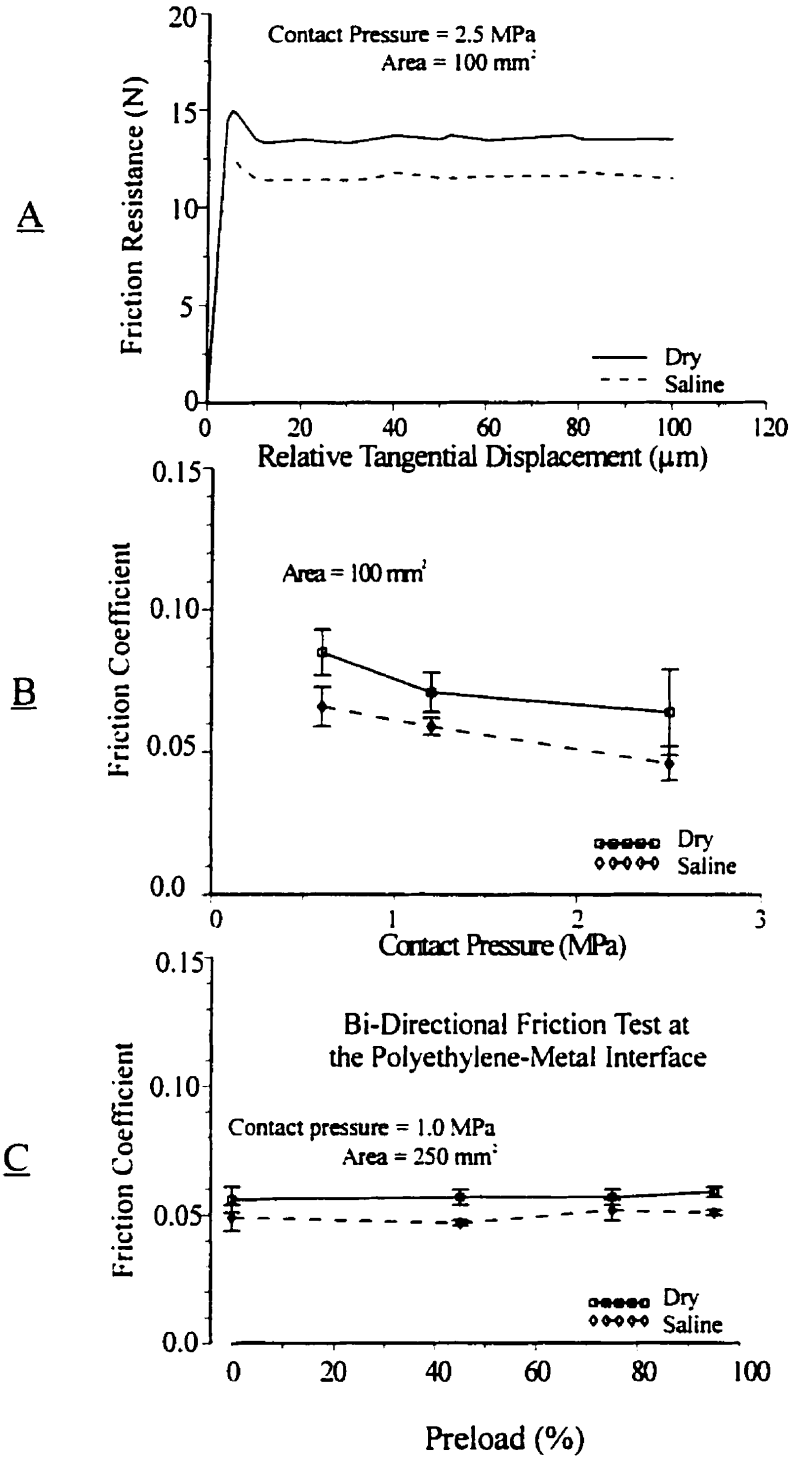

Figure 4.4 Measured results of friction tests at the metal-polyethylene interface for dry and wet surface conditions; A) Typical load-displacement curves, B) Variation of friction coefficient (mean ∓ standard deviation) with contact pressure, and C) Variation of friction coefficient (mean ∓ standard deviation) in one direction in presence of a preload in the other direction. The preload is expressed as % of the mean interface resistance load.

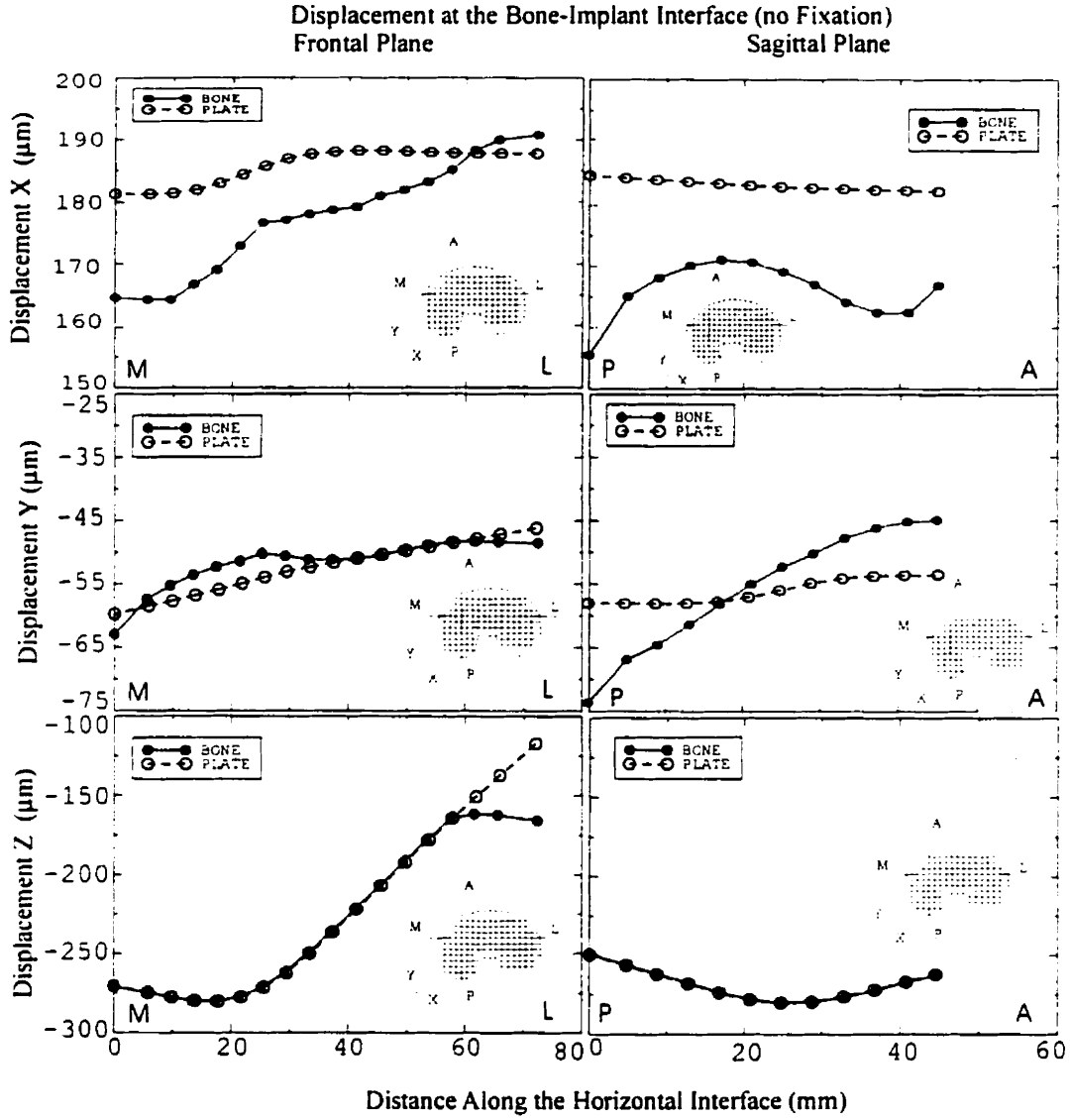

Figure 4.5 Interface bone and baseplate displacements at the final load for the design with no fixation along M-L (on the left, in frontal XZ plane) and P-A (on the right, in sagittal plane) lines in X (on the top), Y (at the middle), and Z (at the bottom) directions.

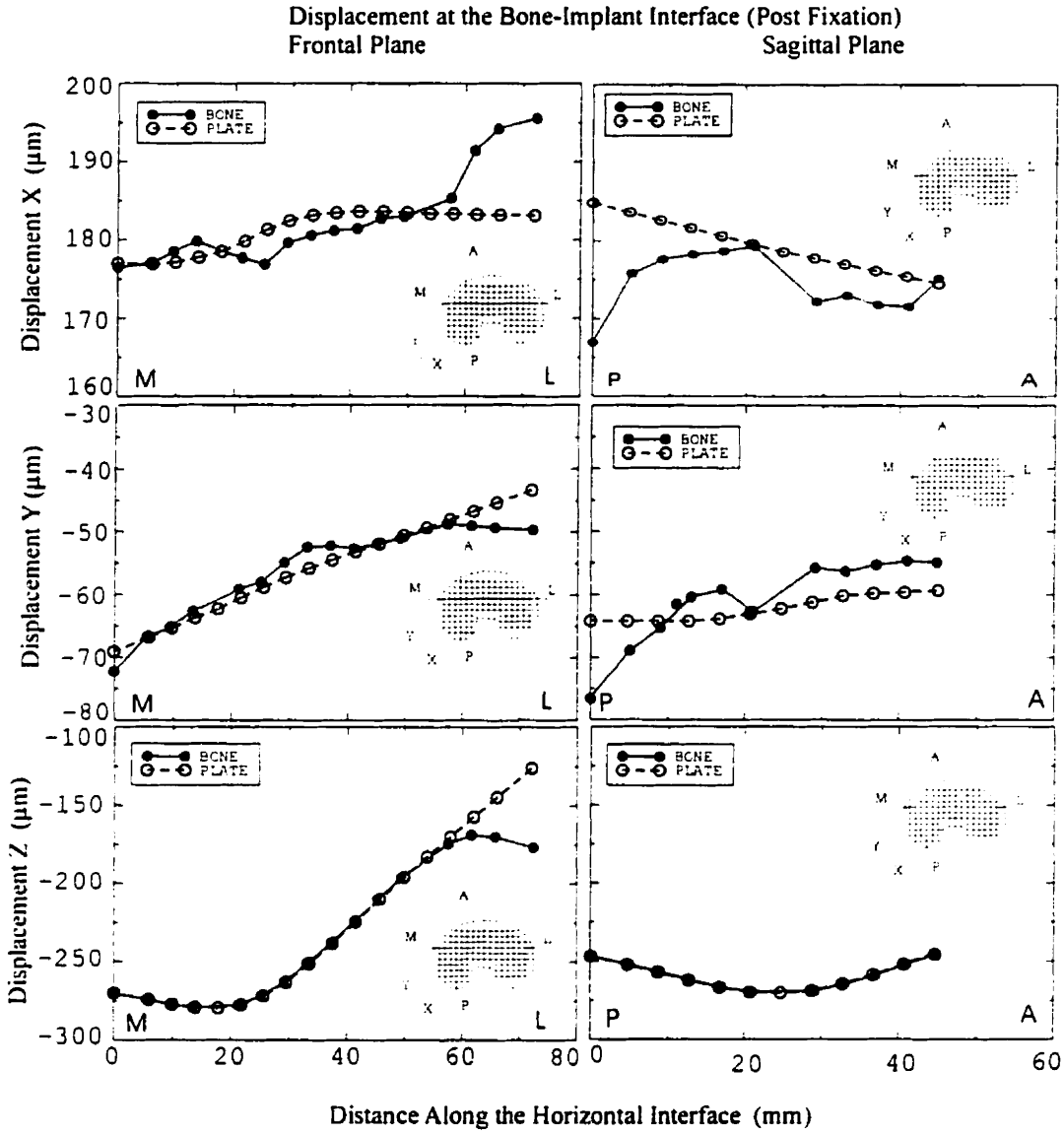

Figure 4.6 Interface bone and baseplate displacements at the final load for the design with two pegs along M-L (on the left, in frontal XZ plane) and P-A (on the right, in sagittal plane) lines in X (on the top), Y (at the middle), and Z (at the bottom) directions.

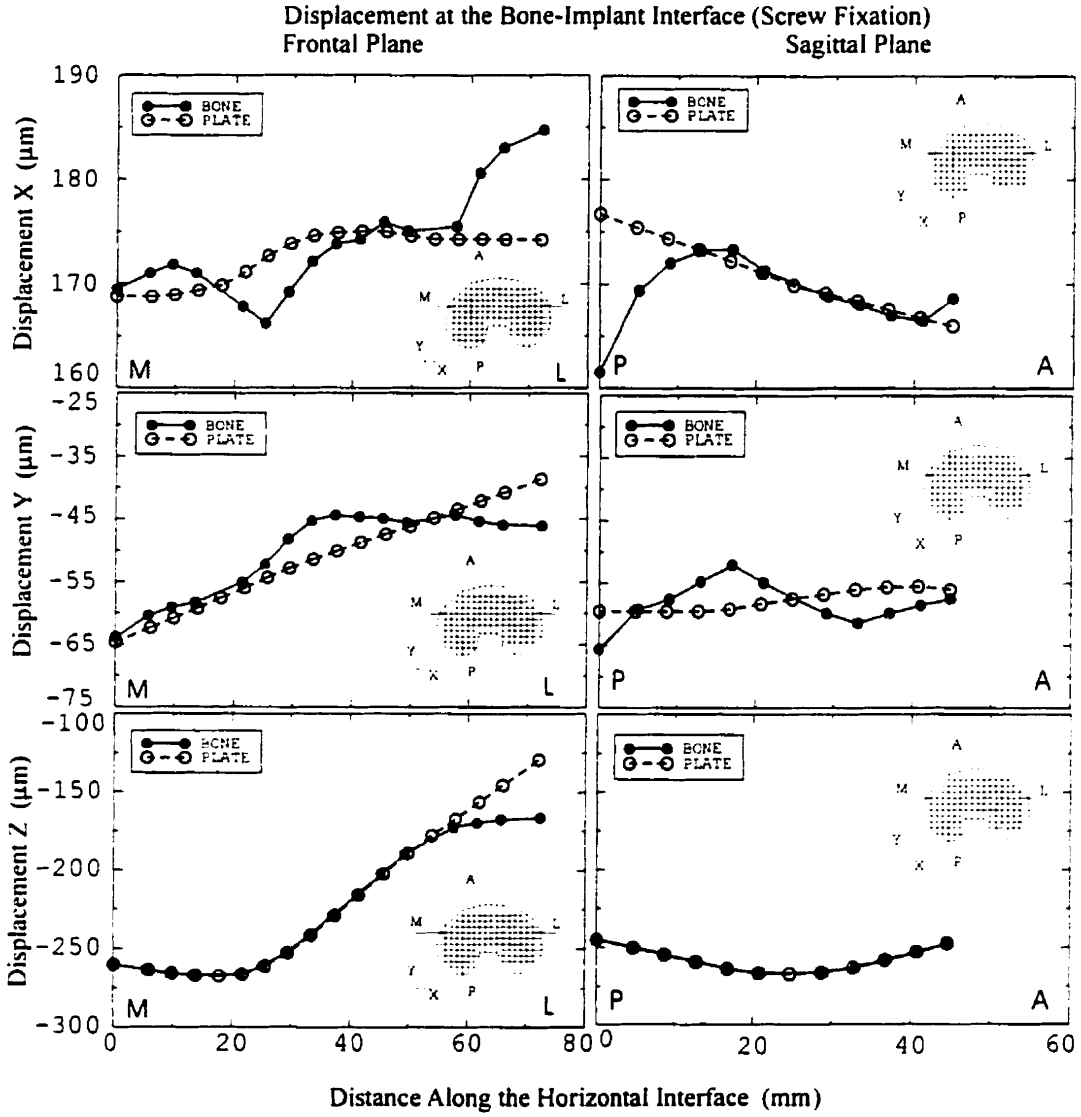

Figure 4.7 Interface bone and baseplate displacements at the final load for the design with screws along M-L (on the left, in frontal XZ plane) and P-A (on the right, in sagittal plane) lines in X (on the top), Y (at the middle), and Z (at the bottom) directions.

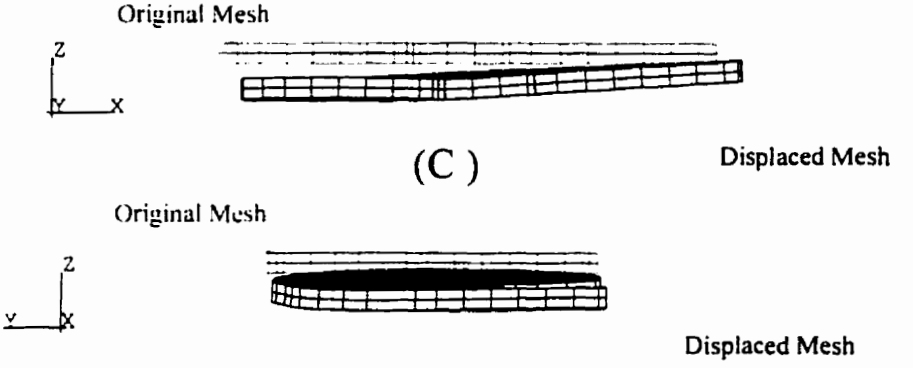

(C)

Displacement Magnification Factor = 20.0

(B)

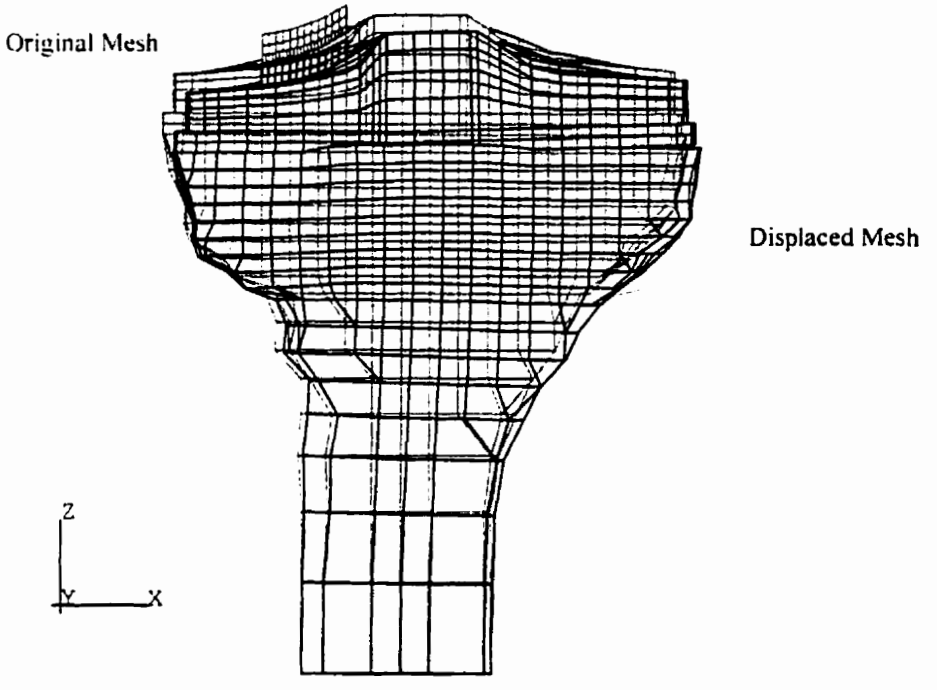

Displacement Magnification Factor = 10.0

(A)

Figure 4.8 Displaced and original undeformed shapes at the final load; A) bone-implant structure in frontal plane, B) baseplate in sagittal plane, and C) baseplate in frontal plane.

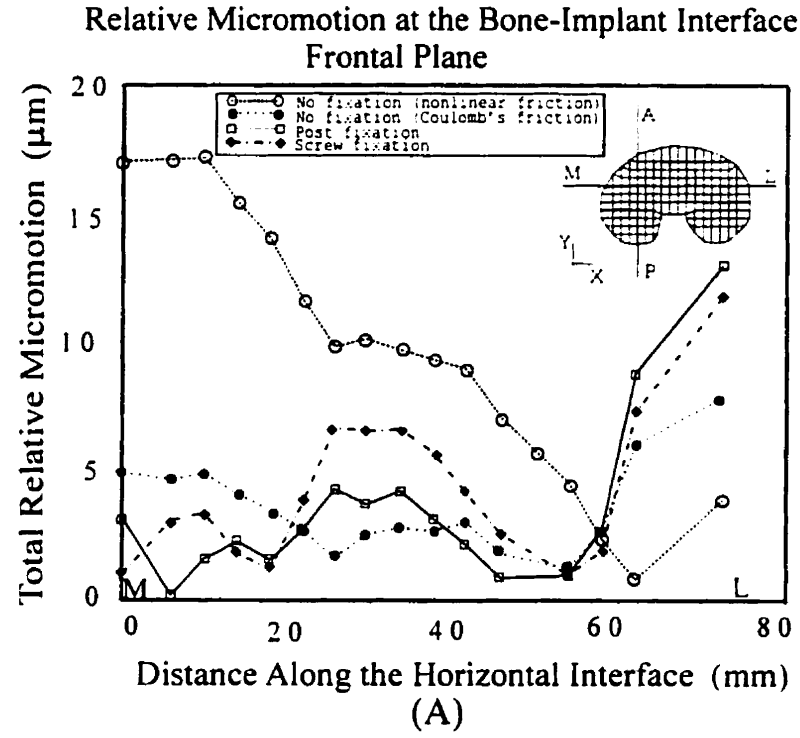

Figure 4.9 Total relative horizontal tangential micromotion at the bone-implant interface for different design configurations and two friction models A) M-L line (frontal plane) and B) P-A line (sagittal plane).

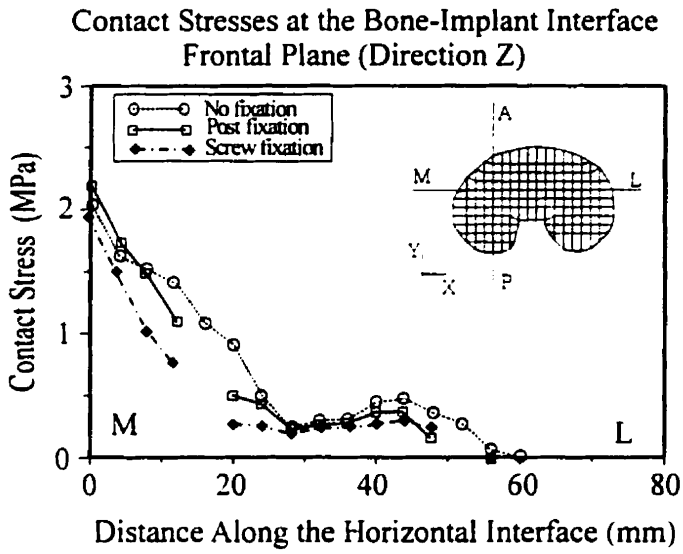

(A)

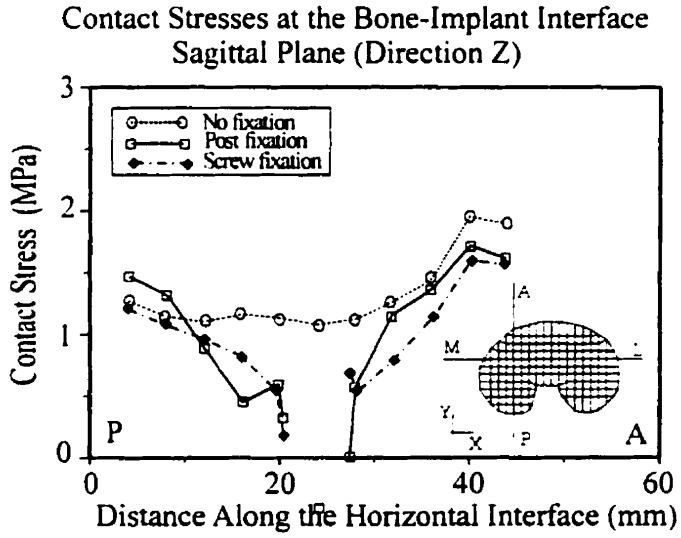

(B)

Figure 4.10 Normal contact stresses at the bone-implant interface for different design configurations along A) M-L line (frontal plane) and B) P-A (sagittal plane).

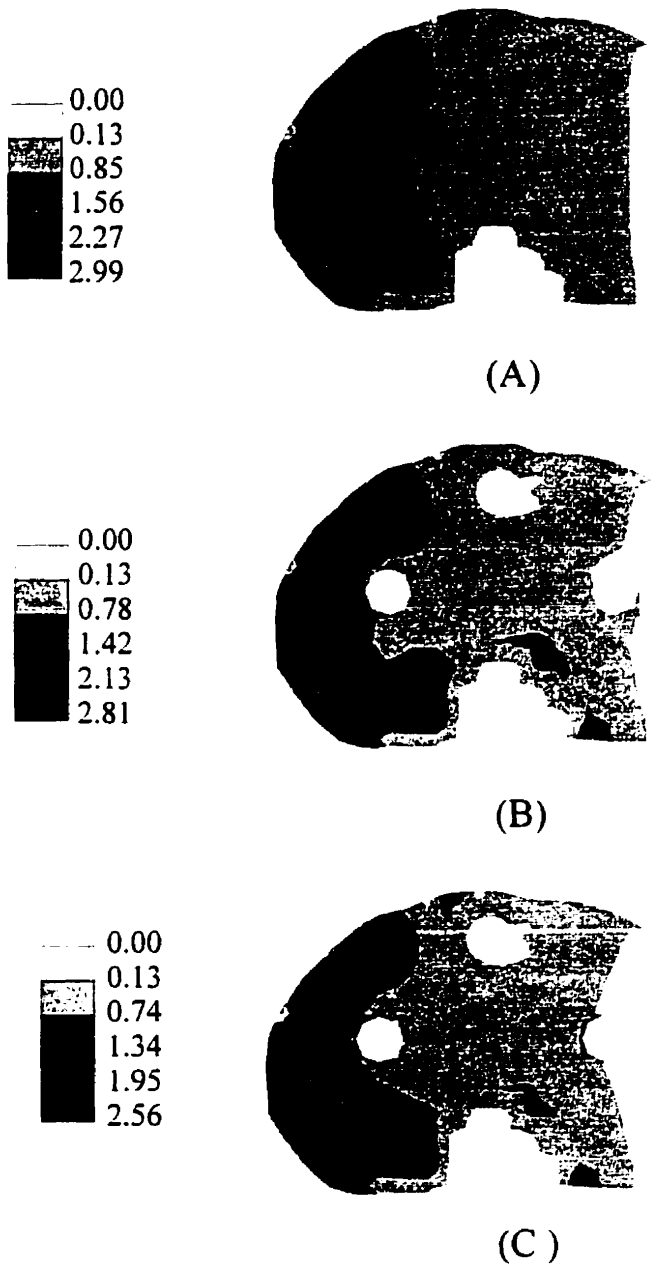

Figure 4.11 Normal contact stresses distribution at the bone-implant interface for the design with A) no fixation, B) post fixation, and C) screw fixation.

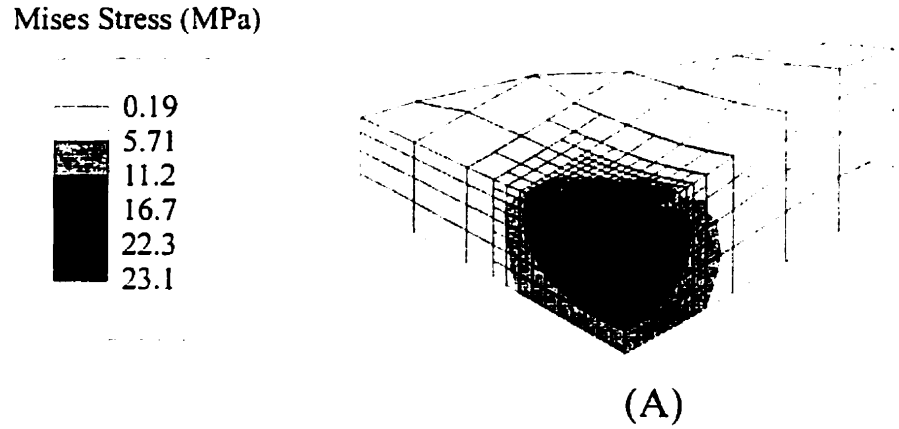

(A)

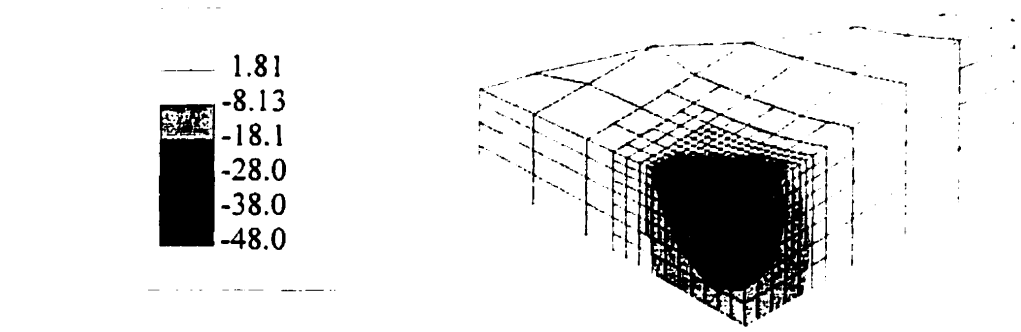

(B)

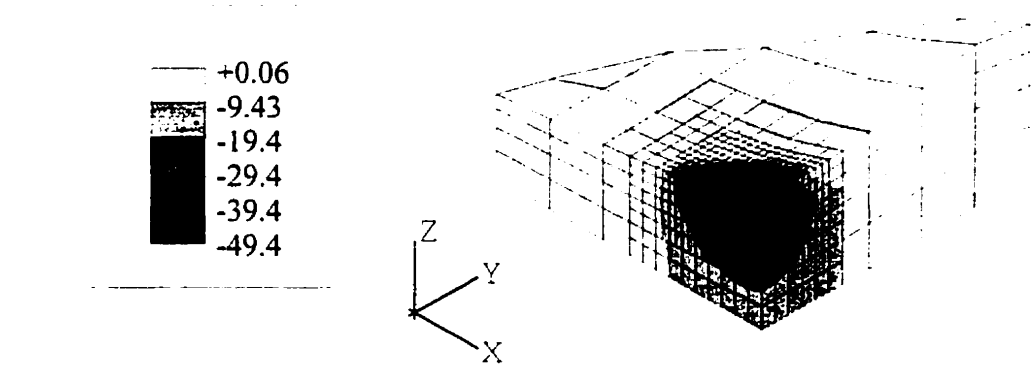

(C)

Figure 4.12 Predicted Mises (A), axial (B), and minimum principal (C) stress distributions within the polyethylene at the medial condyle. Maximum Mises stress occurs at 1-2 mm below the contact surface while maximum compressive principal and axial stresses occur at the contact surface.

CHAPTER 5
DISCUSSION

A three dimensional nonlinear finite element model was developed to investigate the mechanical effect of friction models (Coulomb's vs nonlinear) and tibial fixation designs (plate fixed with three screws, plate fixed with one screw and two short posts and free plate) in total knee arthroplasty in the immediate postoperative period in which no bony ingrowth has occurred. For this purpose, some preliminary steps were taken to prepare the data required to be implemented in the finite element model. First, the friction characteristics at the bone-implant interface were studied to propose the coupled bi-directional friction equations. The nonlinear interface constitutive equations were implemented in the finite element model studies of the bi-directional friction tests to further validate the developed equations and to identify the influence of coupling terms on results. The validated equations were implemented in the finite element model of the knee-implant system. Similar procedure was also taken to study the friction properties at the polyethylene-femoral component interface. Based on the results, the interface between polyethylene and metallic femoral condyle was modeled using Coulomb's friction. The interface between polyethylene insert and metal baseplate was considered to be fixed due to the lock mechanism at the interface. Since in a knee-implant system, screws/posts undergo shear force as well as axial force, the effect of inclination on pull-out response was investigated through experimental and finite element methods. The proposed model for screws/posts was properly included in the 3D finite element model of the knee-implant. The geometry of the constituents of the model was determined by coordinate measuring machine (CMM) or direct measurements. The mechanical properties of the bone and

metallic components were extracted from literature while those of polyethylene were obtained from experiments. A linear elastic isotropic but heterogenous model for bone and an elasto-plastic isotropic hardening model for polyethylene were considered in the finite element model. The axial force of three times body weight, 2000N, was applied through the femoral component on the medial plateau of articular insert to simulate a case with significant varus alignment. The distal end of the tibia was fixed in all directions. To block rigid body motion, the femoral condyle was allowed to move vertically only. The number of loading and fixation configurations was limited due to the complexity of the model. The limitations of the present work which may have influenced the results are elaborated in the next section. Discussion of the results is presented in the subsequent sections.

5.1 Limitations of this work

In the 3D finite element model presented in this work, geometry of the tibia was taken from a tibial specimen of average size. Due to variation in geometries used in this work and those used in the other investigations (both experimental and FEM), a possible discrepancy between the result of this work and that of the others can be expected. It should be noted that the material and interface properties employed in this study are adversely affected by cyclic loadings. Moreover, the interface conditions used here represented those at the immediate post-surgical period with no biological attachment. Therefore, the results should not be used to predict the response in longer-term conditions. Some other parameters which may affect the results are:

- neglecting the inclination of the tibial proximal surface,
- absence of contact with bone at the bottom of posts,
- fixing the femoral component to move vertically only,
- the type of implant (PCA) used,
- refinement of mesh not likely performed adequately in all regions,
- the length of tibia, reported (Eskandari, 1993) to have an impact on the displacement and

relative micromotion at the bone-implant interface,

- the magnitude, location and quasi-static application of the load may not represent the in-vivo loads,
- the model used for screw neglected the tightening effect, i.e., the compressive force generated at the bone-baseplate interface while inserting a screw,
- no relative micromotion at the interface between polyethylene insert and metallic base plate was allowed, and
- the extend of contact between the tibial baseplate and cortical bone.

5.2 Mechanical properties of the polyethylene

Due to the inconsistent reported properties, tension tests based on ASTM D638-94B were performed to obtain the mechanical behavior required for the simulation. The specimens were obtained from polyethylene inserts. The true stress-strain results showed a significant amount of plastic deformation at low stresses (Figure 4.2). The modulus of elasticity and yield stress were determined as 1083.0 ± 69.2 and 13.00 ± 0.83 MPa, respectively. The measured mechanical properties for polyethylene are in agreement with those presented by other researchers (Bartel et al., 1995; Kurtz et al., 1996).

5.3 Friction tests at the polyethylene-metal interface

Polyethylene is known for its low coefficient of friction, good resistance against wear and a high toughness. However, loosening has been recently observed due to polyethylene debris. To study the polyethylene wear, friction characteristics at the polyethylene-prosthesis interface should be determined. For this purpose, small blocks of polyethylene were used to obtain friction behaviors for both dry and wet (with saline) surfaces under various contact pressures. Bi-directional tests

were also performed to investigate the possible coupling phenomenon in response to tangential loads applied in two perpendicular directions.

Uni-directional friction tests at the polyethylene-metal interface showed that friction coefficient for dry contact was slightly higher than that for wet contact (Figure 4A). The measured friction coefficient at the metal-polyethylene interface varying between 0.05-0.10 and 0.04-0.08 for dry and wet surfaces, respectively, was found in the range of values reported in the literature using pin-on-disc testing apparatus (Benabdallah, 1993; Fusaro, 1983; Jones, 1984). Friction behavior was similar to the Coulomb's friction model due to the negligible relative displacement. The relative displacement at the interface prior to sliding was not affected by contact pressure or contact surface condition. It was also noticed that the maximum interface resistance (or friction coefficient) diminished as the contact pressure increased. Statistical analysis revealed a significant effect of contact condition ($p<0.05$) and contact pressure ($p<0.05$) on friction coefficient (Figure 4B). Bi-directional tests revealed that the friction coefficient remained almost unchanged irrespective of the presence of a tangential preload suggesting a weak coupling between different directions ($p>0.05$). The interface between polyethylene and metallic femoral condyle was, hence, modeled using Coulomb's friction model.

5.4 Friction tests at the bone-implant interface

The bi-directional friction tests were performed to quantify the coupled relation between load-displacement at the perpendicular directions. The effect of loading/unloading on uni-directional friction properties at the interface between polyurethane and the porous-surfaced metallic plate was also investigated.

5.4.1 Bi-directional friction tests

The aim of this part of the study was to investigate the friction characteristic at the bone/polyurethane-metal interfaces in the bi-directional motions required in nonlinear 3-D FE analysis of contacting bodies as is the case in the cementless artificial joints. For this purpose, the experimental apparatus used for the uni-directional tests (Shirazi-Adl et al., 1993) was modified to allow the simultaneous recording of loads and relative displacements in perpendicular directions at the interface. In the presence of normal pressure, various preloads were applied in one direction and the response in both directions were simultaneously measured as an incrementally increasing load was applied in the other direction.

The measurements yielded similar load-displacement friction curves for the resultant values in bi-directional tests as those in uni-directional tests, regardless of the bone excision site. Experimental results clearly suggested the presence of coupling between two perpendicular directions. This was found to be the case for the cancellous bone at all bone regions as well as the polyurethane. Friction coefficient was also found to be independent of the relative magnitude of tangential stresses at the interface, and was the same as that found in uni-directional tests.

The measured results of this study, in accord with the earlier studies (Dammak et al., 1997b; Rancourt et al., 1990; Shirazi-Adl et al., 1993) confirmed that the coefficient of friction at the bone-metal interface does not depend on the bone excision site. The measured friction curves were highly nonlinear with large relative displacements in the range of 60-500 μm depending on the bone excision sites. The initial slope was found to be higher at the medial and lateral regions due to the higher elastic modulus of bone in these areas. The interface relative displacements were also found to be independent of the preload magnitudes for both bone and polyurethane specimens.

5.4.2 Frictional contact formulation

An analytical approach based on uni-directional load-displacement curves, suitable for use in bi-directional friction cases was also presented. These equations were developed with the assumptions that, in 2-D interface motions, micromotion occurs in the direction of the resultant force and that it follows the uni-directional load-displacement curve. In the current developments, the friction properties in different directions are, nevertheless, coupled. The coupling of friction properties introduced off-diagonal terms in constitutive relations. These equations were implemented in the FE model studies of bi-directional friction tests. A good agreement was found between the results of predictions and those of experiments (Figure 2.9, 2.10). This satisfactory agreement was achieved by including the coupled terms in the FE models.

The FE simulations of friction tests confirmed the finding that the coupled terms in the friction constitutive relation of the interfaces with nonlinear load-displacement response were essential if accurate results were to be expected from model studies. Such coupling terms properly account for the softening in coupled responses when preloads in other directions are present. The analytical constitutive expressions with coupling terms were validated and could be used in FE model studies of the joint replacement systems. The developed constitutive equations showed that the cross-stiffness terms (i.e., coupling terms) vanished in a uni-directional friction analysis or when a linear friction behavior was implemented for an interface. Thus, these equations can be simplified and accurately used in an axisymmetric or two-dimensional analysis where there is only one shear component at the interface. The idealized Coulomb's friction does not perform satisfactorily even when compared with measured nonlinear uni-directional friction constitutive law (Dammak et al., 1997a). In 3-D cases in which one component of shear force at the interface is much larger than the other one, these coupling terms can be neglected without noticeable loss of accuracy. This could be verified by the model studies of friction tests when a small preload is applied in one direction.

Finally, the formulation presented in this work is limited only to interfaces with isotropic friction properties; i.e., where uni-directional friction properties are not direction dependent. This has been verified by our friction tests to be the case at the porous coated implant interfaces with the cancellous bone or polyurethane. Therefore, in 3-D FE study of contacting bodies with isotropic interfaces as in cementless joint arthroplasty, the experimental results coupled with constitutive formulations presented in this work should be used.

5.4.3 Loading/unloading friction tests

The friction tests were performed under monotonically increasing/decreasing tangential load for porous and smooth-surfaced plates. Nonlinear curves similar to those reported in the earlier studies (Rancourt et al., 1990; Shirazi-Adl et al., 1993) were found. These experiments suggested that the friction response was mainly irreversible, regardless of the surfaces used in the experiment. Polyurethane-porous surfaced metal plate interface generated larger residual displacement in unloading than the polyurethane-smooth surfaced interface. The reloading slope was identical to the unloading one and no significant change in friction properties was observed after repeating the tests for a few cycles. However, repeating the cyclic load seems to have an impact on the relative displacement. This remains as a part of future works requiring a detailed study. The unloading stiffness (slope) found in friction tests was implemented in the FE model study of loading/unloading pull-out tests.

5.5 Pull-out tests

The influence of load inclination and load cycle on the pull-out response was observed in both experimental and FE methods.

5.5.1 Inclined pull-out tests

The objective of this part was to study the effect of inclined load on the load-displacement behavior of pull-out test specimens. For this purpose, both experimental and finite element method were used. Experimental tests were performed using a porous coated post, a stainless smooth-surfaced post and a bone screw. Using a special set-up, the pull-out resistance force versus displacement curves were measured at for different load inclinations. The FE models also used to predict and compare results with those of experiments. This was achieved by using the measured uni-directional friction properties along with coupled constitutive equations. The FE and experimental results for screws support those of King and Cebone (1993).

The axial pull-out force of smooth posts was not affected significantly by increasing the inclination angle of pull-out force. This is due to higher normal stresses at the interface of smooth post sand polyurethane cylinders. However, it was found that increasing the inclination of the load affects the axial pull-out load for porous-coated posts. This is due to changing the normal stresses at the interface. Screw demonstrated a constant reduction in axial pull-out resistance force with inclination. Since the screw was modeled as a post with relatively high interference, the normal stresses at the interface were higher than those of smooth posts. In this study the maximum shear stress that can be transferred at the interface was limited in all models to 1.4 MPa based on shear strength experimental tests. Increasing the inclination can not increase the shear resistance, beyond 1.4 MPa, but reduces the shear resistance in some areas due to lower normal stresses. The overall outcome was a considerable reduction in axial pull-out resistance force with increasing the inclination angle for screw. The aforementioned results were confirmed by both experimental and FE study and in accord with the axisymmetric and experimental studies for axial pull-out tests. Due to the fact that circumferential shear stresses were very small compared to axial shear stresses at the interface, no significant change was observed using the uncoupled friction formulation. That is,

inclined load does not generate considerable circumferential tangential stress at the interface.

5.5.2 Axial loading/unloading tests

The loading-unloading behavior of pull-out tests were investigated using both experimental and FE model studies. Experimental tests revealed nonlinear load-displacement behavior for both posts, particularly for the porous-surfaced one. The FE models of the pull-out specimens accurately represented the global load-displacement behavior. This was accomplished by using nonlinear friction model at the post-polyurethane interface.

The mechanism of load transfer from the post to the polyurethane was determined from the analysis of measurement and FE results. The FE analyses predicts a large shear stress concentration at the tip of the post. Since the interface could only support a limited magnitude of shear stress, slipping between post and polyurethane initiates in this region. As the magnitude of the applied load increases, the region of slipping extends upward from the tip of the post. The entire interface is in a slip state when shear stress at each point exceeds its corresponding shear limit.

During the unloading part, the post-polyurethane interface remained in a stick state along the interface. The unloading and reloading slopes of the curves remained unchanged, regardless of the magnitude of the load prior to unloading. In unloading, a residual displacement was always present which was due to the relative micromotion between post and cylinder during loading. The amount of longitudinal relative motion between post and cylinder depended on the prescribed load, and, hence, on the nonlinear friction at the interface. The normal stresses due to press fit (initial interference) were remained unchanged during the loading/unloading process.

5.6 Finite element model of knee-implant

The objective of the final part of the present study was to develop a 3D finite element model of a knee-implant structure to investigate the mechanical fixation and stability of different design configurations under static condition. For this purpose, nonlinear bi-directional friction properties between bone and porous coated metal plate were considered and compared with the idealized Coulomb's friction. Geometry of the tibia and implant components were obtained by direct measurements whereas the required mechanical properties of constituent materials and contacting interfaces were either measured experimentally or taken from the literature. An elasto-plastic isotropic hardening model was considered for the articular polyethylene insert. A load of approximately three times the body weight was applied at the medial condyle simulating a case with a varus alignment. The number of loading and design configurations considered were limited due to the complexity of models/analyses. It should be emphasized that the material and interface properties used in this study are adversely affected by fatigue loadings; the predictions, hence, should not be applied over longer term conditions. Moreover, the interface conditions considered here represent those at the immediate post-surgical period in which neither bony ingrowth nor fibrous attachment has occurred. In such cases, the friction is the sole mechanism of shear transfer between two opposing surfaces. Any substantial deviation expected in a longer term would violate the basic assumptions and require additional investigations.

5.6.1 Displacements

Displacement magnitudes (Figures. 4.5-4.7) for the tibial implant varied depending on the prosthetic design used. The magnitude of displacements (maximum = 0.20 mm) were in the range reported in the other studies (0.15 mm, Rakotomanana et al., 1994; 0.10 mm, Tissakht et al., 1995). Displacement in the axial (Z) direction showed the least dependency on the fixation

configuration, particularly in the sagittal plane. Displacements at the bone-implant interface nodes were higher in the medio-lateral (X) direction (about 200 μm) than in the anterior-posterior (Y) direction (about 75 μm). The lift-off at the lateral region led to a gap between bone and the implant reducing the effective contact area and increasing, in turn, the compressive load and, hence, subsidence in the opposite medial region. This was predicted by Wyatt et al. (1991), as well. Screw fixation (Table 4.1) in accord with work of Miura et al. (1991), provided the least lift-off followed by the post fixation.

5.6.2 Micromotion

Incompatibility between the bone and implant displacements at the interface generates relative micromotion which was largest in the design with no fixation. The design with screws followed by that with a screw and two pegs yielded the stiffest response which is in agreement with the literature (Dammak et al., 1997a; Kaiser and Whiteside, 1990; Lee et al., 1991; Miura et al., 1991; Volz et al., 1988 ; Wyatt et al., 1991). It was found that the interface friction model significantly influenced the relative micromotion in both medio-lateral and anterior-posterior directions. Coulomb's friction, as compared with the nonlinear friction model, considerably underestimated tangential relative micromotion, an observation made by others as well (Dammak et al., 1997a). The maximum micromotion for screw and post fixation designs was computed to remain below 28 μm which has been reported (Jasty et al., 1997; Pilliar et al., 1986) to be compatible with bony ingrowth. For all design configurations, the maximum micromotion occurred at the perimeter of the implant.

Tissakht et al. (1995) measured the maximum relative micromotion to be 5 μm at the bone-implant interface. They applied a 1000 N load in the center of the implant fixed with 4 short pegs/screws. The 3-D FE study predicted that the maximum relative micromotion varies from about zero for

interface with friction coefficient of 0.45 to 7.5 μm for the frictionless interface. The lowest micromotion was obtained for screw fixation. This investigation predicted the lowest maximum relative micromotion reported in the literature. On the other hand, Keja et al. (14) predicted the largest maximum relative micromotion for peg fixation (up to 100 μm) and knife edge design fixation (up to 90 μm). This study considered a total load of 2500 N applied symmetrically on each condyle and modeled the interface between implant and bone as frictionless to yield the maximum possible relative micromotion. Considering the differences in the location and magnitude of the load, geometry and friction model used by others, the results of the present study (Figure 9) is well situated in the range of the reported results (Beaupre et al., 1986; Lewis et al., 1982; Rakotomanana et al., 1994; Vasu et al., 1986).

5.6.3 Stresses and load transfer

Normal contact stress at the bone-implant interface varied depending on the design. The maximum contact stress at the cancellous bone-implant interface (i.e., 2.81 MPa for the design with pegs and 2.56 MPa for that with screws computed at the medial boundary adjacent to the loaded area) is in the range of values reported in the literature (Beaupre et al., 1986; Murase et al., 1983; Rakotomanana et al., 1994). Design with screws/pegs yielded lower interface contact stresses due to the partial transmission of the applied compression load via shear forces across the interfaces between bone and screws/pegs. In screw-fixation design, 23% of axial load was transmitted by screws as compared with 7% in the post-fixation design (Table 4.2). An increase in interface interference (force-fit) could increase the foregoing proportions whereas repetitive fatigue loading tends to decrease them . An increase in interference is known (Dawson and Bartel, 1992) to be favorable to bone ingrowth due to larger resistance to micromotion.

Apart from the screws/pegs, the total force carried by the cancellous bone and cortical bone varied

between 65%-87% and 10%-13% of total axial force, respectively, with the least values computed for the design with three screws. The use of implant-cortex contact to transmit loads has been encouraged (Bourne and Finlay, 1988; Murase et al., 1983). Such contact can reduce excessive stresses in the underlying cancellous bone. However, resting of the implant edge on the cortical shell has been indicated by finite element studies to have negligible effect on the interface micromotion. Due to higher stiffness of the cortical bone to that of cancellous bone, higher normal contact stresses are expected for cortical bone (Table 4.3). Stresses under the tray at the screw/post areas were lower for plate with fixation than that without fixation (Figures 4.10,4.11).

5.6.4 Polyethylene

A major problem reported in the TKR is the polyethylene wear which could cause component failure and periprosthetic osteolysis. Factors such as patient weight, gender, level of activity and age could play a role in the rate of polyethylene wear (Bartel et al., 1986; Ishikawa et al., 1996; Hood et al., 1983; Landy and Walker, 1985; Mintz et al., 1991; Rose et al., 1984; Wright and Bartel et al., 1986). Fracture mechanics studies have identified the high contact stresses and fatigue cracks in polyethylene as the cause of wear. In agreement with previous studies (Chillag and Bartel, 1991, Mintz et al., 1991; Szivek et al., 1996), the predicted magnitude of normal contact stress (48.0 MPa) was found well beyond the polyethylene yield stress. Maximum Mises stress at polyethylene plate was predicted to occur below the contact surface the magnitude and location of which were found to be independent of the fixation design. It appears, therefore, that the adequate modeling of bone-baseplate interface might not be as crucial if calculation of polyethylene stresses are of primary concern. Stresses in polyethylene have been reported to depend amongst others on its thickness and conformity. The thickness has been recommended to be at least 6-8 mm. Retrieval analyses have indicated that wear resistance depends also on the relative conformity of the articulating surfaces. It has been indicated that the capture mechanism of the insert to

baseplate affects the rate of polyethylene wear. In the current study, however, a fixed interface between the polyethylene and the metal tray was assumed due to the presence of a lock mechanism preventing polyethylene from sliding.

5.7 Clinical perspective

The finite element model study confirmed the earlier results that the use of screws for fixation of implants provides the strongest attachment mechanically achieved. Screws were proven to be effective in preventing lift-off as well as the micromotion. However, their performance may be affected if screws are entitled to the large shear force or cyclic loading. It was shown in the combined pull-out tests that pull-out resistance of screws were highly influenced by increasing the inclination angle (shear force). The fatigue studies also showed that smooth posts has better performance than their counterparts (porous coated posts and screws).

The relative micromotion predicted in this model study is in the range that believed to be required for the bone ingrowth. The maximum micromotion was appeared to be at the perimeter of the implant for all design configurations considered in this work. To reduce the micromotion in this area, increasing the number of screws and locating them more peripherally are recommended.

By applying the load at the medial condyle, the medial screw alone carried 11% of the load. Shear contact stresses at the bone-screw interface carried part of axial load yielding the lowest stress distribution at the bone-implant interface for all designs.

Using a custom made implant or a larger implant to cover the cortex can reduce the interface stresses at the cancellous bone-implant interface. The implant-cortex contact can also prevent the cortical bone atropy.

CHAPTER 6
CONCLUSIONS AND RECOMMENDATIONS

The following steps were taken to develop a three dimensional finite element model to investigate tibial fixation designs and friction models in total knee arthroplasty in the immediate postoperative period. In the first step, geometry of the constituents of the model were measured by CMM or manual instruments. In the second step, mechanical properties of the polyethylene were measured while those for the rest of components in the model were extracted from literature. In the third step, friction characteristics at the contact interfaces (polyethylene-smooth surface metal plate and bone-porous coated metal plate) were determined and proper friction models for each interface were proposed and validated. Then, the validated friction models for interfaces were assigned in the finite element model of the knee-implant. In the fourth step, screw/posts behavior under inclined load was studied by experimental and finite element methods. The results of this study were used to develop a reliable representation of the screw/posts in the finite element model of the knee-implant. In the last step, boundary conditions and loading were applied to the model to simulate a varus misalignment. The studies performed on the friction tests and the pull-out tests as well as the 3-D finite element model of knee-implant yielded to the results which were discussed in the earlier chapters. The important conclusions of the present work followed by some proposals for future research are presented in this chapter.

6.1 Summary of conclusions

The results of this work can be summarized as:

- the true stress-strain results of polyethylene shows a significant amount of plastic deformation at low stresses. The modulus of elasticity and yield stress are 1083.0 and 13.00 MPa, respectively,
- the measured friction coefficient at the metal-polyethylene interface varies between 0.05-0.10 and 0.04-0.08 for dry and wet surfaces, respectively,
- friction coefficient at the polyethylene-metal interface diminishes as the contact pressure increases,
- bi-directional tests has almost no influence on the friction coefficient at the polyethylene-metal interface,
- resultant friction coefficient at the bone-porous coated metal interface measured by bi-directional friction tests are similar to that obtained by uni-directional friction tests,
- bi-directional friction tests at the bone/polyurethane-porous coated metal interface suggest the presence of coupling between two perpendicular directions,
- increasing the inclination angle in pull-out tests influence primarily the screw and porous-coated post behaviors,
- the Coulomb's friction underestimates the predicted micromotion and nonlinear friction should be considered in the knee-implant analysis,
- screw fixation design followed by post fixation design considerably reduces micromotion and lift-off,
- maximum micromotion is obtained at the perimeter of the implant for all the configurations,
- about 10-13% of total axial load was carried by the cortical bone while cancellous bone transfers 65-85% depending on the fixation with the remaining portion transmitted through screws and pegs,

- polyethylene stresses are independent of design configuration and friction model, and
- maximum Mises stress occurred at 1-2 mm below the contact surface within the polyethylene while the maximum normal stress was predicted to be at the contact surface.

6.2 Recommendations for the further studies

The future work can be concentrated on the following subjects:

- Study the effect of cyclic loading on the friction coefficient at the bone-porous coated surfaces.
- Study the surfaces with anisotropic friction properties and develop the required constitutive equations for such surfaces.
- Investigate the cyclic loading effect on the pull-out tests.
- Present a proper finite element model of pull-out tests under fatigue loading.
- Perform a parametric study to determine the effect of parameters like thickness, mechanical properties, loading combination, and . . . on the polyethylene stresses.
- Perform in-vitro study on knee-implant system and compare with the finite element predictions.
- Consider the anisotropic mechanical properties for the bone in finite element model of the knee-implant, and
- Develop a program to extract the 3-D geometry and mechanical properties of the bone from CT images.

6.3 Contributions

Here is a brief description of some of the scientific contributions made by the present work.

- Measurements of mechanical properties of the polyethylene.

- Measurement of the friction properties at the polyethylene-smooth surface metal interface.
- Measurement of the bi-directional friction properties at the bone/polyurethane-porous surface metal interface.
- Measurement of the effect of loading/unloading on uni-directional friction properties.
- Experimental study of inclined pull-out test behavior.
- Experimental study of the loading/unloading behavior of pull-out tests required for future fatigue investigations.
- Development of constitutive equations required to model the bi-directional nonlinear isotropic friction behavior.
- Axisymmetric finite element model study of loading/unloading pull-out tests, initiated for future numerical fatigue investigations.
- 3-D finite element model study of the inclined pull-out tests in order to acquire a proper and accurate model for use within the knee-implant FE model, and
- Development of a 3-D nonlinear finite element model of a knee-implant structure.

REFERENCES

ABAQUS, Finite element program (1992), version 5.2-5.6, Hibbit, Karlsson and Sorenson, Inc., Pawtucket.

American Society for Testing and Materials: Standard D638M-94b; Tensile properties of plastic (metric) (1994), In: Annual Book of ASTM standards, part 8.01, 167-175.

AHMED, A. M., TISSAKHT, M., SHIRVASTAVA, S. C. and CHAN, K., (1990). Dynamic stress response of the implant/cement interface : An axisymmetric analysis of a knee tibial component. J. Orthop. Res., 8, 435-447.

ASHMAN, R. B., RHO, J. Y. and TURNER, C. H. (1989). Anatomical variation of orthotropic elastic moduli of the proximal human tibia. J. Biomechanics, 22, 895-900.

ASKEW, M.J., and LEWIS, J. L. (1981). Analysis of model variables and fixation post length effects on stresses around a prosthesis in the proximal tibia. J. Biomech. Engng., 103, 239-245.

BARTEL, D.L., BICKNELL, V. L. and WRIGHT, T. M. (1986). The effect of conformity, thickness, and material on stresses in ultra-high molecular weight components for total joint replacement. J. Bone Joint Surg., 68A, 1041-1051.

BARTEL, D.L., RAWLINSON, J.J., BURSTEIN, A.H., RANAWAT, C. S. and FLYNN, W.F. (1995). Stresses in polyethylene components of contemporary total knee replacements. Clin. Orthop. Rel. Res., 317, 76-82.

BEAUPRE, G. S., VASU, R., CARTER, D. R. and SCHURMAN, D. J. (1986). Epiphyseal-based designs for tibial plateau components-ii .stress analysis in the sagittal plane. J. Biomechanics, 19, 663-673.

BELL, C.J., SIMMONS, J., KING, P., WALKER, P.S. and BLUNN G. W. (1997). Is oxidation of ultra high molecular weight polyethylene the main cause of delamination wear in total knee replacement. 43rd Annual Meeting, Orthop. Res. Soc., 96 - 16.

BENABDALLAH, S. H. (1993). The running-in and steady-state coefficient of friction of some engineering thermoplastics. Polymer Engineering and Science, 33(2), 70-74.

BENTZEN, S.M., HVID, I. and JORGENSEN, J. (1987). Mechanical strength of tibial trabecular bone evaluated by x-ray computed tomography. J. Biomechanics, 20(8), 743-752.

BOBYN, J.D., PILLIAR, R. M., CAMERON, H.U. and WEATHERLY, G.C. (1980). The optimum pore size for the fixation of porous-surface metal implants by the ingrowth of bone. Clin. Orthop., 150, 263-270.

BLUNN, G. W., WALKER, P. S., JOSHI, A. and HARDINGE, K.(1991). The dominance of cyclic sliding in producing wear in total knee replacements. Clin. Orthop., 273, 253-260.

BOURNE, R. B. and FINLAY, J. B. (1986). The influence of tibia component intramedullary stems and implant - cortex contact on the strain distribution of the proximal tibia following total knee arthroplasty. Clin. Orthop. and Rel. Res., 208, 95-99.

CAMERON, H.U., PILLIAR, R. M. and MACNAB, I. (1973). The effect of movement on the

bonding of porous metal to bone. J. Biomed. Mat. Res., 7, 301-311.

CHEAL, E. J., HAYES, W. C., LEE, C. H., SNYDER, B. D., and MILLER, J. (1985). Stress analysis of a condylar knee tibial component: Influence of metaphyseal shell properties and cement injection depth. J. Orthop. Res., 3, 424-434.

CHILLAG, K.J. and BARTH, E. (1991). An analysis of polyethylene thickness in modular total knee components. Clin. Orthop. Rel. Res., 273, 261-263.

COLLIER, J. P., MAYOR, M.B., McNAMARA, J. L., SURPRENANT, V. A., and JENSES, R.E. (1991). Analysis of the failure of 122 polyethylene inserts from uncemented tibial knee components. Clin. Orthop. Rel. Res., 273, 232-242.

COLLINS, J.J. (1995). The redundant nature of locomotor optimization laws. J. Biomechanics, 28, 251-267.

COLLINS, D. N., HEIM, S. A., NELSON, C. L., SMITH III, P. (1991). Porous-coated anatomic total knee arthroplasty., Clin. Orthop. Rel. Res., 267, 128-136.

DAMMAK, M., HASHEMI, A., SHIRAZI-ADL, A. and ZUKOR, D.J. (1996). Experimental and finite element fixation studies of posts and screws. Engineering Systems Design and Analysis, ASME, PD-Vol.77, 11-18.

DAMMAK, M., SHIRAZI-ADL, A. and ZUKOR, D. J. (1997a). Analysis of cementless implants using interface nonlinear friction - Experimental and finite element studies. J. Biomechanics, 30, 121-129.

DAMMAK, M., SHIRAZI-ADL, A., HASHEMI, A., and ZUKOR, D.J. (1994). Fixation mechanics of posts in joint arthroplasty - Comparison of various friction properties. Advances in Bioengineering, ASME WAM, Chicago, 411-412.

DAMMAK, M., SHIRAZI-ADL, A., SCHWARTZ JR, M., GUSTAVSON, L. (1997b). Friction properties at the bone-metal interface - comparison of four different porous metal surfaces. J. Biomed. Mat. Res., 35, 329-336.

DAWSON, J. M. and BARTEL, D. L. (1992). Consequences of an interface fit on the fixation of porous-coated tibial components in total knee replacement. J. Bone Joint Surg., 74A, 233-238.

DEHEER, D. C. and HILLBERRY, B. M. (1992). The effect of thickness and nonlinear material behavior on contact stresses in polyethylene tibial components. 38th Annual Meeting, Orthop. Res. Soc., 327.

DENG, M. and SHALABY, S. W. (1995). Effects of gamma irradiation, gas environments, and post irradiation aging on ultrahigh molecular weight polyethylene. J. Appl. Polymer Science, 58, 2111-2119.

DODD, C. A. F., HUNGERFORD, D. S., KRACKOW, K. W. (1990). Total knee arthroplasty fixation. Clin. Orthop. Rel. Res., 260, 66-70.

DUCHEYNE, P., DeMEESTER, P., AERNOUDT, E., MARTENS, M. and C. MULIER (1977). Consequences of an interface fit on the fixation of porous-coated tibial components in total knee replacement. J. Biomed. Mat. Res., 11, 811-838.

ENGH, G. A., DWYER, K. A. and HANES, C. K. (1992). Polyethylene wear of metal-backed tibial components in total and unicompartmental knee prostheses. J. Bone Joint Surg., 74B, 9-17.

ESKANDARI, H. (1993). Bone-prosthesis interface relative displacement of the knee tibial component: finite element analysis and measurement. M. Eng. Thesis, Mechanical Department, McGill University.

FINLAY, J.B., HARADA, I., BOURNE, R.B., RORABECK, C.H., HARDIE, R. and SCOTT, M.A. (1989). Analysis of the pull-out strength of screws and pegs used to secure tibial components following total knee arthroplasty. Clin. Orthop. Rel. Res., 247, 220-231.

FLEMING, J. R. and SUH, N. P. (1977). Mechanics of crack propagation in delamination wear. Wear, 44(1), 39-56.

FORCIONE, A. and SHIRAZI-ADL, A. (1990). Biomechanical analysis of a porous-surfaced knee implant: A finite element contact problem with nonlinear friction., Mechanical Engineering Forum, Canadian Society of Mechanical Engineers, Toronto., 2, 19-24.

GIBSON, L.J. (1985). The Mechanical behavior of cancellous bone. J. Biomechanics, 18(5), 317-328.

GEORGE, D.C., KRAG, M.H., JOHNSON, C.C., VAN HAL, M.E., HAUGH, L.D. and GROBLER, L.J. (1991). Hole preparation techniques for transpedicles screws: Effect on pull-out strength from human cadaveric vertebrae. Spine, 16(2), 181-184.

GOLDSTEIN, S. A., WILSON, D. L., SONSTEGARD, D.A. and MATTHEWS, L. S. (1983).

The mechanical properties of human tibial trabecular bone as a function of metaphyseal location. J. Biomechanics, 16, 965-969.

HARRINGTON, I. J. (1976) A bioengineering analysis of force actions at the knee in normal and pathological gait. Biomedical Engineering, 11, 167-172.

HASHEMI, A., SHIRAZI-ADL, A. and DAMMAK, M. (1996). Bi-directional friction study of cancellous bone-porous coated metal interface. J. Biomed. Mat. Res. (Appl. Biomat.), 33, 257-267.

HECK, D. A., CLINGMAN, J. K. and KETTELKAMP, D. G. (1992). Gross polyethylene failure in total knee arthroplasty. Orthopaedics, 15, 23-28.

HOOD, R. W., WRIGHT, T. M. and BURSTEIN, A. H. (1983). Retrieval analysis of total knee prostheses: A method and its application to 48 total condylar prostheses. J. Biomed. Mat. Res., 17, 829-842.

HUISKES. R. and CHAO, E.Y.S. (1983). A survey of finite element analysis in orthopaedic biomechanics: the first decade. J. Biomechanics, 16, 385-409.

HUNGERFORD, D.S. and KENNA, R.V. (1983). Preliminary experience with a total knee prosthesis with porous coating used without cement. Clin. Orthop. Rel. Res., 176, 95-107.

HUNGERFORD, D. S. and KRACKOW, K. A. (1985). Total joint arthroplasty pf the knee. Clin. Orthop. Rel. Res., 192, 23-33.

HVID, I., BENTZEN, S.M., LINDE, F., MOSEKILDE, L. and PONGSOIPETCH, (1989). X-ray quantitative computed tomography: The relations to physical properties of proximal tibial trabecular bone specimens. J. Biomechanics, 22(8-9), 837-844.

ISHIKAWA, H., FUJIKI, H. and YASUDA, K. (1996). Contact analysis of ultra high molecular weight polyethylene articular plate in arthificial knee joint during gait movement. J. Biomech. Engng., 118, 377-386. ***

JAHANMIR, S. and SUH, N. P. (1977). Mechanics of subsurface void nucleation in delamination wear. Wear, 44(1), 17-38.

JONES, L.C. and Hungerford, D.S. (1987). Cement disease. Clin. Orthop., 225, 255-262.

JONES, S. M. G., PINDER, I. M., MORAN, C. G. and MALCOLM, A.J. (1992). Polyethylene wear in uncemented knee replacements. J. Bone Joint Surg., 74B, 18-22.

KAISER, A. D. and WHITESIDE, L. A. (1990). The effect of screws and pegs on the initial fixation stability of an uncemented unicondylar knee replacement. Clin. Orthop. Rel. Res., 259, 169-178.

KEAVNEY, T. M., GUO, X. E., WACHTEl, E. F., McMAHON, T. A. and HAYES, W. C. (1994). Trabecular bone exhibits fully linear elastic behavior and yields at low strains. J. Biomechanics, 27, 1127-1136.

KEER, L.M., BRYANT, M. D. and HARIOTS, G. K. (1982). Subsurface and surface cracking due to Hertzian contact. J. Lubrication Technology, 104(3), 347-351.

KEER, L.M. and BRYANT, M. D. (1983). A pitting model for rolling contact fatigue. J. Lubrication Technology, 105(2), 198-205.

KEJA, M., WEVERS, H.W., SIU, D. and H. GROOTENBOER (1994). Relative motion at the bone-prosthesis interface. Clinical Biomechanics, 9, 275-283.

KIENAPFEL, H., SUMNER, D.R. and TURNER, T.M. (1992). Efficacy of autograft and freeze-dried allograft to enhance fixation of porous-coated implants in the presence of interface gaps. J. Orthop. Res., 10, 422-423.

KILGUS, D. J., MORELAND, J. R., FINERMAN, G. A. M., FUNAHASHI, T.T. and TIPTON, J.S. (1991). Catastrophic wear of tibial polyethylene inserts. Clin. Orthop. Rel. Res., 273, 223-231.

KING, T.Stj. and CEBONE, D. (1993). An alternative to screws for plating osteoporotic bone. J. Biomed. Eng., 15, 79-82.

KLUSTER, M.S., WOOD, G.A., STACHOWIAK, G.W. and GACHTER, A. (1997). Joint load considerations in total knee replacement. J. Bone Joint Surg., 79B, 109-113.

KURTZ, S. M., RIMNAC, C.M., SANTNER, T. J. and BARTEL, D. L.(1996). Exponential model for the tensile true stress-strain behavior of as-irradiated and oxidatively degraded ultra high molecular weight polyethylene. J. Orthop. Res., 14, 755-761.

LANDY, M. and WALKER, P.S. (1985). Wear in condylar replacement knees - A 10 year follow up. 31st Annual Meeting, Orthop. Res. Soc., 96.

LANDON, G.C., GALANTE, J.D., and MALEY, N.M. (1986). Noncemented total knee arthroplasty. Clin. Orthop. Rel. Res., 205, 49-57.

LEE, R. W., VOLZ, R. G., and SHERIDAN, D. C. (1991). The role of fixation and bone quality on the mechanical stability of tibia knee components. Clin. Orthop. Rel. Res., 273, 177-183.

LEWIS, J.L., ASKEW, M.J. and JAYEOX, D.P. (1982). A comparative evaluation of tibial component designs of total knee prostheses. J. Bone Joint Surg., 64A, 129-135.

LITTLE, R. B., WEVERS, H. W., SIU, D. and COOKE, T. D. V. (1986). A three dimensional finite element analysis of the upper tibia. J. Biomech. Engng., 108, 111-119.

MANN, K.A., BARTEL, D.L., WRIGHT, T.M. and INGRAFFEA, A.R. (1991). Mechanical characteristics of the stem-cement interface. J. Orthop. Res., 9(6), 798-808.

McNAMARA, J.L.,COLLIER, J.P., MAYOR, M.B. and JENSEN, R.E. (1994). A comparison of contact pressures in tibial and patellar total knee components before and after service in vivo. Clin. Orthop. Rel. Res., 299, 104-113.

MINTZ, L., TSAO, A. K., McCRAE, C. R., STULBERG, S. C. and WRIGHT, T. (1991). The arthroscopic evaluation and characteristics of severe polyethylene wear in total knee arthroplasty. Clin. Orthop. Rel. Res., 273, 215-222.

MIURA, H., WHITESIDE, L. A., EASLEY, J.C. and AMADOR, D. D. (1990 or 1991). Effects of screws and a sleeve on the initial fixation in uncemented total knee tibia components. Clin. Orthop. Rel. Res., 259, 160-168.

MORELAND, J.B. (1988). Mechanisms of failure in total knee arthroplasty. Clin. Orthop. Rel. Res., 226, 49-64.

MORREY, B. F., CHAO, E. Y. S. (1988). Fracture of the porous-coated metal tray of a biologically fixed knee prosthesis. Clin. Orthop. Rel. Res., 228, 182-189.

MORRISON, J.B. (1970). The mechanics of the knee joint in relation to normal walking. J. Biomechanics, 3, 51-61.

MURAKAMI, Y., KANATA, M. and YATSUZKA, H. (1985). Analysis of surface crack propagation in lubricated rolling contact. ASLE Transactions, 28(1), 60-68.

MURASE, K., CROWNINSHIELD, R.D., PEDERSEN, D.R. and CHANG, T.S. (1983). An analysis of tibial component design in total knee arthroplasty. J. Biomechanics, 16, 13-22.

NATARAJAN, R. and ANDRIACCHI, T.P. (1989). New analytical method for the analysis of bone ingrowth in porous tibial component. San Diego, ASME Biomechanics Symposium, 281-284.

NOLAN, J. F. and BUCKNILL, T. M. (1992). Aggressive granulomatosis from polyethylene failure in an uncemented knee replacement. J. Bone Joint Sur., 74B, 23-24.

PETERS, C.L. and ROSENBERG, A.G. (1995). Bone ingrowth and total knee replacement. The knee, 1, 189-196.

PILLIAR, R. M., LEE, J. M. and MINIATOPOULOS, C. (1986). Observations of the effects

of movement on bone ingrowth into porous-surfaced implants. Clin. Orthop., 208, 108-113.

PLOETZ, W.E. (1992). The influential of bone density on the friction properties of porous surfaces on bone. 38th Annual Meeting, Orthop. Res. Soc., 375.

PRAEMER, A., FURNER, S. and RICE, D.P. (1992). Musculoskeletal conditions in the united states. American Academy of Orthopaedic Surgeons, 200.

PRUITT, L., BAILEY, L. and NASSIRI, R. (1997). The role of manufacturing process on the fatigue crack propagation resistance of medical grade ultra high molecular weight polyethylene. 43 rd Annual Meeting, Orthop. Res. Soc., 790.

POLINENI, V. K., ESSNER, A., WANG, A., STARK, C. and DUMBLETON, J. H. (1997). Effect of sterilization methods on the wear behavior of UHMWPE acetabular cups - A hip joint wear simulator study. 43rd Annual Meeting, Orthop. Res. Soc., 779.

RAKOTOMANANA, R. L., LEYVRAZ, P.F., CURNIER, A., HEEGAARD, J.H. and RUBIN, P.J. (1992). A finite element model for evaluation of tibial prosthesis-bone interface in total knee replacement. J. Biomechanics, 25, 1413-1424.

RAKOTOMANANA, R. L., LEYVRAZ, P.F., CURNIER, A., MEISTER, J-J and LIVIO, J-J. (1994). Comparison of tibial fixations in total knee arthroplasty: An evaluation of stress distribution and interface micromotions. The Knee, 1, 91-99.

RANCOURT, D., SHIRAZI-ADI, A., DROUIN, G. and PAIEMENT, G. (1990). Friction properties of the interface between porous-surfaced metals and tibial cancellous bone. J. Biomed.

Mat. Res., 24, 1503-1519.

RAND, J. A. (1991). Cement or cementless fixation in total knee arthroplasty. Clin. Orthop. Rel. Res., 273, 52-62.

ROSE, R. M., RIES, M. D., PAUL, I. L., CRUGNOLA, A. M. and ELLIS, E. (1984). On the true wear rate of ultrahigh molecular weight polyethylene in the total knee prosthesis. J. Biomed Mat. Res., 18(2), 207-224.

RYD, L., ALBREKTSSON, B.E.J., HERBERTS, A., LINDSTRAND, P. and SELVIK, G. (1988). Micromotion of a cemented freeman-samuelson knee prosthesis in gnoarthrosis. Clin. Orthop. Rel. Res., 229, 205-212.

RYD, L., CARLSSON, L. And HERBERTS, P. (1993). Micromotion of a noncemented tibial component with screw fixation. Clin. Orthop. Rel. Res., 295, 218-225, 1993.

RYD, L., LINDSTRAND, A., STENSTORM, A. and SELVIK, G. (1990). Porous coated anatomic tricompartmental tibial components: the relationship between prosthetic position and micromotion. Clin. Orthop., 251, 189-197.

SATHASIVAM, S. and WALKER, P. S. (1997). A computer model with surface friction for the prediction of total knee kinematics. J. Biomechanics, 30(2), 177-184.

SHEPPARD, S., BARBER, J. R., and COMNINOU, M. (1985). Short subsurface cracks under conditions of slip and stick caused by a moving compressive load. J. Appl. Mech., 52(4), 811-817.

SHIRAZI-ADL, A. and AHMED, A.M. (1989). A parametric axisymmetric study on the interface motions in porous-surfaced tibial implant. Annuals of Biomedical Engineering, 17, 411-421.

SHIRAZI-ADL, A., DAMMAK, M. and PAIEMENT, G. (1993). Experimental determination of friction characteristics at the trabecular bone/porous-coated metal interface in cementless implants. J. Biomed. Mat. Res., 27, 167-175.

SHIRAZI-ADL, A., DAMMAK, M. and ZUKOR, J. (1994). Fixation pull-out response measurement of bone screws and porous-surfaced posts. J. Biomechanics, 27, 1249-1258.

SHIRAZI-ADL, A. and FORCIONE, A. (1992). Finite element stress analysis of a push-out test part ii: free interface with nonlinear friction properties. J. Biomech. Engng., 114, 155-161.

STRICKLAND, A.B., NATARAJAN, R., and ANDRIACCHI, T.P. (1989). Transverse motion at the interface between the tibial component and bone in a total replacement: an analytical model. AMD (ASME, Applied Mechanics Division), Biomechanics Symposium, Third joint ASCE/ASME Mechanics Conference, 285-288.

SUMNER, D. R., BERZINS, A., TURNER, T. M., IGLORIA, R., NATARAJAN, N. (1994). Initial in vitro stability of the tibial component in a canine model of cementless total knee replacement. J. Biomechanics, 27, 929-939.

SUMNER, D. R. and GALANTE, J.O. (1990), Surgery of the musculoskeletal system. In C.M. Evarts, editor, Bone ingrowth, New York, Churchill Livingstone, 131-76.

SUMNER, D. R. and TURNER, T. M. (1991). Enhancement of biological fixation in cementless

total knee arthroplasty. In Goldberg V., Total Knee Arthroplasty, New York, Raven Press.

SZIVEK, J. A., ANDERSON, P. L. and BENJAMIN, J. B. (1996). Average and peak contact stress distribution evaluation of total knee arthroplasties. J. Arthroplasty, 11, 952-963.

TANNER, M. G., WHITESIDE, L. A. and WHITE, S. E. (1995). Effect of polyethylene quality on wear in total knee arthroplasty. Clin. Orthop. Rel. Res., 317, 83-88.

TAYLOR, S.J., WALKER, P.S., PERRY, J., CANNON, S.R. and WOLEDGE, R. (1997). The forces in the distal femur and knee during different activities measured by telemetry. 43 rd Annual Meeting, Orthopaedic Research Society, 259.

TISSAKHT, A., ESKANDARI, H., and AHMED, A. M. (1995). Micromotion analysis of the fixation of total knee tibial component. Computers and Structures, 56, 365-375.

TURNER, T.M., SUMNER, D.R., URBAN, R.M., RIVERO, J.O. and GALANTE, D.P. (1986). A comparative study of porous coatings in a weight bearing total hip arthroplasty model. J. Bone Joint Surg. (A), 68A, 1396-1409.

VASU, R., CARTER, D.R., SCHURMAN, D.J. and BEAUPRE, G.S. (1986). Epiphyseal-based designs for tibial plateau components-i. stress analysis in the frontal plane. J. Biomechanics, 19, 647-662.

VOLZ, R. G., NISBET, L. K., LEE, R. W. and McMURTRY, M. G. (1988). The mechanical stability of various noncemented tibial components. Clin. Orthop. Rel. Res., 226, 38-42.

WALKER, P. S., BLUNN, G. W. and LILLEY, A. (1996). Wear testing of materials and surfaces for total knee replacement. J. Biomed. Mat. Res. (Applied Biomaterials), 33, 159-175.

WAUGH, T.R. (1985). Total knee arthroplasty in 1984. Clin. Orthop. Rel. Res., 192, 40-45.

WHITESIDE, L. A., PAFFORD, J. (1997). Load transfer characteristics of a noncemented total knee arthroplasty. Clin. Orthop. Rel. Res., 239, 168-177.

WRIGHT, T.M. and BARTEL, D.L. (1986). The problem of surface damage in polyethylene total knee components. Clin. Orthop. Rel. Res., 205, 67-74.

WYATT, R. W. B., ALPERT, J. P., DANIEL, A. U., HOFMANN, A. A. and DUNN, H. K. (1991). The effect of screw fixation on the initial rigidity of tibial knee components. J. Appl. Biomat., 2, 109-113.

APPENDIX A :

NUMERICAL AND EXPERIMENTAL STUDY OF INTERFACES WITH NONLINEAR FRICTION

APPENDIX A
NUMERICAL AND EXPERIMENTAL STUDY OF INTERFACES WITH NONLINEAR FRICTION

A.1 ABSTRACT

The purpose of this study is to develop proper constitutive relations for the interfaces with nonlinear friction properties to be implemented in the finite element analysis of cementless human knee joint implants. In the first part, bi-directional friction tests are performed to determine the primary and coupled relations between tangential stresses and relative displacements in two perpendicular directions at the beaded porous coated metal-polyurethane interface. In the second part, to validate the developed constitutive relations, the foregoing tests are simulated by finite element models. The influence of the coupling terms on results is investigated by comparison of predictions with measurement results. In the last part, a metal plate resting freely on top of a polyurethane block is analysed under normal and tangential loads to further study the influence of the interface friction coupling terms on results. The measured and computed results indicate that the coupling terms should be present in the bi-directional nonlinear friction constitutive relations. These terms, however, disappear when the friction is uni-directional or the interface load-displacement relation is linear. In the event where one component of the shear stress at the interface is much larger than the other one, such coupling terms would play a negligible role and, hence, can be dropped. Moreover, bi-directional tests suggest that the resultant load-displacement relation is nearly identical to that obtained in a uni-directional testing condition.

A.2 INTRODUCTION

In an arthritic joint, the pain can be relieved and near-normal activity be regained by a prosthetic replacement (ie, an artificial joint). The number of total joint replacements has grown significantly in the last two decades, a trend that is expected to continue with the aging population of the western societies. Cemented and cementless implants are two distinct types that are currently used in the joint arthroplasty. While in cemented implants, the cement is used as the bonding agent between the prosthetic components and the bone, in cementless implants the prosthesis is in direct contact with the host bone. In this latter, the short- and long-term fixation stability is provided by both the porous-coating of the implant at the interfaces with the bone and the screws/posts. The porous-coating is employed to promote bone ingrowth and, hence, a biologic attachment of the artificial joint to the host bone. The success of the operation depends, therefore, on the achievement of such biologic integration. Many factors are known to influence the ingrowth of bone, for example, the size of surface pores and the magnitude of relative displacements at the bone-implant interface. Excessive relative motions at the bone-porous coated metal interface are generally recognized as a factor which decreases bone proliferation into surface pores of implants (Cameron et al., 1973, Ducheyne et al., 1977), thereby resulting in adverse fibrous ingrowth (Pilliar et al., 1986).

In a cementless implant, the friction at the bone-prosthesis interface plays an important role in the mechanical response of the system, particularly in the immediate post-operative period where no bony ingrowth has yet occurred and the friction is the only means of load transfer in the direction tangential to the common interfaces. To study the relative significance of friction in the joint mechanics, uni-directional friction properties at the interface between porous-and smooth-surfaced metals and the tibial cancellous bone/polyurethane have previously been measured under single and repetitive fatigue loadings (Rancourt et al., 1990; Shirazi-Adl et al., 1993). It was found that, in

contrast to the idealized Coulomb's friction, the tangential load-displacement at the interface is highly nonlinear in which relatively large tangential displacements are recorded before the ultimate load is reached. The measured interface nonlinear properties were implemented in axisymmetric finite element analysis of push-out tests (Shirazi-Adl and Forcione, 1992) and tibial knee implants (Forcione and Shirazi-Adl, 1990). These limited case studies demonstrated the important role of friction in fixation mechanics of cementless artificial joints. The earlier finite element studies of cementless tibial components in total knee replacement have been limited in either using the idealized Coulomb's friction (Dawson and Bartel, 1992; Rakotomanana et al., 1994) or assuming a frictionless contact at the bone-implant interface (Keja et al., 1994; Shirazi-Adl and Ahmed, 1989).

The foregoing experimental and model studies treated the friction between two bodies in only a uni-directional context in which two opposing bodies in contact are bound to move along a line and, hence, transfer shear load only along the same line of motion. In a three dimensional contact problem, the articulating bodies could undergo relative movements and develop shear force in any direction on the common interface. This direction could also change during the course of deformation. The phenomenon of bi-directional friction between two bodies, therefore, needs to be studied in an experimental study the results of which can, then, be employed to develop appropriate constitutive laws necessary to perform realistic model studies of cementless artificial joints. Based on the above discussion, the aim of this study is set as to develop appropriate bi-directional nonlinear constitutive equations at the bone-polyurethane metal interface needed for three dimensional finite element analysis of human joint implants. Since, the three dimensional finite element model experiences two dimensional relative motions at the common interfaces, bi-directional friction tests between polyurethane specimens and a porous-surfaced metal are initially performed to quantify the required coupling terms in the nonlinear friction constitutive relations. Proper analytical expressions are developed for the bi-directional nonlinear friction which

account for the coupling terms. The model predictions, implementing the bi-directional friction laws, are subsequently compared and validated with the measurement results. Finally, in order to identify the relative importance of new coupling terms, the response of a plate resting freely on a polyurethane cube is investigated under combined compression and shear forces. The displacements are compared to demonstrate the significance of the bi-directional constitutive relations as compared with the uni-directional relations when studying interfaces with nonlinear friction properties. Evidently, such distinction cannot be made for the surfaces with Coulomb or bi-linear friction properties.

A.3 METHOD

A.3.1 Measurements

To perform friction tests, a beaded porous-surfaced metal plate (made of Vitallium, Howmedica, Rutherford, NJ) with the surface texture similar to those currently used in cementless implants is used. Polyurethane cubes are also prepared as the opposing body in friction tests. The use of polyurethane is due to its availability, homogeneity, and material and structural properties similar to the human tibial cancellous bone. We have also used similar polyurethane material in our previous pull out test investigations of posts and screws (Shirazi-Adl et al, 1994). The experimental apparatus developed earlier for our uni-directional friction tests (Shirazi-Adl et al, 1993) is slightly modified to allow for the simultaneous application of loads and measurement of motions in perpendicular directions. A schematic representation of the bi-directional friction test is shown in Fig. A.1. The normal load is applied on top of the moving specimen to generate a uniform pressure at the interface while the tangential loads are applied via cables at the interface level to avoid undesired moments. The bi-directional nature of the tests requires monitoring the load-displacement behavior in two perpendicular directions. Continuation of this work to measure the bone-porous

coated implant bi-directional friction properties is currently underway.

To perform the tests, specimens of polyurethane (about 20 x 20 x 10 mm) are cut and placed on top of the beaded porous-surfaced metal plate and a normal pressure of 0.2 MPa is applied which remains constant during the test. Our previous extensive friction studies have demonstrated that the interface friction resistance does not depend on the magnitude of the normal load and the rate of loading (Rancourt et al, 1990, Shirazi-Adl et al., 1993). A constant tangential preload is applied in one direction (say x) while another tangential load is applied and incrementally varied to its maximum value in the perpendicular direction (say y). The tests are terminated as soon as the maximum interface resistance is reached at which load the cube starts sliding on the metal plate. These tests are repeated for four different preload magnitudes of 32%, 42%, 72%, and 90% of the mean maximum tangential force evaluated from prior uni-directional friction tests. Each test is repeated for a minimum of four times to perform subsequent statistical analyses.

A.3.2 Finite Element Model

Frictional Contact Formulation Measured nonlinear friction properties of the uni-directional contact tests have been implemented in an in-house nonlinear finite element code and used to perform axisymmetric finite element stress analysis of push-out tests and tibial knee implants (Shirazi-Adl and Forcione, 1992; Forcione and Shirazi-Adl, 1990). In this study, the uni- and bi-directional nonlinear constitutive relations are developed and used in the ABAQUS (1992) program to perform the subsequent finite element analyses. To develop the relations, two formulations, one without coupling terms for uni-directional friction and the other with coupling terms for bi-directional friction, are presented. These are later compared and validated with the measurement results to evaluate their limitations and applicabilities.

Case A: Without coupling

In this case, it is assumed that friction response in each direction is independent of that in the other direction. The shear resistance is, therefore, a function of relative displacement at that direction only; ie, no coupling between different directions. The stress-strain relation for both directions are also assumed to be identical; ie, the isotropy of the response. For an isotropic uni-directional friction behavior, the constitutive relation is expressed as:

$$\tau_i = f(\gamma_i) \qquad i = x, y \tag{A.1}$$

where τ and γ are tangential stress and relative displacement, respectively, and f is a nonlinear friction function based on measurements in uni-directional friction experiments. The gradient of the frictional stress with respect to γ_i, (i=x,y) can be evaluated as:

$$\frac{\partial \tau_i}{\partial \gamma_j} = \begin{cases} \dfrac{\partial f(\gamma_i)}{\partial \gamma_i} & \text{when} \quad i = j \\ 0 & \text{when} \quad i \neq j \end{cases} \tag{A.2}$$

It is to be noted that the tangential stiffness of the interface in each direction is a function of the relative displacement at that direction only. In this case, the off-diagonal terms (cross-stiffness parameters) are nil and no coupling between different perpendicular directions is introduced in constitutive equations.

Case B: With coupling

In this formulation, it is assumed that the frictional properties in different directions are coupled. That is, a shear stress in one direction depends not only on the relative displacement in its own direction but also on that in the other direction perpendicular to the first one. This dependency introduces off-diagonal terms in constitutive matrix that causes coupling effects. In this case, it is

actually assumed that the resultant tangential forces and relative displacements occur in the same direction and follow the nonlinear uni-directional friction curve. With these assumptions and defining the τ_{eq} and γ_{eq} as resultant shear stress and relative displacement, shear stress components in perpendicular directions can be calculated as:

$$\tau_i = \tau_{eq} \frac{\gamma_i}{\gamma_{eq}} \qquad i = x, y \tag{A.3}$$

in which

$$\tau_{eq} = f(\gamma_{eq}) \tag{A.4}$$

where f is the uni-directional nonlinear friction function obtained from experiments.

The gradients of the interface friction stress with the relative displacements γ_x and γ_y yield both diagonal and off-diagonal stiffnesses as follows:

$$\frac{\partial \tau_x}{\partial \gamma_x} = f'(\gamma_{eq}) \frac{\gamma_x^2}{\gamma_{eq}^2} + f(\gamma_{eq}) \frac{\gamma_y^2}{\gamma_{eq}^3} \tag{A.5}$$

$$\frac{\partial \tau_y}{\partial \gamma_y} = f'(\gamma_{eq}) \frac{\gamma_y^2}{\gamma_{eq}^2} + f(\gamma_{eq}) \frac{\gamma_x^2}{\gamma_{eq}^3} \tag{A.6}$$

$$\frac{\partial \tau_x}{\partial \gamma_y} = \frac{\partial \tau_y}{\partial \gamma_x} = \left(f'(\gamma_{eq}) - \frac{f(\gamma_{eq})}{\gamma_{eq}} \right) \frac{\gamma_x \gamma_y}{\gamma_{eq}^2} \tag{A.7}$$

One observes that, in contrast to the uncoupled formulation in case A, all stiffnesses are a function of two perpendicular relative tangential displacements. Moreover, It is noted that the cross-stiffness parameters (ie, coupling terms) in Eq. A.7 disappear if the friction response becomes linear or uni-directional. Our earlier uni-directional friction measurements (Rancourt et al., 1990; Shirazi-Adl et al., 1993) demonstrated the linear dependence of the shear stress and the independence of the tangential displacement on the normal stress at the interface. In the foregoing developments given in Eqs. A.1-A.7, therefore, the normal pressure term is left out, without loss of completeness.

Finite Element Models To investigate the relative accuracy and performance of the foregoing constitutive laws, two finite element models are developed and analysed using the ABAQUS (1992) program. In the first model study, the experimental friction tests of polyurethane cubes on metal plate are simulated using a three dimensional model that includes 52 eight-node brick elements, 148 nodes and 16 contact elements, as shown in Fig.A.2. Both constitutive models with and without coupling are considered in order to validate the assumptions made in each case. To compare the predictions with the results of experimental friction tests, the geometry, boundary conditions, and loading are taken identical to those used in tests.

In second model study, a three dimensional finite element model of a beaded porous-surfaced metal plate resting freely on a polyurethane block fixed at the bottom is developed, as shown in Fig. A.3. The friction at the interface is modelled using both formulations discussed in the above cases A and B. The dimensions for the metal plate and polyurethane specimen are 75 x 50 x 3 (thickness) mm and 85 x 60 x 40 (thickness) mm, respectively. To perform this study, 1320 eight-node brick elements, 1932 nodes, and 150 contact elements are used. The normal and tangential loads are applied in three consecutive steps, first the normal and then the two perpendicular tangential forces in x and y directions, reaching maximum values of 1000 N, 250 N, and 250 N, respectively. The elastic moduli of the plate and polyurethane materials for these

studies are taken as 200000 MPa and 40 MPa, respectively. The Poisson's ratio for both materials is 0.3.

A.4 RESULTS

A.4.1 Experimental Studies

Experimental results of two dimensional friction tests performed on porous-surfaced metal plates and polyurethane cubes are shown in Figs. A.4 and A.5, normalized for normal pressure of (Pn) 1 MPa. Each curve represents the mean value of friction results obtained in four tests with the standard deviation shown only for the final point of each curve in order not to overload the graphs. Four different tangential preloads are taken in the x direction. The load-displacement is highly nonlinear exhibiting relatively large displacements before the maximum interface resistance is reached. It is seen that the presence of a preload in the x direction affects the response not only in the y direction but also the coupled tangential motion in the x direction. Moreover, the coupling effect is seen to increase as the relative magnitude of the preload increases. The measured variation of resultant forces and displacements evaluated from these bi-directional tests is verified to be similar to that measured in uni-directional tests.

A.4.2 Finite Element Studies

The predicted variation of tangential load-displacement in the y direction in presence of various preloads in the x direction are shown in Figs. A.6 and A.7 for a polyurethane cube on a porous-surfaced metal plate. These studies simulate the bi-directional experimental tests the results of which are shown in Figs. A.4 and A.5. Comparison of predictions with measurements suggests a satisfactory agreement. It also confirms the constitutive formulation accounting for the coupling

terms and indicates that the response cannot be accurately computed if these terms are neglected.

As for the finite element model studies of the metal plate resting freely on a polyurethane block, a substantial difference is computed between the results obtained by both constitutive formulations, one with the coupled terms and one without. The predictions are shown in Figs. A.8-A.13. Both the primary displacements (ie, those in the direction of applied load as shown in Figs. A.9 and A.11) and coupled ones (ie, those not in the direction of applied load as shown in Figs. A.8 and A.10) demonstrate a substantial difference between two cases. The results indicate that the case with zero off-diagonal terms markedly underestimates the tangential displacements. In the normal direction, however, almost identical displacements are predicted irrespective of the constitutive relations used, as shown in Fig. A.14. These latter results show that the plate subsides in the region adjacent to the loads and lifts up away from the loads resulting in complete separation of the metal plate and polyurethane block.

A.5 DISCUSSION

The objective of the present study was to develop appropriate nonlinear constitutive equations required for three dimensional finite element analysis of contacting bodies as is the case in the cementless artificial joints. Experimental friction studies at the beaded porous coated metal-polyurethane interface were performed to evaluate the bi-directional friction characteristics of the interface. For this purpose, in the presence of normal pressure, various preloads were applied in one direction and the response in both directions was measured as an incrementally increasing load was applied in the other direction.

Experimental results clearly suggest the presence of coupling between these two perpendicular directions. As the preload increases, the primary and coupled response under the applied load

softens. The measurements yield similar load-displacement friction curves for the resultant values in bi-directional tests as those in uni-directional tests. Friction coefficient evaluated as the ratio of the interface tangential resistance to the normal pressure was also found to be independent of the combination of tangential stresses at the interface, and is the same as that found in uni-directional tests.

The finite element simulations of above tests confirm the findings that the coupled terms in the friction constitutive relation of the interfaces with nonlinear load-displacement response are essential if accurate results are to be expected from model studies. Such coupling terms properly account for the softening in both primary and coupled responses when preloads in other directions are present. The analytical expressions for the case with coupling are, therefore, validated and can be used in future model studies of the human joint implant systems.

Both constitutive relations with and without coupling terms were used for the study of the response of a metal plate resting freely on a polyurethane block. The results confirm the substantial influence of these coupling terms on the computed displacements in the tangential directions. Both the primary and coupled motions were affected. Moreover, the constitutive law with coupling terms exhibit a softening response as far as the tangential displacements are concerned. The idealized Coulomb's friction was found in our earlier studies (Dammak, 1995; Dammak et al, 1995) not to perform satisfactorily as compared with nonlinear uni-directional friction constitutive law and, hence, was not considered in this study.

Based on the Eq. A.7, it is seen that the cross-stiffness terms (ie, coupling terms) vanish in a uni-directional analysis or when a linear friction behavior is implemented in the program. Such formulation can, therefore, be accurately used in an axisymmetric or two-dimensional analysis where there is only one shear component at the interface. Moreover, in three-dimensional cases

in which one component of shear stress at the interface is much larger than the other one, these coupling terms can be neglected without noticeable loss of accuracy. This is confirmed by both bi-directional test results shown in Figs. A.4-A.7 and our model studies of the pull out tests under inclined loads that were not reported here. Finally, it is to be noted that the formulation presented here is limited only to interfaces with isotropic friction properties; ie, where uni-directional friction properties are not direction dependent. This has been verified by our friction tests to be the case at the implant interface with the bone or polyurethane.

ACKNOWLEDGEMENTS This work is supported by a grant from the Natural Sciences and Engineering Research Council of Canada (NSERC).

REFERENCES

ABAQUS, 1992, Hibbit, Karlson and Sorenson Inc.

Cameron, H. U., Pilliar, R.M., and Macnab, I., 1973, "The effect of movement on the bonding of porous metal to bone". J. Biomed. Mat. Res., Vol. 7, pp. 301-311.

Dammak, M., 1995, "Etudes experimentale et numerique de protheses noncimentees du genou human". PhD thesis, Genie mecanique, Ecole Polytechnique, Montreal, Canada.

Dammak, M., Shirazi-Adl, A., and Zukor, D., 1995, "Fixation analysis of posts, screws, and plates -experimental and finite element studies". J. Biomechanics., Submitted.

Dawson, J.M., and Bartel, D.L., 1992, "Consequences of an interface fit on the fixation of porous-coated tibial components in total knee replacement". J. Bone Joint Surg., Vol. 74-A, No.2, pp. 233-238.

Ducheyne, P., DeMeester, P., Aernoudt, E., Martens, M. and Mulier, C., 1977, "Influence of a functional dynamic loading on bone ingrowth into surface pores of orthopaedic implants". J. Biomed. Mat. Res., Vol. 11, pp. 811-838.

Forcione, A., and Shirazi-Adl, A., 1992, "Biomechanical analysis of a porous surfaced knee

implant: A finite element contact problem with nonlinear friction". Mechanical Engineering Forum, Canadian Society of Mechanical Engineers, Toronto., Vol. 2, pp. 19-24.

Keja, M., Wevers, H.W., Siu, D., and Grootenboer, H., 1994, "Relative motion at the bone-prosthesis interface". Clin. Biomech., Vol. 9, No. 5, pp. 275-283.

Pilliar, R.M., Lee, J.M., and Miniatopoulos, C., 1986, Observations of the effects of movement on bone ingrowth into porous-surfaced implants". Clin. Orthop., Vol. 208, pp. 108-113.

Rakotomanana, R.L., Leyvraz, P.F., Curnier, A., Meister, J-J., and Livio, J-J., 1994. "Comparison of tibial fixations in total knee arthroplasty: An evaluation of stress distribution and interface micromotions". The Knee, Vol. 1, No.2, pp. 91-99.

Rancourt, D., Shirazi-Adl, A., and Drouin, G., 1990, "Friction properties of the interface between porous-surfaced metals and tibial cancellous bone". J. Biomed. Mater. Res., Vol. 24, pp. 1503-1519.

Shirazi-Adl, A., and Ahmed, A. M., 1989, "A parametric axisymmetric study on the interface motions in porous-surfaced tibial implants". Annuals of Biomedical Engineering, Vol. 17, pp. 411-421.

Shirazi-Adl, A., Dammak, M., and Paiement, G., 1993, "Experimental determination of friction characteristics at the trabecular bone/porous-coated metal interface in cementless implants". J. Biomed. Mater. Res., Vol. 17, pp. 167-175.

Shirazi-Adl, A., Dammak, M., and Zukor, D., 1994, "Fixation pull-out response measurement of bone screws and porous-surfaced posts". J. Biomechanics, Vol. 27, No. 10,pp. 1249-1258.

Shirazi-Adl, A., and Forcione, A., 1992. "Finite element stress analysis of a push-out test part II: free interface with nonlinear friction properties". J. Biomech. Engng., Vol. 114, pp. 155-161.

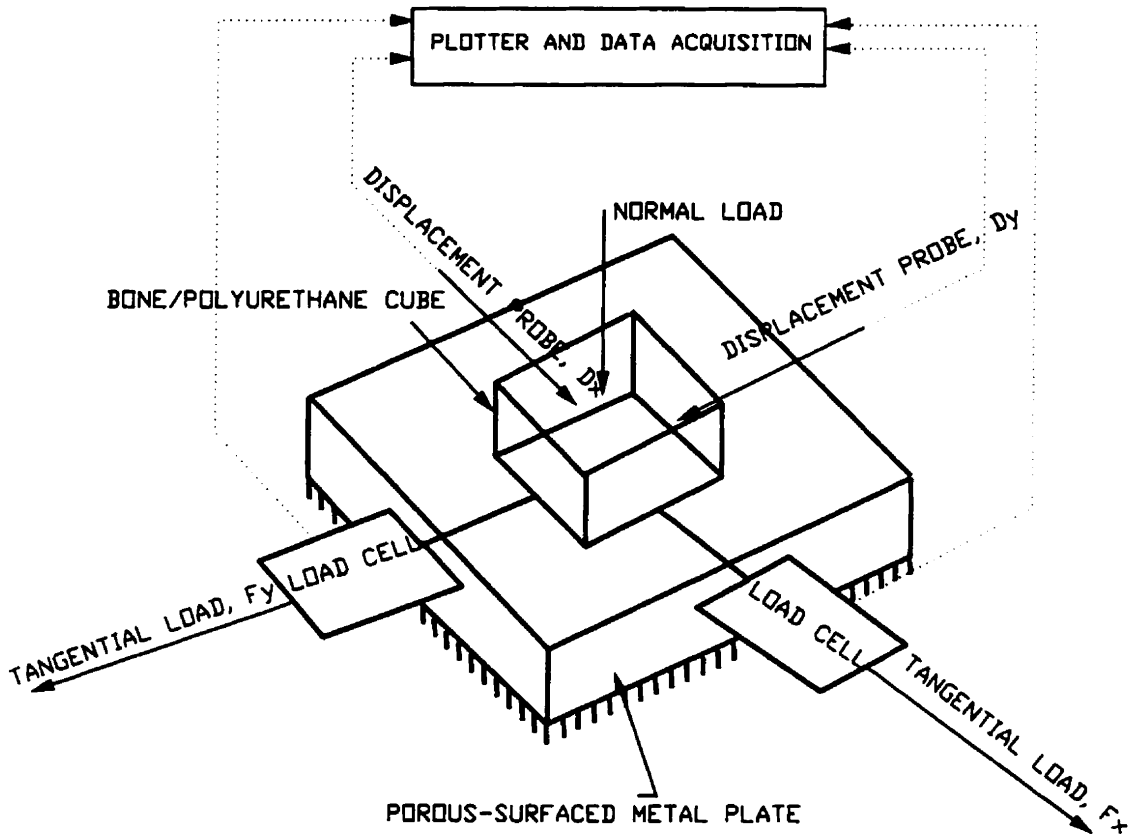

Figure A.1 A schematic representation of the experimental setup for bidirectional friction tests of bone or polyurethane samples on a porous-surfaced metal plate.

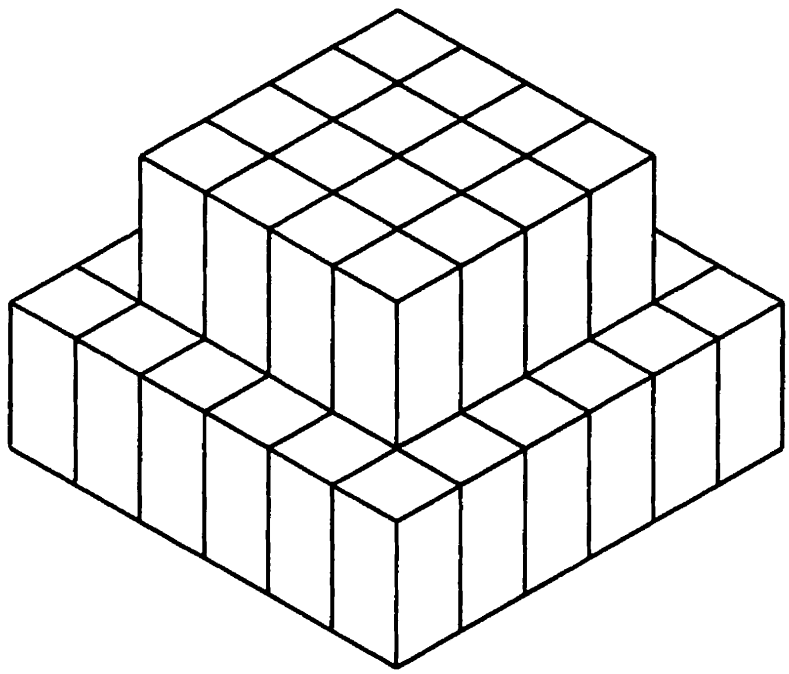

Figure A.2 The three dimensional finite element model of the experimental friction test of Figure 1 simulating a polyurethane cube resting on top of a porous-surfaced metal plate.

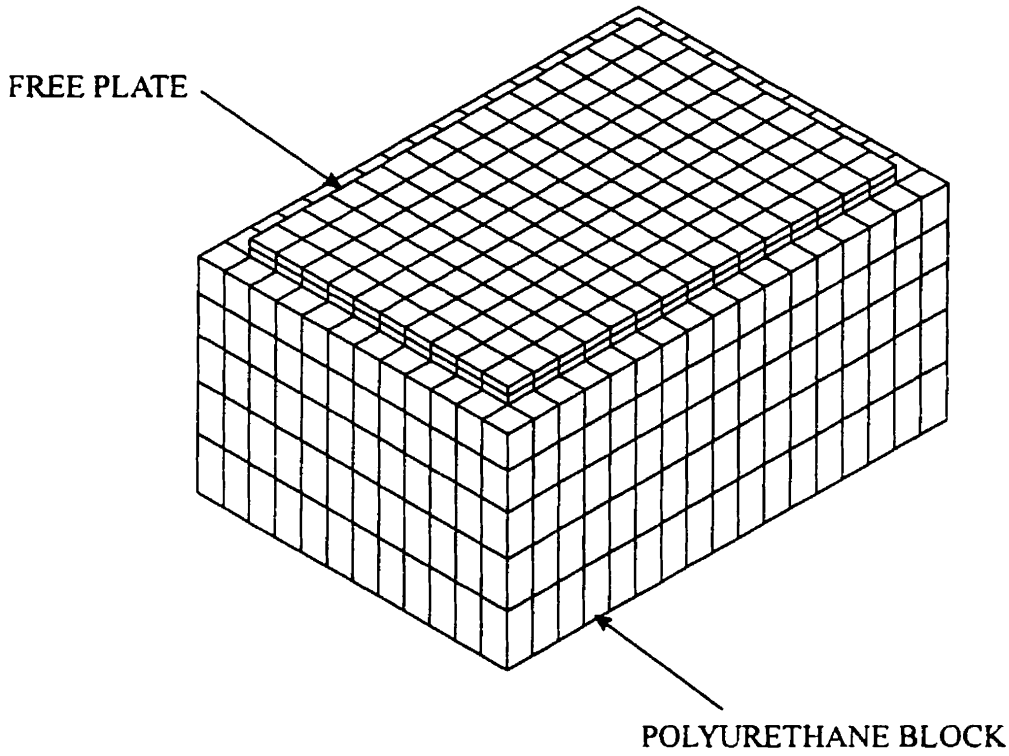

Figure A.3 Finite element mesh of a plate (75 x 50 x 3 mm) resting freely on top of a polyurethane block (85 x 60 x 40 mm) fixed at the bottom. Normal and tangential forces are applied eccentrically on the metal plate.

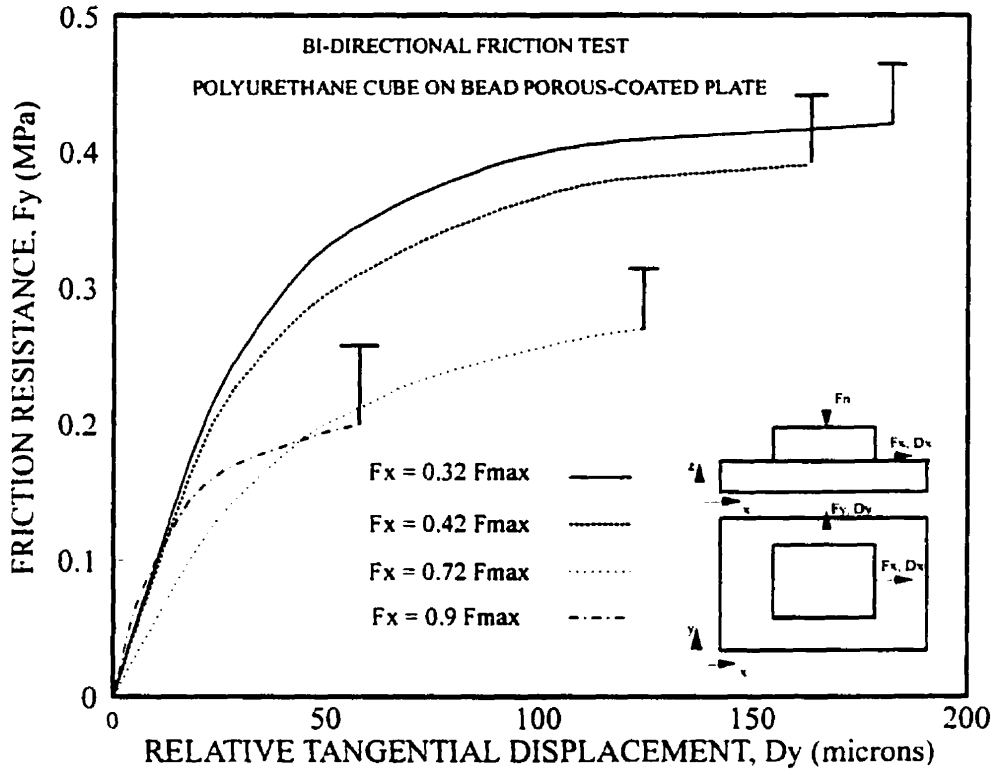

Figure A.4 Experimental friction load (y)-dislacement(y) curve under monotonically increasing tangential load F_y preloaded in perpendicular direction x by F_x expressed as a percentage of F_{max} which is the mean interface resistance force in uni-directional test. The standard deviation is given for each case at the final point only.

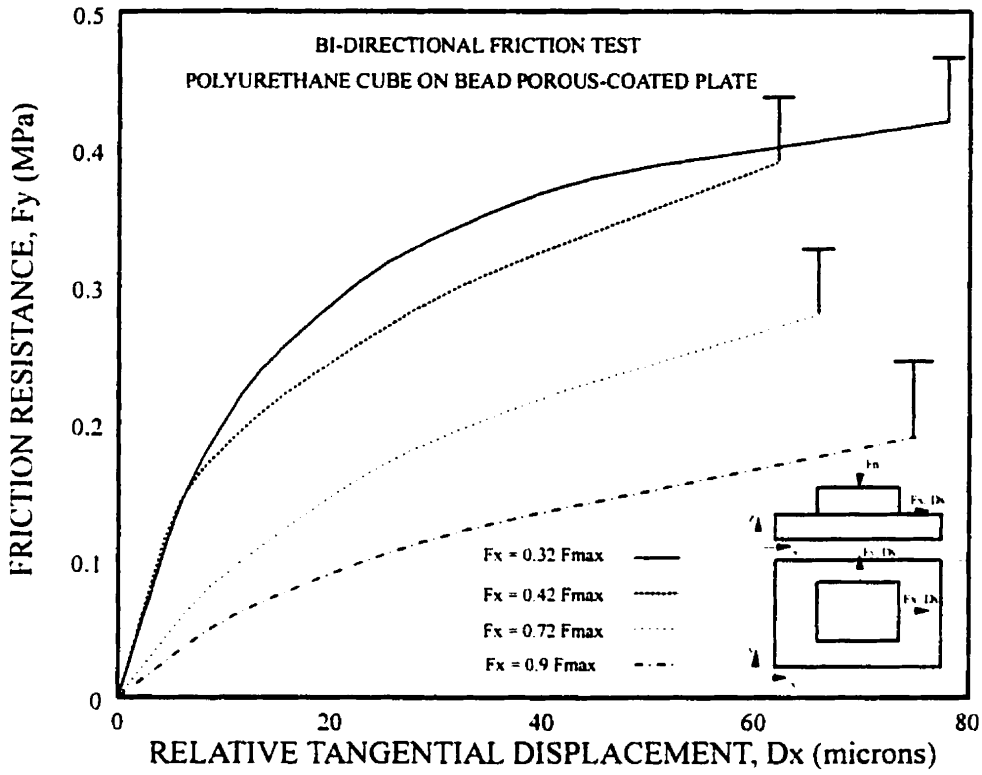

Figure A.5 Experimental friction load (y)-dislacement (x) curve under monotonically increasing tangential load F_y preloaded in perpendicular direction x by F_x expressed as a percentage of F_{max} which is the mean interface resistance force in uni-directional test. The standard deviation is given for each case at the final point only.

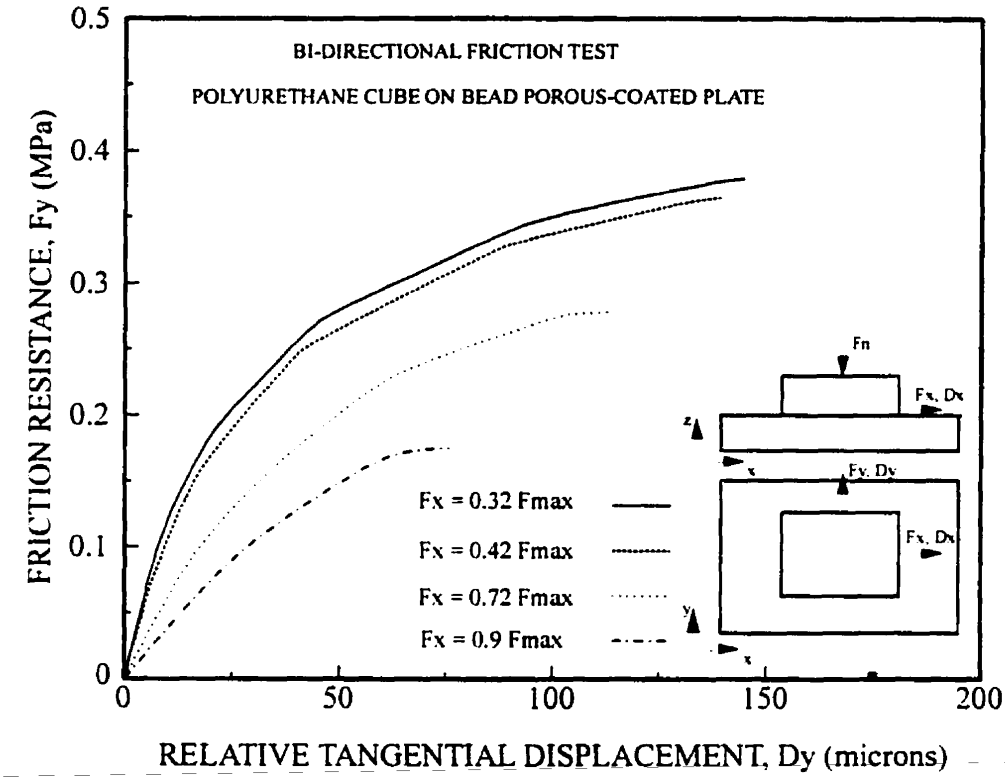

Figure A.6 Predicted load (y)-dislacement (y) curve of bi-directional friction tests in presence of various preloads in the x direction. F_{max} is the mean maximum tangential force measured in uni-directional test.

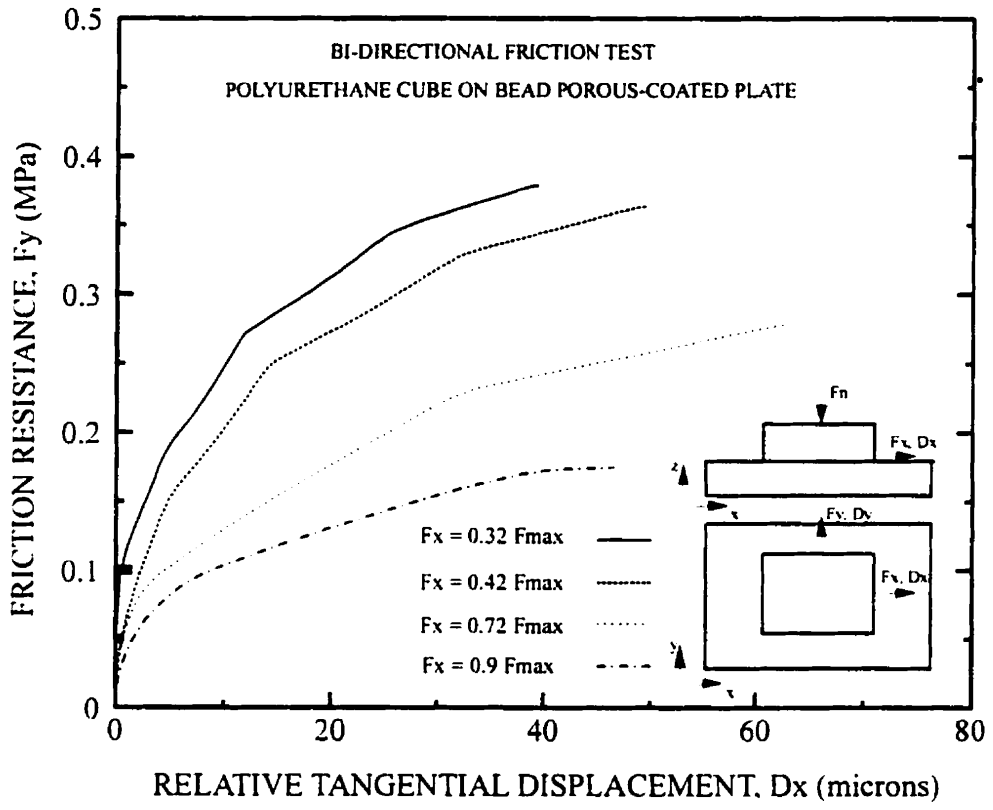

Figure A.7 Predicted load (y)-dislacement (x) curve of bi-directional friction tests in presence of various preloads in the x direction. F_{max} is the mean maximum tangential force measured in uni-directional test.

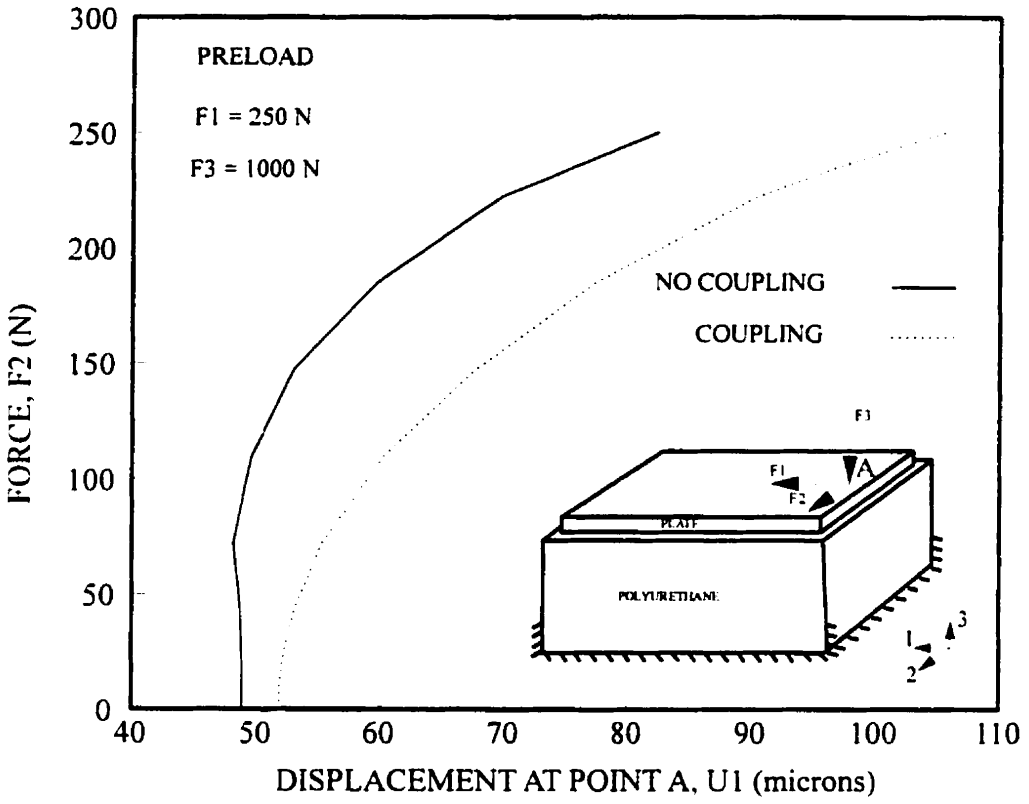

Figure A.8 Predicted shear force (F_2)-dislacement (U_1) response at point A under the preloads in directions 1 and 3 for the cases with and without coupling terms.

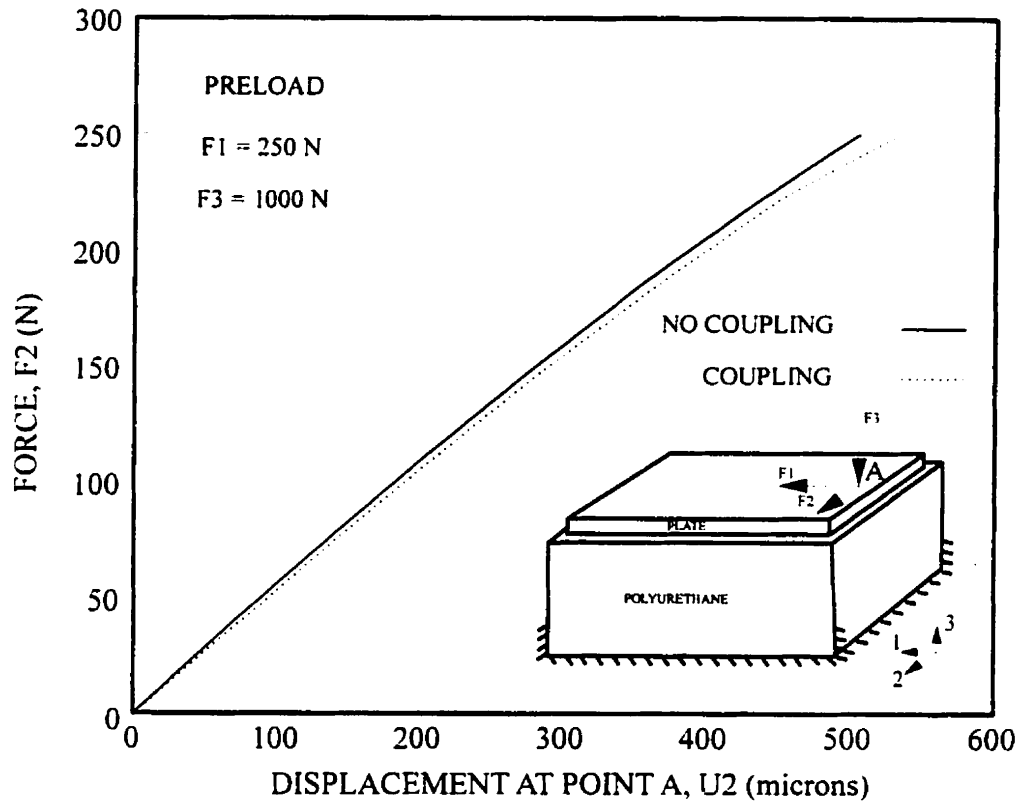

Figure A.9 Predicted shear force (F_2)-dislacement (U_2) response at point A under the preloads in directions 1 and 3 for the cases with and without coupling terms.

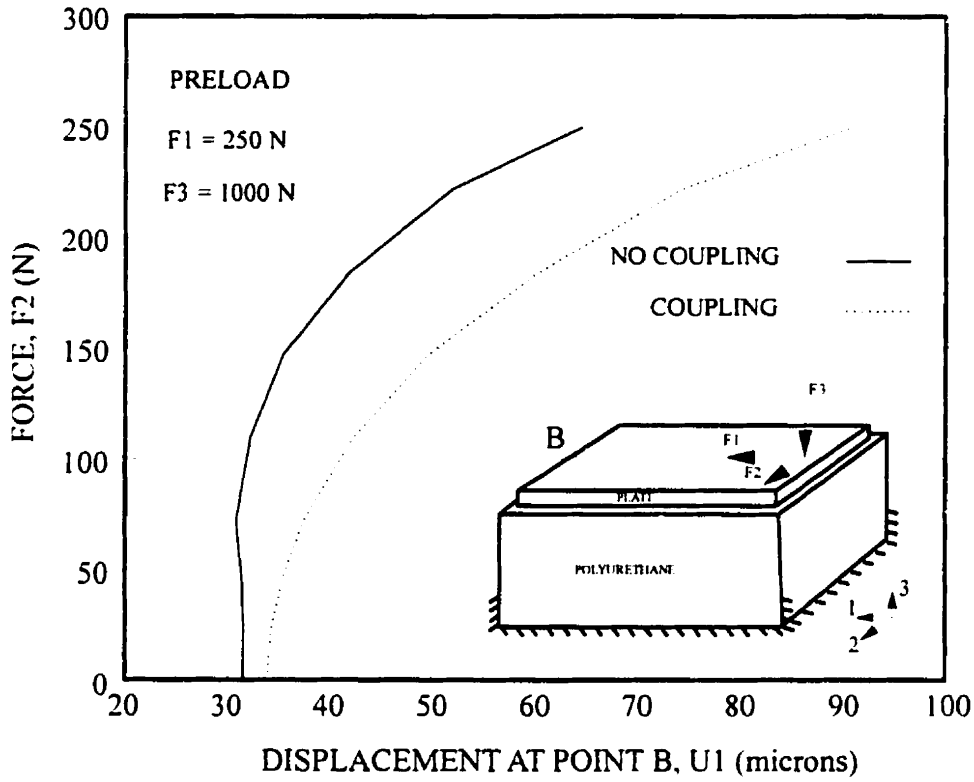

Figure A.10 Predicted shear force (F_2)-dislacement (U_1) response at point B under the preloads in directions 1 and 3 for the cases with and without coupling terms.

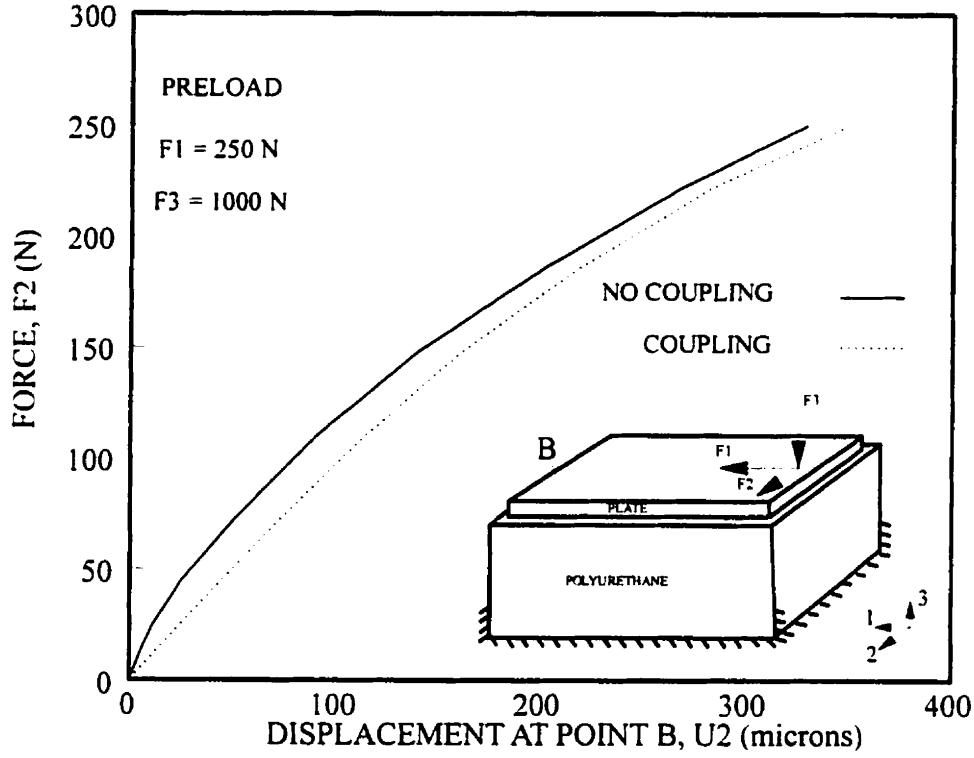

Figure A.11 Predicted shear force (F_2)-dislacement (U_2) response at point B under the preloads in directions 1 and 3 for the cases with and without coupling terms.

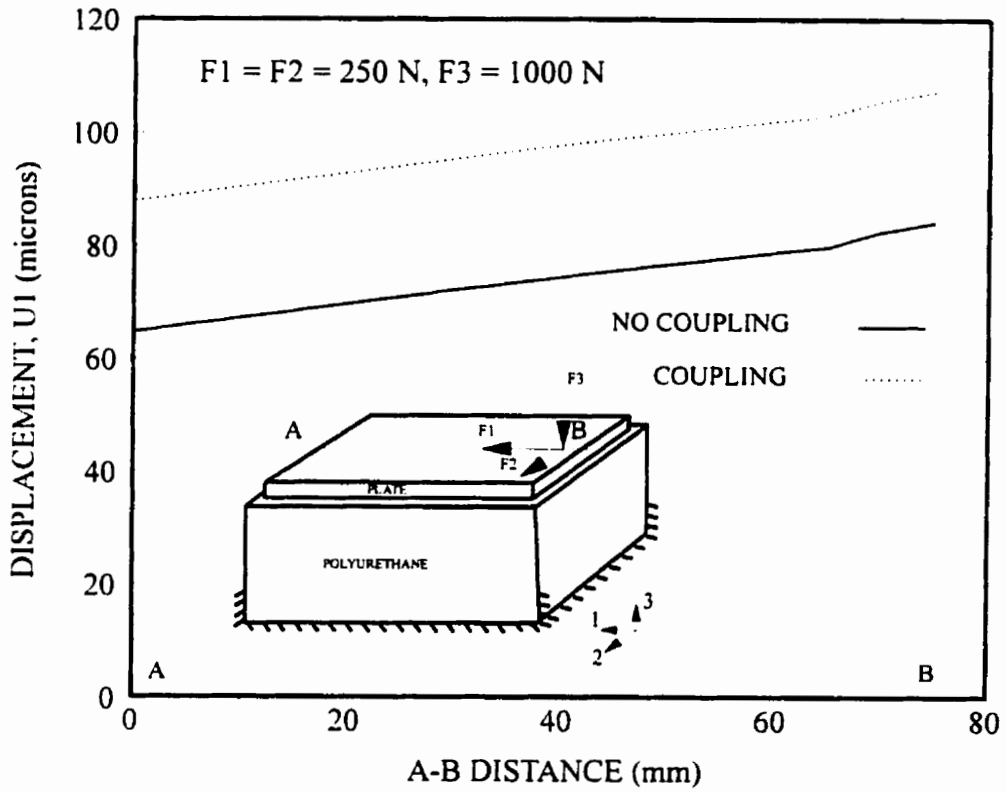

Figure A.12 Predicted tangential displacement (U_1) along AB on top of the plate under final loads for the cases with and without coupling terms.

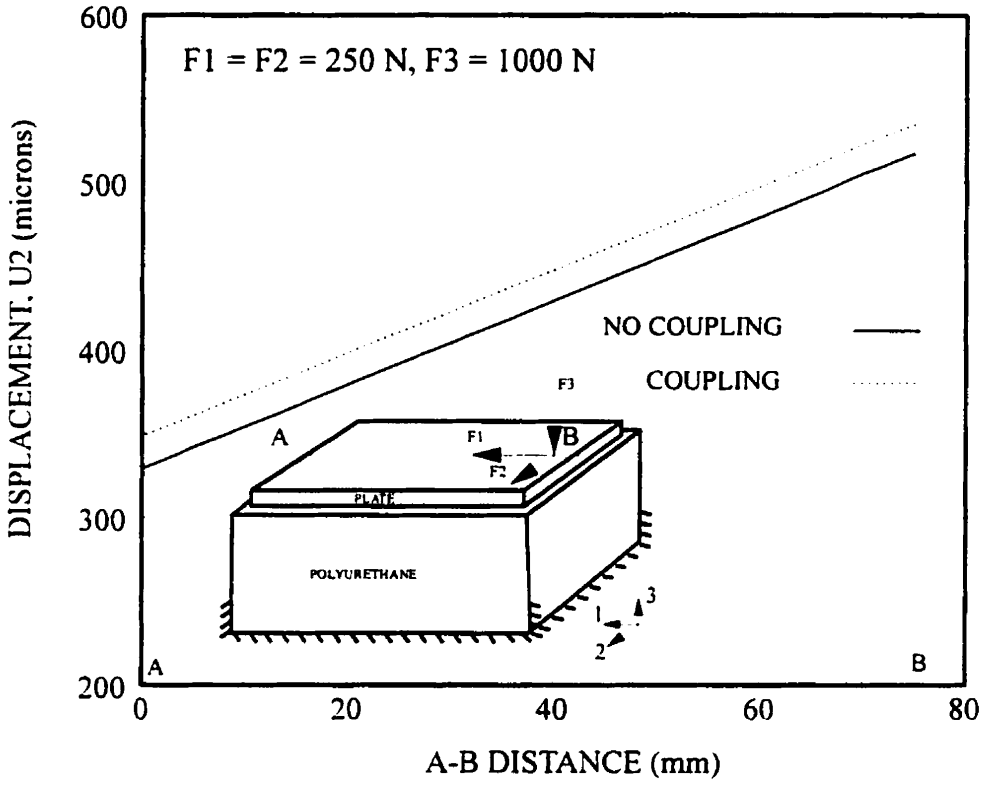

Figure A.13 Predicted tangential displacement (U_2) along AB on top of the plate under final loads for the cases with and without coupling terms.

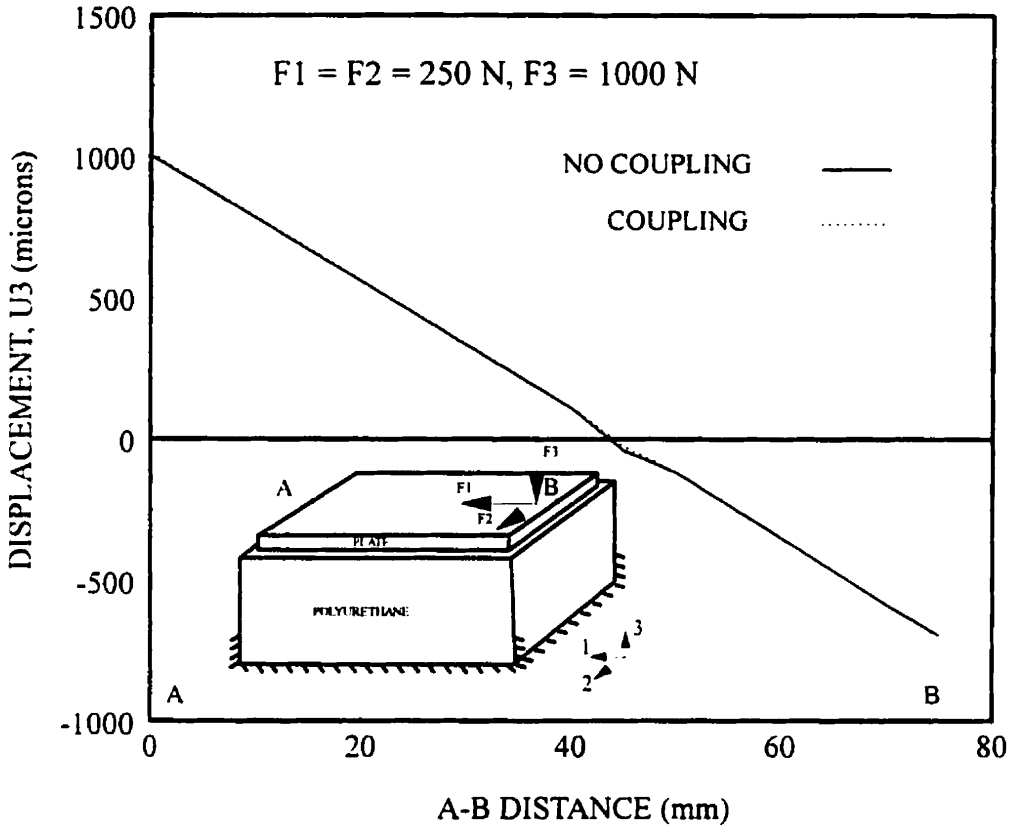

Figure A.14 Predicted tangential displacement (U_3) along AB on top of the plate under final loads for the cases with and without coupling terms.

APPENDIX B

EFFECT OF LOADING/UNLOADING CYCLE ON THE FRICTION PROPERTIES AND PULL-OUT TESTS

APPENDIX B

EFFECT OF LOADING/UNLOADING CYCLE ON THE FRICTION PROPERTIES AND PULL-OUT TESTS

B.1 INTRODUCTION

The important role of friction and screws/posts on the fixation stability of the implant has been discussed in chapters 2, 3 and appendix A. In those studies the load was assumed to be monotonic. Since knee-implant systems undergo cyclic loading, fatigue analysis will be required to simulate long-term performance of prostheses. To study the effect of a full loading/unloading cycle on the knee-implant structure, the interface friction properties and pull out responses were investigated. These parameters, like friction properties at the interface of bone and implant, and pull-out resistance force of posts and screws have direct impact on the overall implant cyclic response. For this purpose and in order to initiate such study, a few cycles of friction tests and axial pull-out tests are performed and proper FE models are also developed and validated. The measured fatigue performance of the interface between the bone and the porous surface plate, after being validated in pull-out model studies, could be used in FE study of tibial knee implants to predict the permanent migration of the implant over the long term period (Ryd et al., 1988; Ryd et a., 1993).

B.2 METHODS

Experimental model of friction tests performed at the interface between polyurethane and porous surface metal are presented. Then, pull-out response in a cycle of loading/unloading is discussed using both experimental and FE model studies.

B.2.1 Friction tests

Experimental friction tests were aimed to investigate the friction properties at the polyurethane-porous coated metal interface in a uni-directional loading and unloading cycle required for a fatigue study.

Test apparatus The experimental apparatus developed earlier (Shirazi-Adl et al., 1993) for the uni-directional friction tests was used to perform loading-unloading friction tests. A schematic representation of the friction test apparatus is shown in Figure 2.3.

Preparation of specimens A beaded porous-surfaced metal plate (made of Vitallium, Howmedica, Rutherford, NJ) with the surface texture similar to those currently used in cementless implants was used. This plate was used in the earlier studies in uni-directional friction tests (Shirazi-Adl et al., 1993). Polyurethane specimens of similar dimensions were also cut for the friction tests. The use of polyurethane (at least four specimens in each case) was due to its availability, homogeneity, and material and structural properties similar to those of the human tibial cancellous bone. A smooth-surfaced stainless steel plate was also used in the uni-directional loading/unloading friction tests.

Experimental procedure To perform uni-directional friction tests, cubic specimens of

polyurethane were placed on the top of metal plates (porous/smooth-surfaced metal plates). The Normal pressures of 0.2 and 0.35 were used for porous/smooth-surfaced metal plates, respectively. Tangential force was applied via cable at the interface level to avoid undesired moments. Similar to the earlier uni-directional tests, tangential load-displacement curve at the interface was measured. During the tests, the tangential force was removed at various load levels and the unloading part of the curve was recorded as well.

B.2.2 Pull-out loading/unloading behavior

Experimental test To determine the parameters affecting fixation behavior of screws and posts, pull-out tests were performed. Loading-unloading pull-out tests were performed to determine residual stresses and/or displacements at the interface. Experimental results were used to validate the axisymmetric FE models of pull-out tests. The test procedure was similar to those performed by Shirazi-Adl et al., (1994). A porous-coated post provided by Howmedica (Howmedica, Rutherford, NJ) and a stainless smooth-surfaced post were used in these experiments. The diameter of posts was 8.75 mm. Polyurethane cylinders with 30 mm diameter and 40 mm height were prepared. The inside diameter of cylinders before inserting the posts (i.e., drill size) was 8 mm. A special fixation set-up was used to hold these cylinders in place during the pull-out tests. The outer surface of cylinders was fixed. The pull-out resistance force versus displacement curves were measured. During these tests, unloading behavior at different load levels was also registered. Each loading step included loading up to a prescribed load, unloading to zero load, and reloading to the previous prescribed load. These steps were repeated two times for each test specimens. Four specimens were used for each test.

FE model Pull-out tests were analyzed using nonlinear, axisymmetric FE analyses. The FE models composed of 163 quadrilateral bilinear elastic elements for the metallic post and

polyurethane cylinder, and twelve nonlinear contact elements along the interface. Contact elements relate the amount of shear stress that can be transferred along the interface element to amount of relative displacement that is occurred at the interface. These elements were not allowed to transfer tensile stresses but can transfer compressive stresses. The ultimate shear stress was related to the normal stress by friction coefficient. If the shear stress exceeds the measured ultimate shear strength of the surrounding material, the contact condition changes from stick to slip state. Elastic moduli of 220 GPa and 40 MPa were assigned to the post and polyurethane materials, respectively. A Poisson's ratio of 0.3 was used for both materials. The measured nonlinear loading/unloading curves were used to model the interface. Friction coefficient of 0.38 and 0.2 were used for the porous and smooth-surfaced posts, respectively. The FE mesh of cylinder and inserted post is shown in Figure B.1. The ABAQUS code was used to perform these analyses.

B.3 RESULTS

B.3.1 Friction tests

The friction curve measured under monotonically increasing/decreasing tangential load for porous-surfaced plate is presented in Figure B.2. These experiments suggest that the friction response is mainly irreversible. At normal load equal to one (normalized), the unloading stiffness is found to be 24.2±2.8 (mean ± SD) and 29.7±2.1 (N/μm) for porous and smooth-surfaced plates, respectively. Repeating the loading/unloading cycle at different load levels did not affect these values.

B.3.2 Loading/unloading pull-out tests

A typical pull-out load/unload-displacement response for porous posts is shown in Figure B.3. The

FE results for a porous- and smooth-coated posts are presented in Figure B.4 and B.5, respectively. Two different stiffnesses were used in analysis; One based on friction tests while the other based on a perfectly plastic behavior of friction. As it is seen the unloading stiffness based on the friction tests yields results that are in better agreement with experimental results than those based on infinite unloading stiffness. The comparison is more evident in porous-coated posts due to their larger relative displacements. The program is developed so that it can be used for different unloading stiffnesses including the infinite one.

B.4 DISCUSSION

In this work, the effect of loading/unloading on uni-directional friction properties at the interface between polyurethane and the porous/smooth-surfaced metal plate was investigated. Moreover, the influence of repetitive loading on pull-out response was analyzed using both experimental and FE methods.

B.4.1 Friction tests

The friction tests were performed under monotonically increasing/decreasing tangential load for porous and smooth-surfaced plates. Nonlinear curves similar to those of the earlier studies (Rancourt et al., 1990; Shirazi-Adl, 1993) were found. These experiments suggested that the friction response is mainly irreversible, regardless of the surfaces used in the experiment. Polyurethane/porous-surfaced metal plate interface generated larger residual displacement in unloading than the polyurethane/smooth-surfaced interface. The reloading slope was identical to the unloading one and no significant change in friction properties was observed after repeating the tests for a few cycles. The unloading stiffnesses (slopes) found in friction tests were implemented in FE model study of pull-out tests.

B.4.2 Axial loading/unloading pull-out tests

The loading-unloading behavior of pull-out tests were investigated using both experimental and FE model studies. Experimental tests revealed nonlinear load-displacement behavior for both posts, particularly for the porous-surfaced one. The FE models of the pull-out specimens accurately represented the global load-displacement behavior. This was accomplished by using nonlinear friction interface elements at the post-polyurethane interface. The mechanism of load transfer from the post to the polyurethane was determined from the analysis of measurement and FE results. The largest strain at the interface elements occurred at the tip of the post. The FE analyses predicted a large shear stress concentration at the tip of the post. Since the interface could only support a limited magnitude of shear stress, slipping between post and polyurethane initiated in this region. As the magnitude of the applied load increased, the region of slipping extended upward from the tip of the post. The entire interface was in a slip state when shear stress at each point exceeds its corresponding shear limit.

During the unloading part, the post-polyurethane interface remained in a stick state along the interface. The unloading and reloading slopes of the curves remained unchanged, regardless of the magnitude of the load prior to unloading. In unloading, a residual displacement was always present which was due to the relative micromotion between post and cylinder during loading. The amount of longitudinal relative motion between post and cylinder depended on the prescribed load, and, hence, on the nonlinear friction at the interface. The normal stresses due to press fit (initial interference) were remained unchanged during the loading/unloading process.

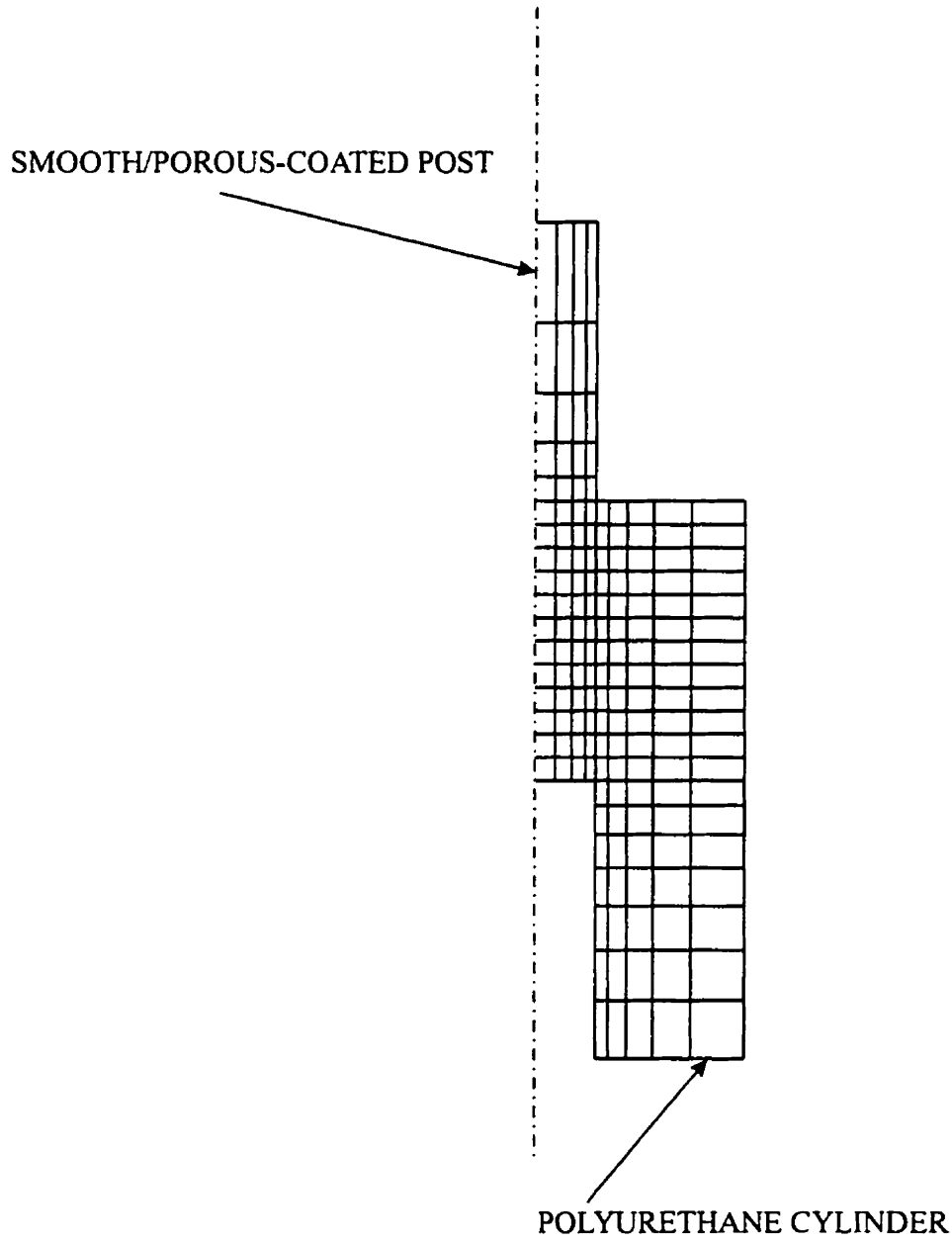

Figure B.1 Axisymmetric finite element mesh representation of the pull-out test specimen. The cylinder is fixed completely along the outer surface.

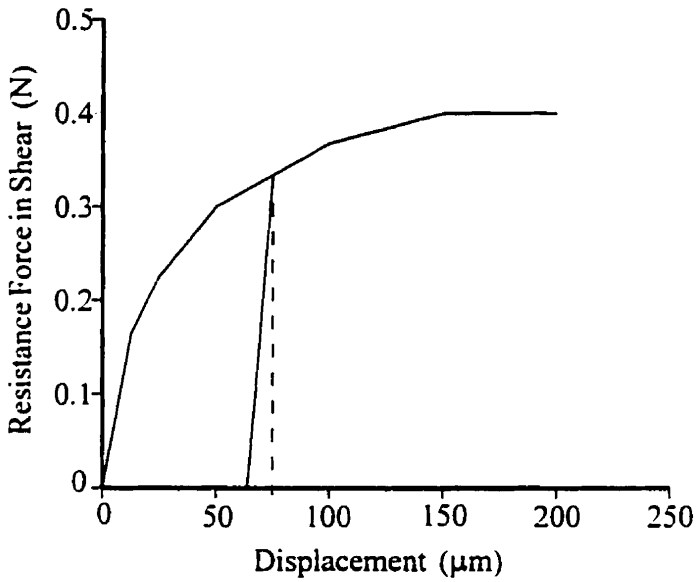

Figure B.2 The tangential load/unload-displacement response of a beaded porous-surfaced plate in contact with polyurethane. Solid line is based on experiments while the dashed line presents the completely irreversible friction behavior (Pn=1 N).

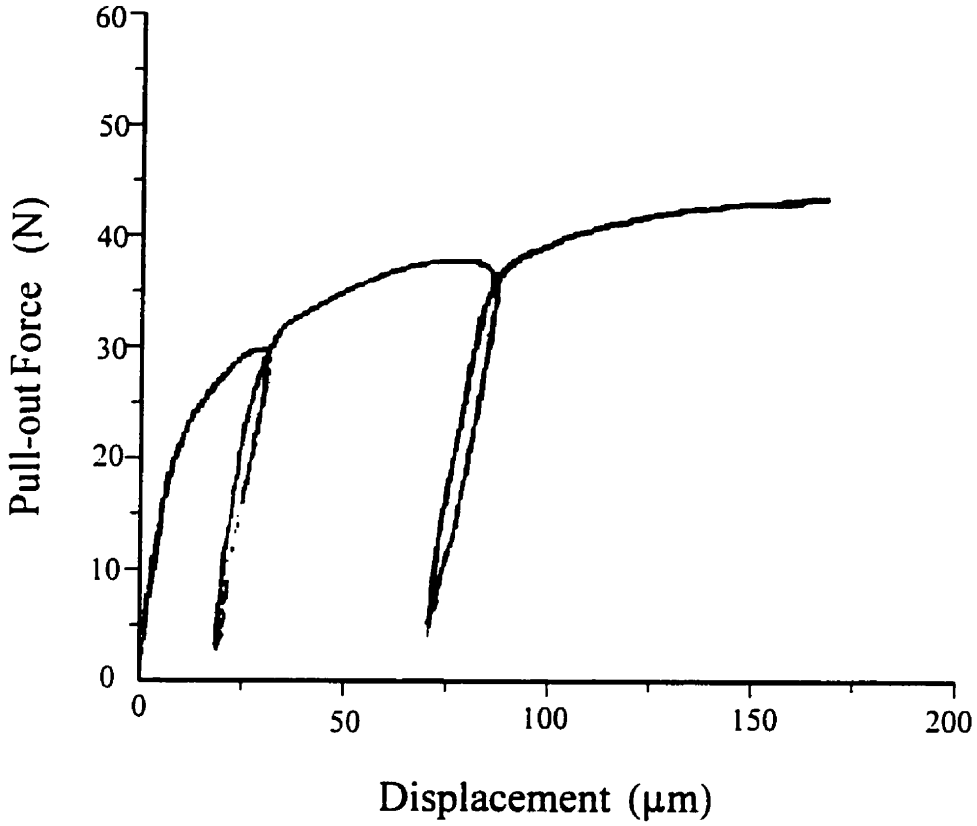

Figure B.3 A typical pull-out load/unload-displacement response of a beaded porous-coated post in polyurethane. (Post diameter D=8.75 mm, cylinder diameter D=30mm, drill size DS=8.0 mm, insertion depth L=20 mm).

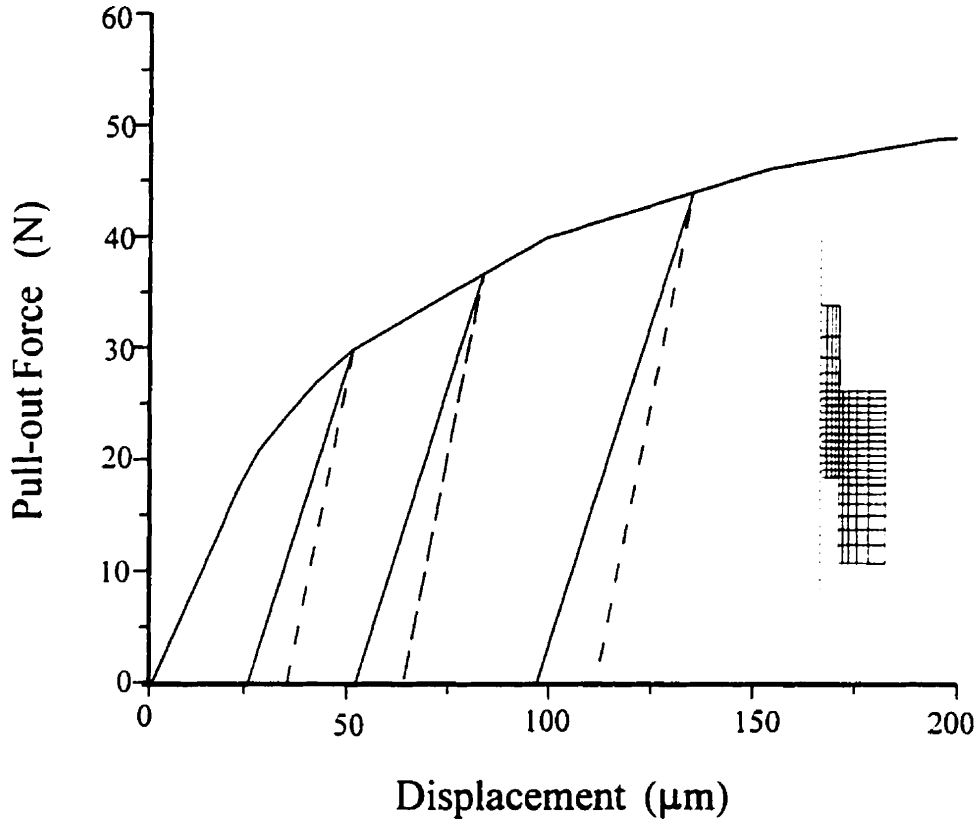

Figure B.4 A pull-out load/unload-displacement response of a beaded porous-coated post in polyurethane. Unloading curves are for 60%, 75% and 90% of ultimate pull-out load. Friction unloading stiffness is equal to 24.2 (N/mm) and ∞ for solid line and dashed line, respectively.

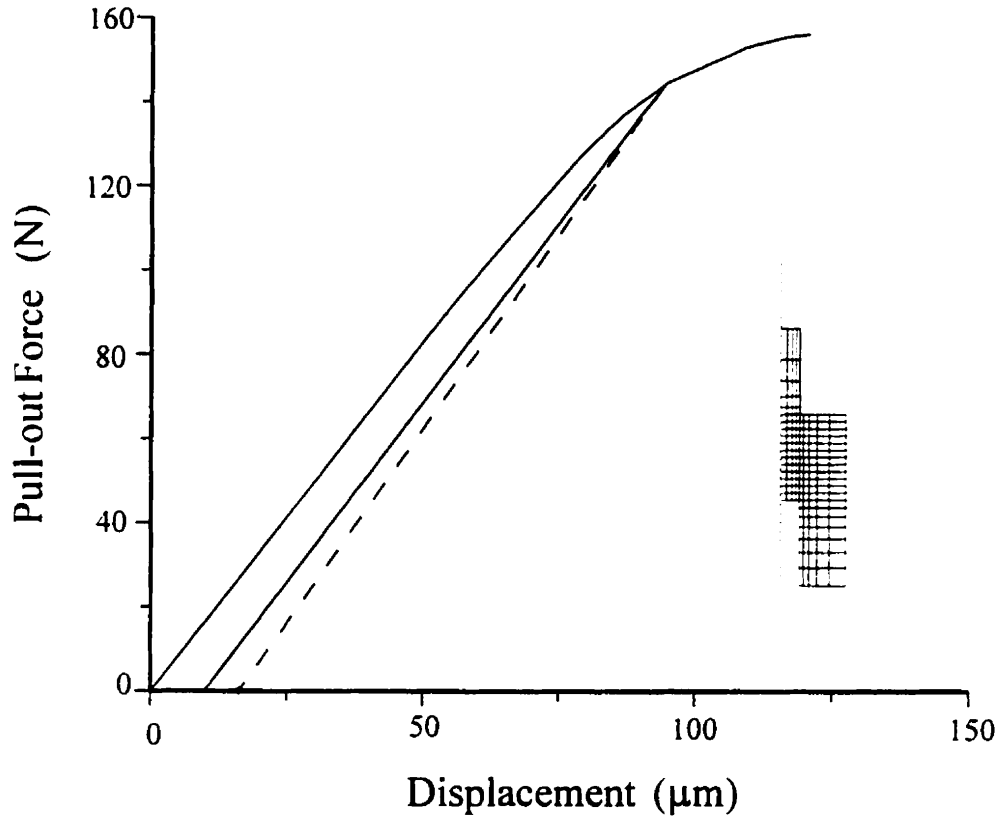

Figure B.5 A pull-out load/unload-displacement response of a smooth surfaced post in polyurethane. Unloading curve is for 90% of ultimate pull-out load. Friction unloading stiffness is equal to 29.7 (N/mm) and ∞ for solid line and dashed line, respectively.

APPENDIX C:

SUPPLEMENTARY RESULTS OF THE FINITE ELEMENT ANALYSIS OF TIBIAL IMPLANTS

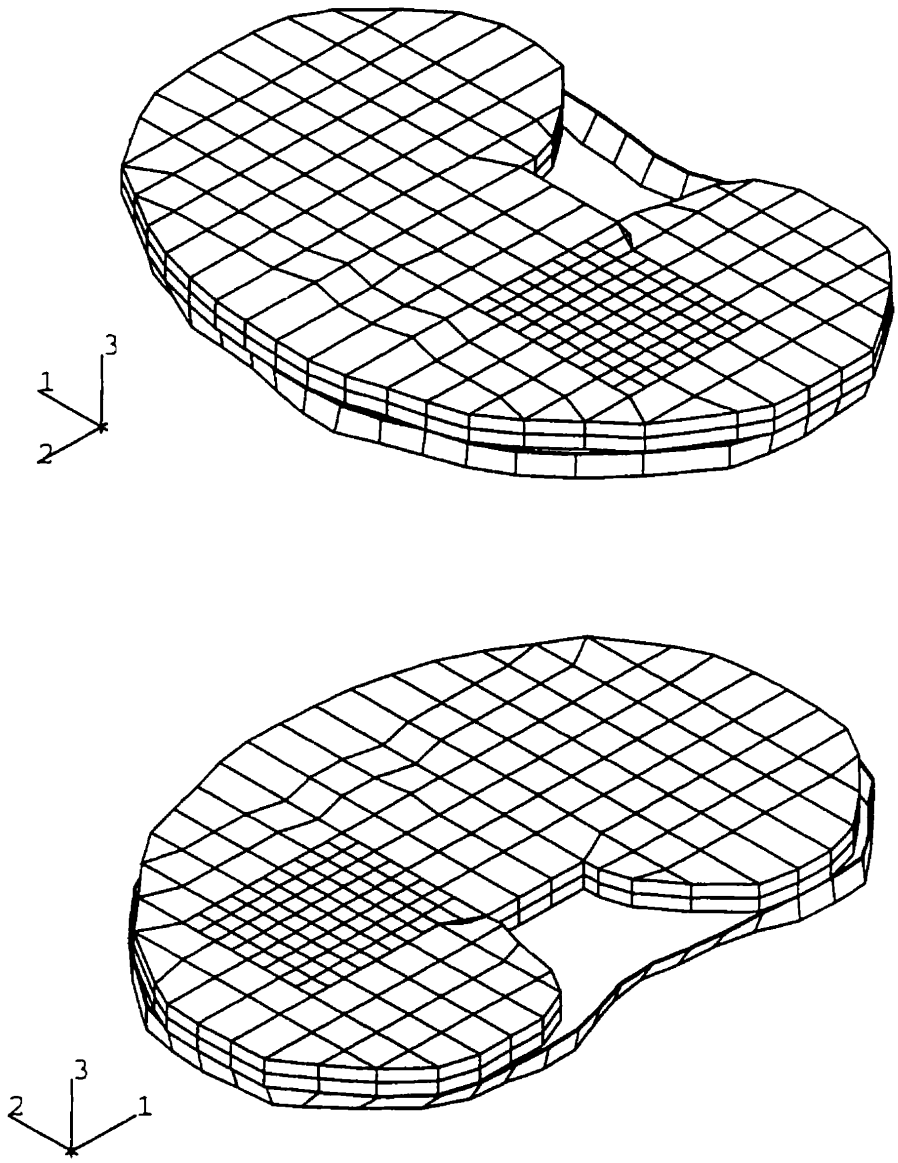

Figure C.1 Relative position of tibial baseplate component to cortical bone from two perspectives. The baseplate is sitting entirely on the cortical bone except in some regions.

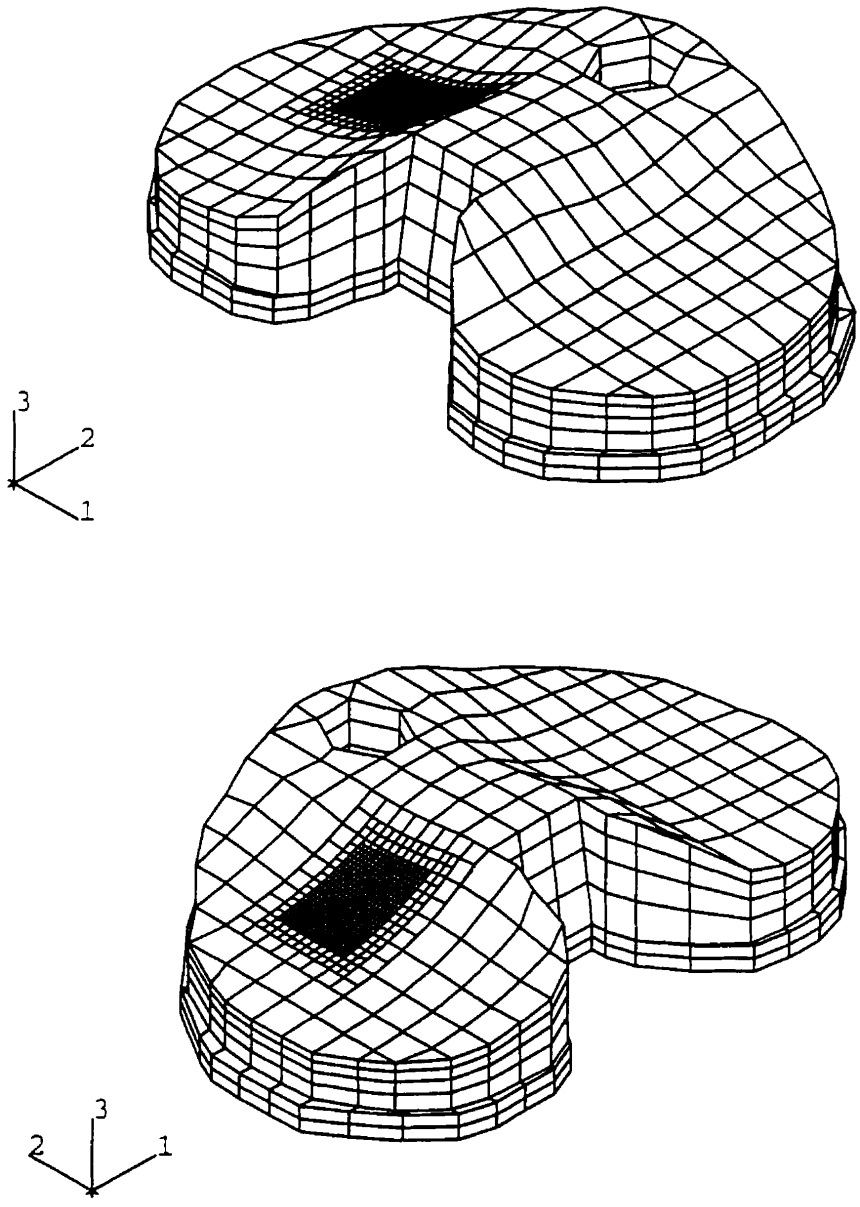

Figure C.2 Relative position of polyethylene insert to tibial baseplate from two perspectives. Baseplate overlaps polyethylene.

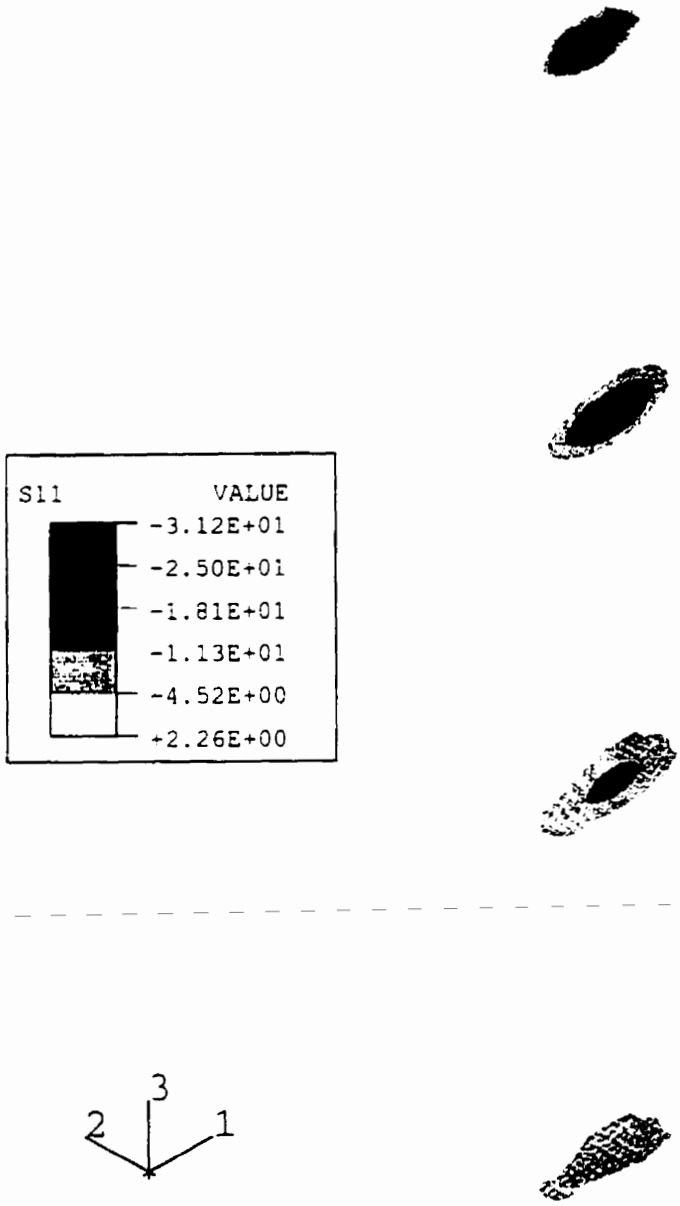

Figure C.3 Normal stress distribution, S_{11}, (M-L) in different layers of the polyethylene component.

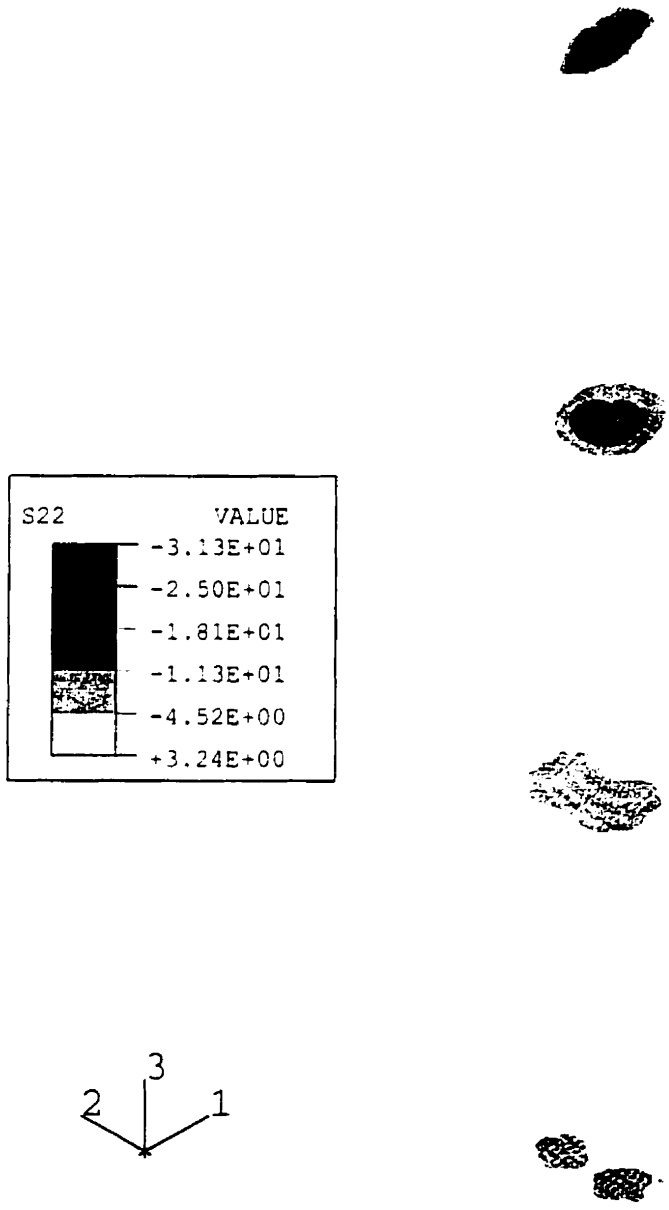

Figure C.4 Normal stress distribution, S_{22}, (A-P) in different layers of the polyethylene component.

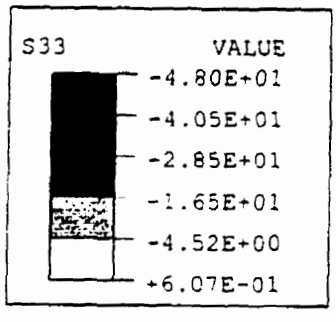

Figure C.5 Normal stress distribution, S_{33}, (axial) in different layers of the polyethylene component.

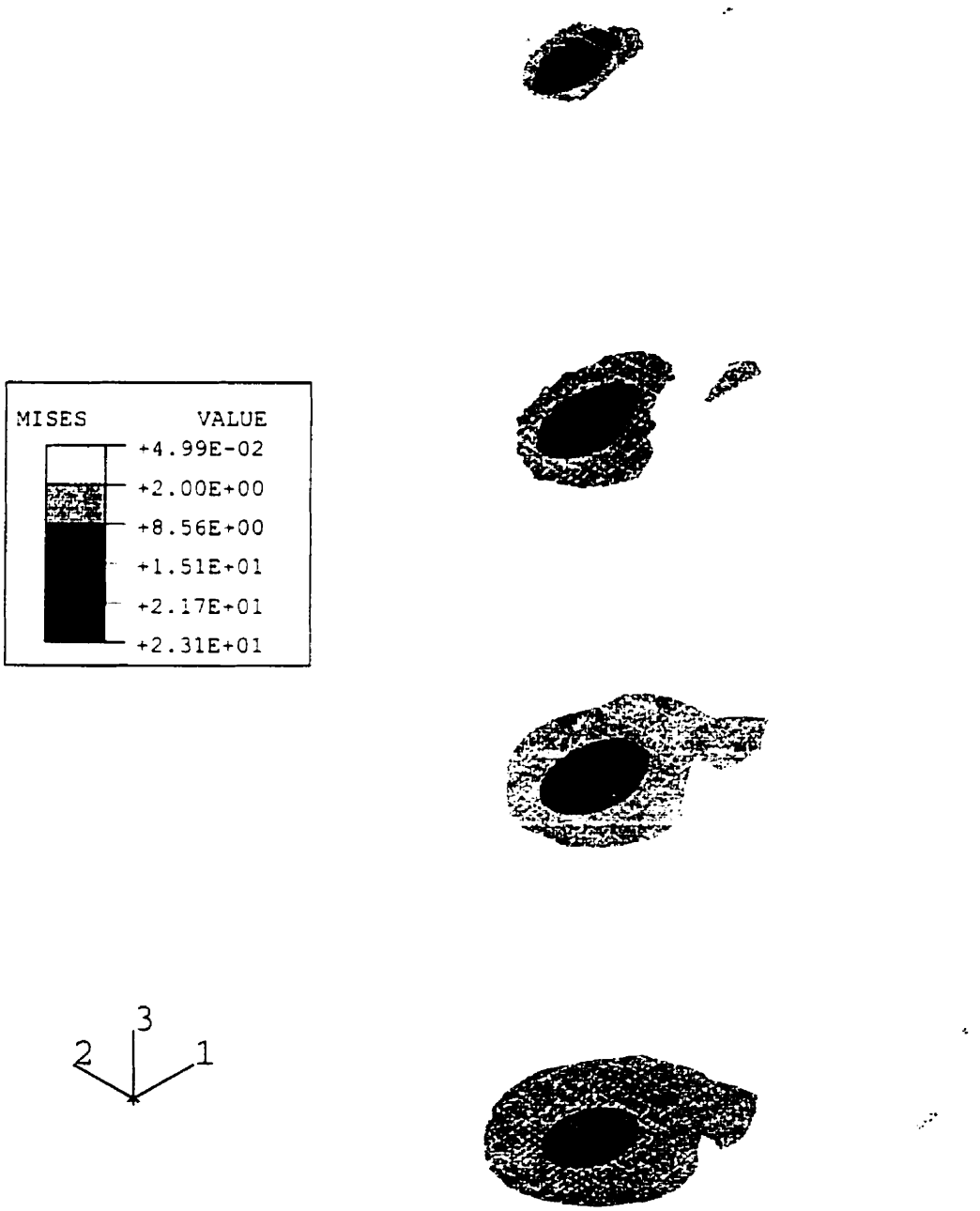

Figure C.6 Mises stress distribution in different layers of the polyethylene component.

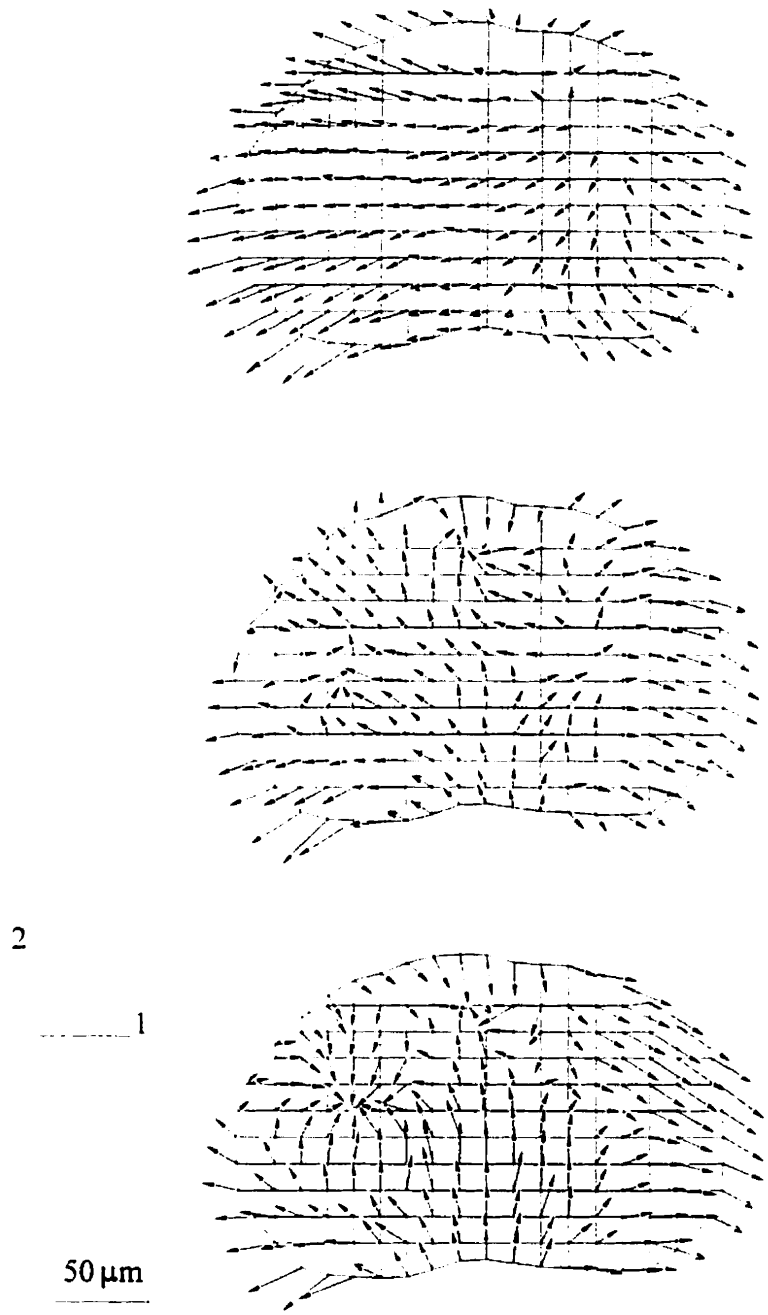

Figure C.7 Relative micromotion distribution at the bone-implant interface, for no fixation, post fixation and screw fixation, respectively (top to bottom).

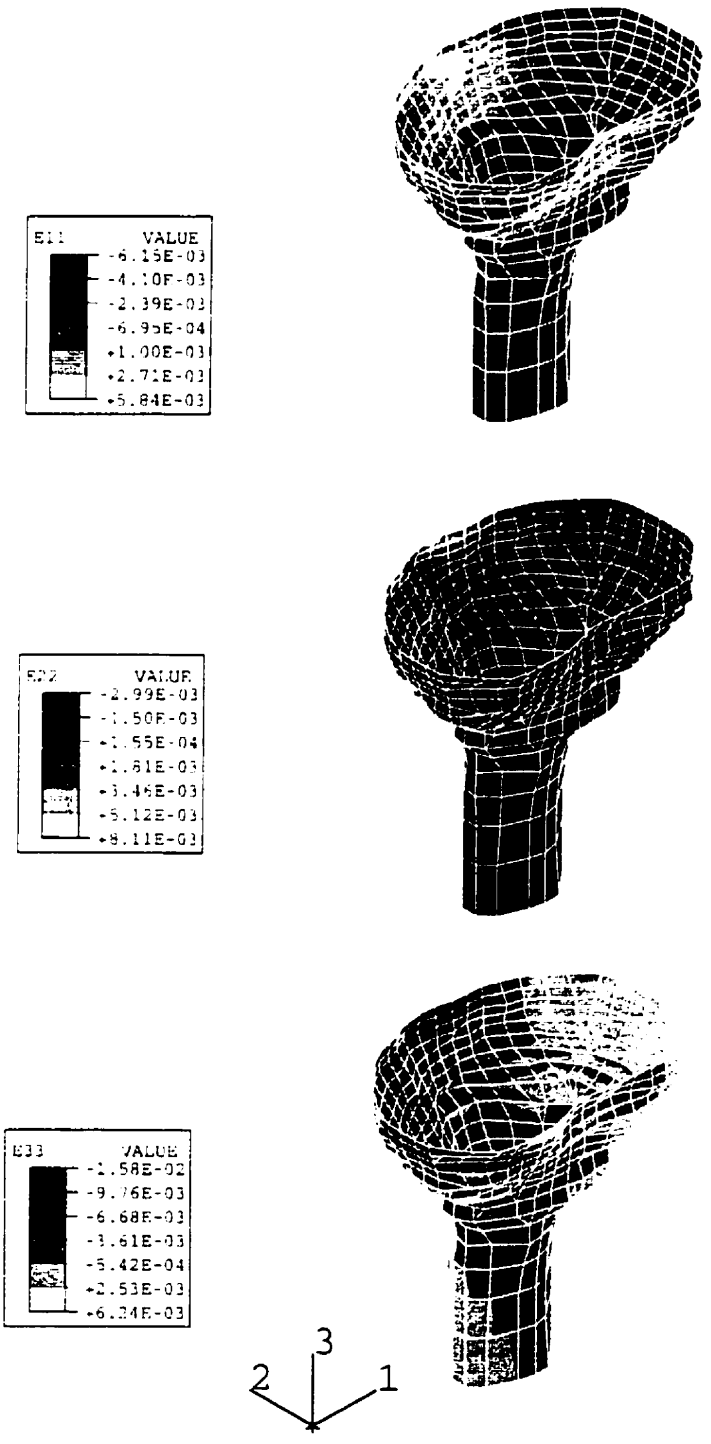

Figure C.8 Distribution of normal strain components within the cortical bone for no fixation configuration

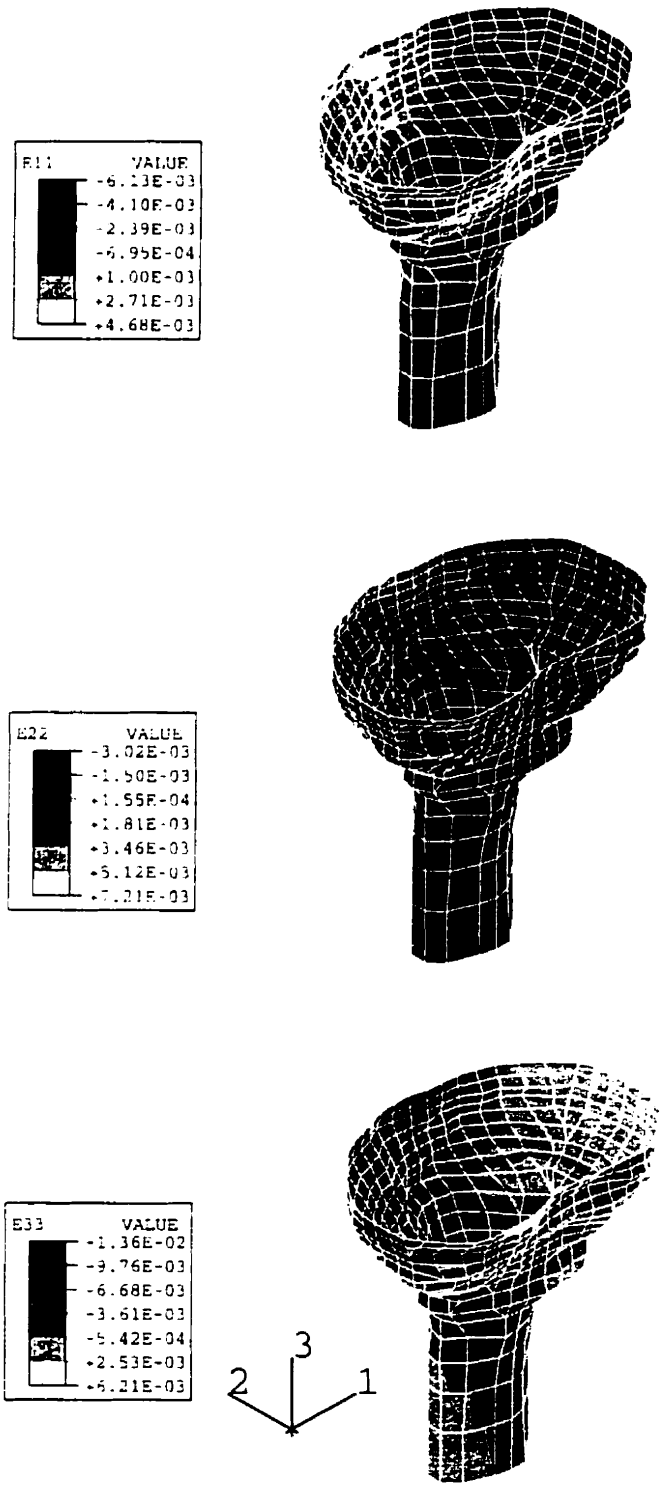

Figure C.9 Distribution of normal strain components within the cortical bone for post fixation configuration

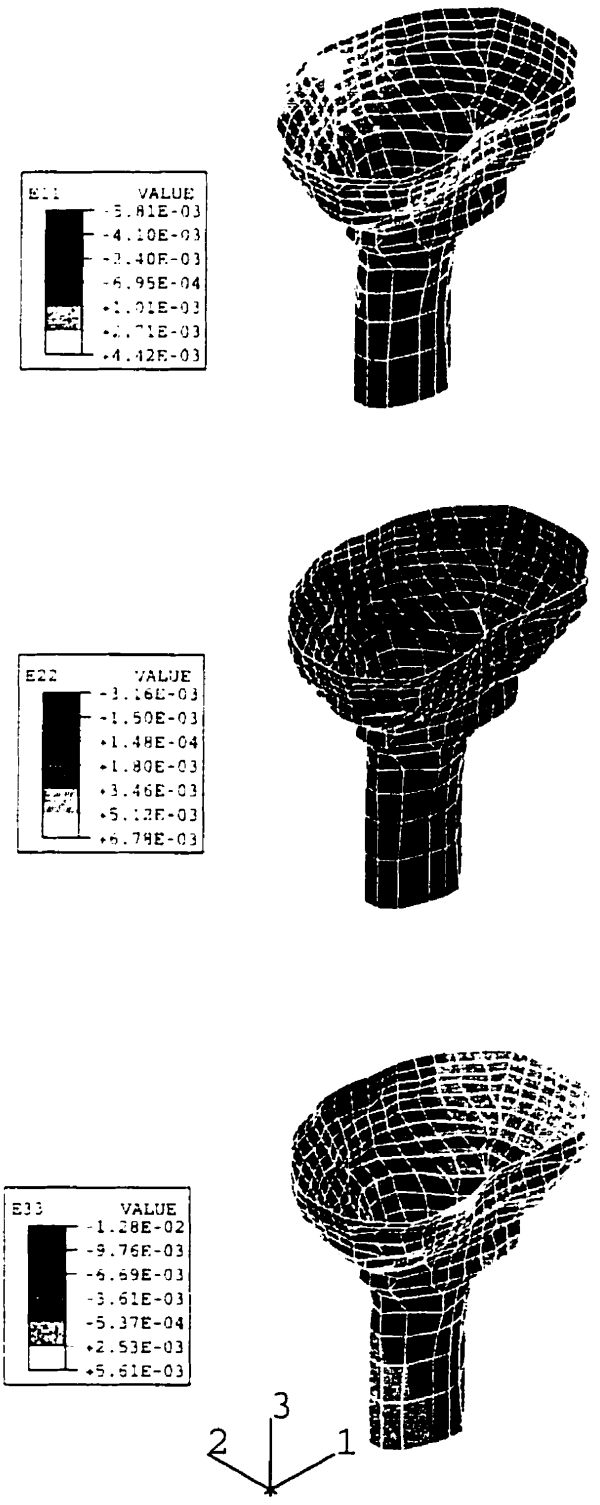

Figure C.10 Distribution of normal strain components within the cortical bone for screw fixation configuration